FABRICATION AND MECHANICAL CHARACTERIZATION OF A TWO-PLY CROSS FIBER STENT AND FIBERS COMPRISING BLENDS OF POLY(L-LACTIC ACID)

by

SUSHMA GAMPA

Presented to the Faculty of the Graduate School of

The University of Texas at Arlington

And

The University of Texas Southwestern Medical Center at Dallas

in Partial Fulfillment of the Requirements

for the Degree of

MASTER OF SCIENCE IN BIOMEDICAL ENGINEERING

THE UNIVERSITY OF TEXAS AT ARLINGTON

December 2005

ACKNOWLEDGEMENTS

I would like to sincerely thank my supervising professor Dr. Robert Eberhart, for his constant support and encouragement throughout the course of this project. It has been a wonderful experience working with him. Most importantly, I would like to thank my dearest husband and friend, Chandra Shekar, for his love, encouragement and support throughout this project. He never let me give up when I was faced with physical and emotional challenges. I would like to thank Dr. Charles Chuong and Dr. Kytai Nguyen for accepting to be on my thesis committee.

My special thanks to Pankaj Satasiya whose training and advice helped me get started on this project. Thanks to Dr. Kevin Nelson, Dr. Timmons, Dhiman Bhattacharya, Russ Emerick, Kipton Sheek and Dr. Karen Pawloski for generously sharing their experience and knowledge of the SEC techniques. It was a pleasant experience to work with Jenet, Anup and Chris. I greatly appreciate Dr. Steve Collins, Winston Layne, Miles and Joe for their immense help with the use of DSC and Instron. Thanks to Dr. Roger Goolsby and Tom Lees for their help with MTS.

I would also like to acknowledge my parents, Gampa Eshwaraiah and Vijaya Laxmi, and my in-laws, Garrepally Tirupathaiah and Anasuya for their selfless love and support.

November 21, 2005

ABSTRACT

FABRICATION AND MECHANICAL CHARACTERIZATION
OF A TWO-PLY CROSS FIBER STENT AND
FIBERS COMPRISING BLENDS OF
POLY(L-LACTIC ACID)

Publication No. _____

Sushma Gampa, M.S.

The University of Texas at Arlington
And
The University of Texas Southwestern Medical Center at Dallas, 2005

Supervising Professor: Robert C Eberhart

Recent studies indicate that stabilization of vulnerable atherosclerotic plaques is critical for minimizing acute coronary syndromes. In this regard a new biodegradable stent design, the Two-ply cross fiber stent, has been developed to reduce stent-imposed stresses on such plaque and to provide increased drug reservoir capability. A comparative study of the mechanical properties of Two-ply and Single-ply stent designs was performed. Fibers comprising PLLA blends were developed and their thermal and

mechanical properties were determined. Lateral spreading of helical fibers upon deployment of the Two ply design was observed that, in theory, may reduce stresses on the plaque surface. The results indicate that the 1.5 mm furled Two-ply cross fiber stent can be expanded fully, to 3.1 ± 0.1 mm diameter, with an inflation pressure of less than 5 atm. Use of two fiber plies increased the hoop strength without significantly affecting the longitudinal flexibility, thereby maintaining maneuverability whilst improving collapse resistance after deployment. Calorimetry measurements indicate that blends containing up to 50% of 100kD PLLA are suitable for incorporation of the anti-inflammatory drug Curcumin by melt extrusion.

TABLE OF CONTENTS

LIST OF ILLUSTRATIONS

LIST OF TABLES

CHAPTER 1

INTRODUCTION

According to the recent estimates of the American Heart Association (AHA) about 70,100,000 Americans suffer from one or more types of cardiovascular disease. It is widely prevalent among all the population groups in United States and has been documented as the major cause of mortality since 1900. Atherosclerosis cardiovascular disease is an inflammatory disease in which deposits of cholesterol, calcium and other cellular waste products accumulate in the artery walls (plaque) resulting in the arterial wall thickening and hardening. Severe atherosclerotic plaques cause several complications like ischemia, angina, myocardial infarction and occlusive coronary thrombus. Nearly 3/4 of all the deaths from cardiovascular diseases are due to atherosclerosis [1].

Atherosclerosis often results in narrowing of the luminal area which when severe can cause some of the symptoms mentioned above. For treatment, these focal atherosclerotic plaques are compressed against the arterial wall using Percutaneous transluminal coronary angioplasty (PTCA). Though this procedure resulted in acute gain in lumen diameter, late lumen loss due to restenosis, elastic recoil due to negative arterial remodeling and abrupt vessel closure required repetitive revascularization procedures. In this context, stent emerged as a cardiovascular device capable of providing prolonged mechanical support to the arterial wall and maintaining luminal

patency. The number of PTCA interventions performed each year has expanded considerably since the early days of stent development. According to the AHA, the rate of coronary stent insertion has increased almost 150 percent between 1996 and 2000 [1] due to the availability of a wide variety of stents for applications in lesions with various levels of complexities.

All the available stents can be broadly classified as balloon-expandable or self-expandable stents. In the balloon-expandable design, stents are mounted over an angioplasty balloon catheter, whose inflation helps to expand the stent to a larger diameter due to plastic deformation of its struts. In the self-expandable design, stent is covered with a constraining sheath whose release helps to elastically expand the stent to a predetermined size [2, 3]. Among the two types balloon-expandable metallic stents are used more often and they constitute 99% of the implantable devices used in the treatment of coronary artery disease [4].

Stents are manufactured using different techniques and different kinds of metals and polymers. The different metals used for stent construction include stainless steel, tantalum, nitinol, cobalt-chromium alloy, platinum and other metal alloys [2, 4]. Construction of stents like Gianturco-Roubin I and II and Wiktor™ involve weaving strands of metal wire into coils while stents like Palmaz-Schatz, Bx Velocity™ and MULTI-LINK® are manufactured by cutting patterns into thin metal tubes using lasers. NIR® stents are manufactured by first cutting patterns into thin metal sheets followed by rolling into tubes and welding. S670 and S7 stents from Medtronic are manufactured by welding together multiple links cut from metal tubing [4]. Most of the balloon-

expandable stents that are available are made from 316L stainless steel. Recently concern has been raised over nickel leaching, which results in chronic inflammation. Stainless steel has about 5% nickel content and when used in patients with a positive patch test for nickel allergy it could result in increased instent restenosis [4].

Many patients with stent implantations were observed to develop a stent-related problem called in-stent restenosis caused by exaggerated vascular neointimal proliferation which when severe can cause significant narrowing of the lumen. Depending on vessel anatomy and other clinical risk factors the incidence of restenosis can vary from 8% to 80% at 6 months following stent implantation [5]. In order to counter this problem both systemic and local drug treatment options have been studied. The systemic use of pharmaceutical agents has unfavorable effects like systemic toxicity and inadequate drug dosage at the lesion of interest. Local targeted delivery using stents as substrates for therapeutic agents is ideal because they are deployed against the vessel wall and hence can help to localize the effect of the drug by use of significantly lower doses of drugs. Stent-drug systems can be of three different categories (1) Drugs can be bound to the surface or embedded within microscopic reservoirs of metal stents; (2) Drugs can be loaded into a polymer layer (bioresorbable or non-bioresorbable) which is coated/sprayed onto the struts of the metal stent; (3) Drugs can be loaded into the bulk of the stents made of biodegradable polymers, figure 1.1 [6, 7]. Pharmaceutical agents used in stent-based antirestenotic therapy include immunosuppressive agents, anti-proliferative agents, anti-inflammatory agents, antithrombotic agents and pro-healing agents.

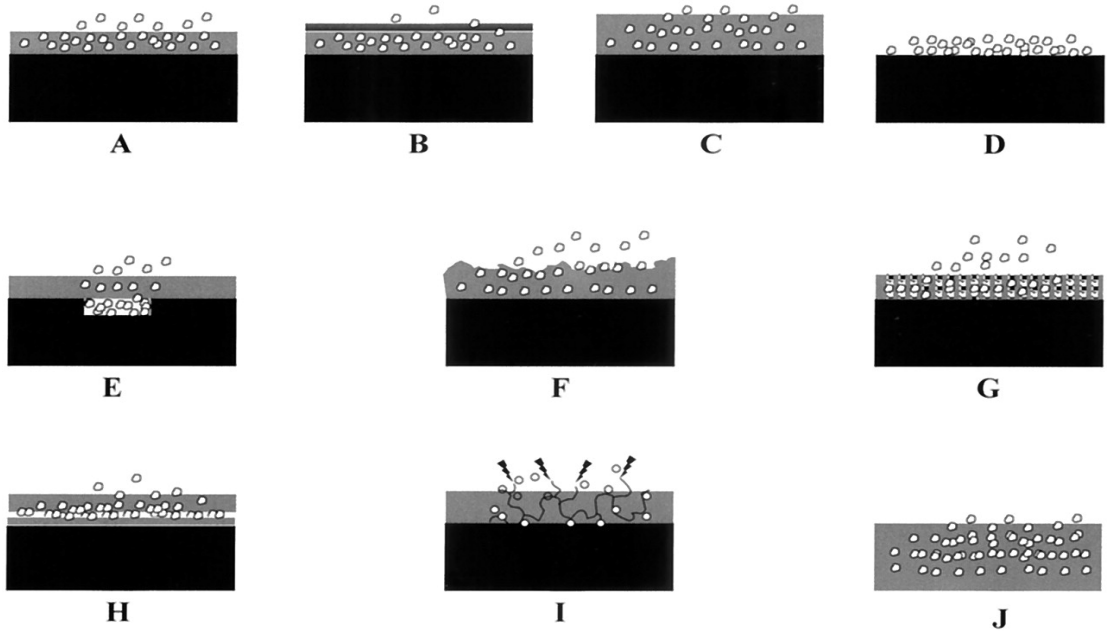

Figure 1.1 Different types of stent-based drug eluting systems. (black represents stent strut and gray coating). (A)Drug-polymer blend, release by diffusion; (B)Drug diffusion through additional polymer coating; (C) Drug release by swelling of coating; (D)Non–polymer-based drug release; (E)Drug loaded in stent reservoir; (F)Drug release by coating erosion; (G)Drug loaded in nanoporous coating reservoirs; (H)Drug loaded between coatings (coating sandwich); (I) Polymer-drug conjugate cleaved by hydrolysis or enzymic action and (J) Bioerodible, polymeric stent [7].

In the Unites States currently two types of drug eluting stents are approved by the Food and Drug Administration for clinical use. They are the Sirolimus-eluting CYPHER stent (Cordis/Johnson and Johnson) and the Paclitaxel-eluting TAXUS stent (Boston Scientific) [6]. These and many other stent-based drug delivery systems are being developed at a rapid pace to counter the problem of restenosis.

Coronary stents are currently employed to achieve luminal patency and restore unobstructed blood flow to the arterial lesions exhibiting greater than 75% cross

sectional area luminal narrowing. In spite of major advancements in the stent technology, the coronary heart disease remains the major cause of deaths in the United States. Patients who have already been revascularized by PTCA or CABG procedures continue to have a high risk of coronary artery disease progression and experience acute coronary syndromes (ACS). Also, a large number of people who appear to be normal with no symptoms of angina have been reported to experience acute coronary symptoms (fatal or nonfatal) like myocardial infarction, unstable angina and/or sudden cardiac death [8, 9]. Necropsy specimens from sudden death victims revealed that the lesion responsible for the cardiac event (culprit lesion) had coronary thrombus in 50–75% of the cases and greater than 75% luminal narrowing without thrombus in the rest [10]. Using coronary angiograms obtained prior to the acute coronary event in patients presenting with ACS, Little et al showed that 2/3 of lesions had less than 50% stenosis at the site of original coronary occlusion [11, 12]. In another study by Ambrose et al a linear relationship could not be established between the severity of the vessel stenosis and the probability of developing an ACS [11]. The occlusive thrombi observed in ACS victims were associated more often with angiographically insignificant lesions that do not warrant PTCA and stenting using coronary angiography. In order to investigate the underlying cause of ACS many retrospective studies were performed using autopsy or cross sectional studies using IVUS on the victims of ACS. Using autopsy material Glagov et al demonstrated that the arterial wall thickens outward and partially preserves the luminal areas at the atherosclerotic sites [13]. Using IVUS in a retrospective study Schoenhagen et al reported that outward arterial wall remodeling (positive) increases

wall thickness while preserving the luminal area and inward (negative) remodeling shrinks the arterial wall thickness, reducing the luminal area. Positive remodeling and larger plaque areas were associated with unstable clinical presentation, whereas negative remodeling was more common in patients with stable clinical presentation [14]. Kotani et al showed that a large proportion of lesions responsible for ACS had positive remodeling, higher proportion of plaque, and were rich in lipids [15]. These and several other studies have revealed that positive remodeling occurs due to the expansion of the internal elastic lamina caused by hemorrhage, inflammation, large lipid cores, macrophages and calcified deposits in the plaque. Though positive remodeling helps preserve the lumen area and reduce the probability of chronic stable angina it can be potentially lethal because of its accumulation and brewing of thrombotic and inflammatory contents. Gertz et al analyzed the morphologic features of the atherosclerotic lesions in infarct-related arteries and found that 30% of the ruptured plaques had lipid components compared to only 5% in the non-ruptured plaques [16]. The results of these several retrospective studies were confirmed by the prospective study performed by Yamagishi et al using IVUS. They reported that angiographically insignificant lesions that resulted in an ACS had larger, eccentric plaques compared with those lesions that did not result in the precipitation of an ACS. They also reported that 60% of the lesions that developed an ACS demonstrated outward remodeling [17]. Van der Wal et al reported that there was an infiltration of inflammatory cells, predominantly macrophages and T-lymphocytes, at the site of plaque rupture or erosion in the thrombotic coronary segments. Immunohistochemical

examination revealed the presence of activated inflammatory cells representing an ongoing inflammatory process [18].

From all the above studies it can be summarized that the pathology of the plaques responsible for the sudden cardiac events, the "Culprit" plaques, associated with occlusive thrombi and positive wall remodeling have (1) ruptured plaque with a large lipid pool, inflammation and thin fibrous cap (70%) [8, 19, 20] or (2) non ruptured plaque covered with a de-endothelialized surface (30%) [8, 10].

Several other plaques have been identified as "Vulnerable" plaques based on their morphologies which indicate that they might cause occlusive thrombus formation in the future, figure 1.2.

The vulnerable plaque or rupture prone plaque that most closely resembles a ruptured Culprit plaque, referred to as "Thin-cap fibroatheroma" [21], typically has a positively thickened arterial wall with large lipid core (>40% of plaques total volume) covered with a thin fibrous cap and is marked with ongoing inflammation and neovascularity [16, 22, 21], figure 1.3. The rupture of this plaque has been identified as the possible cause of acute coronary events. The contents of the large lipid core such as lipoprotein and tissue factor producing macrophages are highly thrombogenic and their luminal exposure due to plaque rupture can result in the formation of potentially occlusive thrombus near, or distal to the lesion site [23-26].

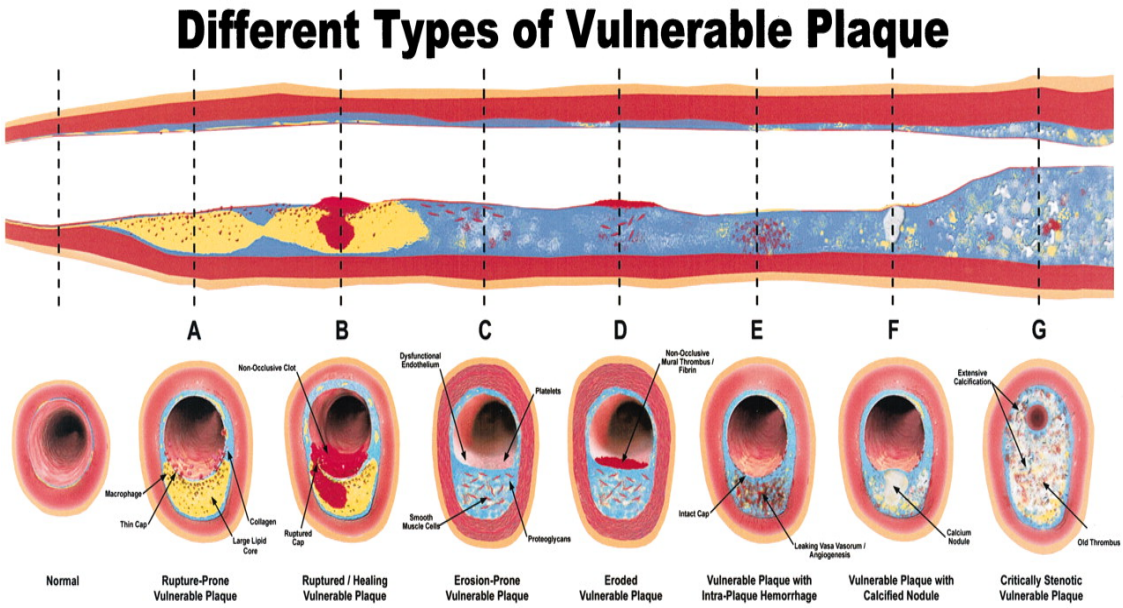

Figure 1.2 Different types of vulnerable plaques (A) Rupture-prone plaque with large lipid core and thin fibrous cap infiltrated by macrophages, (B) Ruptured plaque with subocclusive thrombus and early organization, (C) Erosion-prone plaque with proteoglycan matrix in a smooth muscle cell-rich plaque, (D) Eroded plaque with subocclusive thrombus, (E) Intraplaque hemorrhage secondary to leaking vasa vasorum, (F) Calcific nodule protruding into the vessel lumen and (G) Chronically stenotic plaque with severe calcification, old thrombus, and eccentric lumen [8].

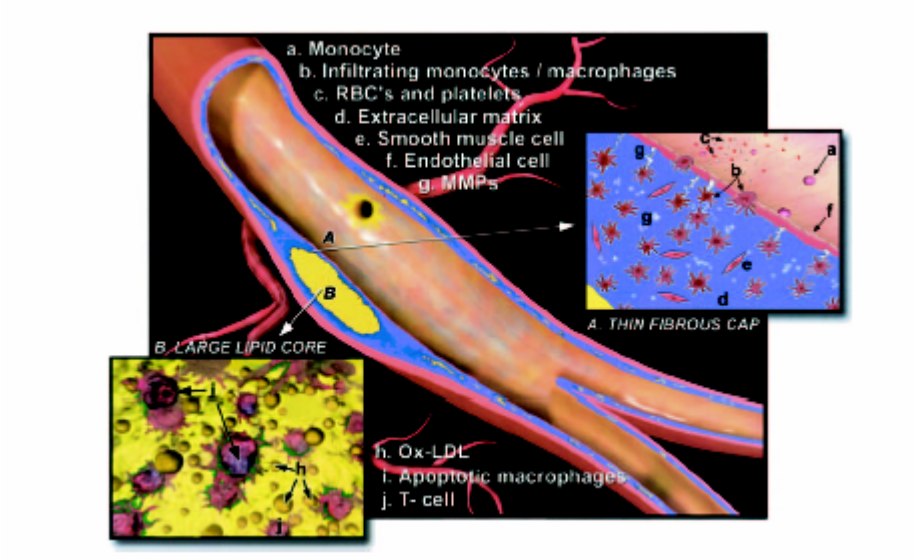

Figure 1.3 Schematic illustration of vulnerable plaque [8].

The contents of the plaque and the physiology surrounding the plaque both determine the stability and rupture of the plaque. Large amounts of lipid components like cholesteryl ester can soften the lipid core while large amounts of cholesterol crystals stiffen it and thereby impact the plaque stability [27]. Inflammatory cells, like activated T cells, infiltrating the plaque synthesize INF-γ which inhibits collagen synthesis and smooth muscle cell proliferation, activates macrophages and macrophage derived foam cells which in turn produce matrix-degrading metalloproteinases. This cascade of inflammatory actions ultimately results in the thinning of the fibrous cap [28, 29]. The increased neovascularisation found in the intima and adventitia of the plaque [22] also contributes to the thinning process by recruiting greater numbers of inflammatory cells at the plaque site. If the plaque surface is irregular it could cause significant disturbance to blood flow pattern resulting in turbulence, excessive shear force and uneven stress distribution. The rhythmic pulsation of blood and heart muscle can cause constant stretching and compression forces and weaken the fibrotic cap [30, 31].

Timely detection of the plaque can lead to earlier treatment to prevent/reduce the acute coronary events. Some of the major imaging techniques being investigated include invasive techniques like intravascular ultrasound (IVUS) (conventional, radiofrequency and elastography), angioscopy, optical coherence tomography, thermography, spectroscopy (Raman and Near Infra Red) and intravascular magnetic resonance imaging (MRI) and non-invasive techniques like computed tomography and high-resolution MRI [20]. All these techniques use the typical morphological features

and bioactive processes found in the vulnerable plaque to identify patients who might be at high risk for future ACS. Conventional IVUS provides very good visualization of the structural topography of both the vessel lumen and wall. In the vulnerable plaque setting it can detect the type of vessel wall remodeling, eccentric plaque and significant echolucency (correlates with plaque burden). In order to improve the imaging resolution for better identification of plaque components IVUS using radiofrequency signals (IVUS-RF) is being developed. Another technique called elastography goes further by using IVUS-RF signals at different intravascular pressures to measure tissue strain [32]. Several serum markers such as high sensitive C-reactive protein (hs-CRP), serum amyloid A, interleukin-6 and soluble intercellular adhesion molecule 1 are also being studied as potential inflammation markers that could help predict future cardiovascular events [20].

Stabilization of the plaque by pacifying the intensity of the inflammatory and/or thrombotic activity and/or improving the endothelial cell function on its surface may help reduce the risk of plaque rupture. Some of the systemic drug choices that are under investigation include lipid lowering agents, anti-thrombotic agents, Angiotensin converting enzyme (ACE) inhibitors, Calcium antagonists, β-blockers and anti-oxidants [32]. While most of these drugs target inflammation, thrombogenicity or endothelial cells Statins (lipid lowering agents) have been postulated to act on more than one of these. Since the bulk of the plaque is made up of a large lipid pool a lipid lowering agent would be the best choice to reduce the size of the plaque. In fact Angiographic and IVUS studies demonstrated considerable reduction in plaque dimensions, increased

fibrous tissue and reduced lipid pool with the use of statin treatment [33, 34]. Two other studies also showed that more than 30% reduction of first acute coronary events was observed in the group subjected to statin therapy compared to those treated with placebo [35, 36]. Apart from their action on lipid metabolism they can also reduce inflammation and platelet reactivity, enhancing thickness of fibrous cap and improve the functionality of the endothelial cells [37, 38]. Because of its action on several pathways statin treatment can be applied to treat both the rupture prone plaques as well as plaques with erosion. In spite of these attractive features one limitation of using systemic statin therapy is that the timeframe required to obtain favorable reduction in the plaque lipid pool is long (up to six months) [32].

Because of the prolonged treatment times involved systemic therapy may have unfavorable effects like bleeding (anti-thrombotic agents), systemic toxicity and insufficient dosage at the plaque site. Alternatively, the use of stent-based targeted drug delivering systems can help to significantly reduce the stabilization time with lower concentrations of drugs compared to systemic treatment. With regard to stent technology, these findings suggest that: 1) these stents must minimally stress the lesion, i.e. must expand gently and seal, or otherwise protect against plaque rupture; 2) should be placed at the lesion site only during therapeutic stabilization process 3) should facilitate single or multiple agent elution over prolonged time; 4) enhance arterial remodeling to reduce fragility of the lesion followed by plaque stabilization.

Most of the stent-based drug delivery systems currently available and those under investigation use conventional bare metal stent as the backbone over which a

layer of elastomeric biostable polymeric matrix of thickness 5-10 μm is coated [4]. The thin polymer matrix and the limited surface area of the metal stent limits the amount of drug that can be loaded. Bioresorbable stents on the other hand can be built with larger drug elution capacity because the entire stent bulk can help as drug reservoir. Thus the local release of drug can be expanded beyond the vulnerable plaque to include adjacent areas of diffuse disease, otherwise treatable only by systemic drug therapy. Also, the elasticity of the polymer matrix attached to the metal stents should be sufficient enough so as to not to tear away during stent expansion but with biodegradable stents no such complications would arise because the stent itself serves as the drug reservoir. The high deployment pressures used with metal stents are not suitable for lesions with vulnerable plaques. Low profile bioresorbable stents can be expanded at low pressure. Bioresorbable stents are temporary, meaning once the culprit lesion is stabilized and remodeling is well underway, the bioresorbable stent disappears, enhancing the chances for healing. The continued presence of the metal stent even after drug depletion continues to aggravate the remodeling tissue, reducing the chances for effective healing. Therefore, resorbable stents better enable tailored medical therapy, with timed strategies in patients with impending vulnerable plaque rupture. Bioresorbable stents provide another opportunity and advantage in this setting. After resorption of the primary stent, additional stents can be deployed, for second-stage mechanical and pharmacologic support, if necessary.

The following objectives have been pursued in this project:

1. Development of the Two-ply cross fiber stent design and testing of the feasibility of its fabrication.
2. Comparative study of mechanical properties of Two-ply and Singe-ply stent designs
3. Development of binary polymer blends and fibers as possible substrates for loading drugs in the Two-ply cross fiber stent configuration
4. Thermal and mechanical characterization of stent fiber blends

CHAPTER 2

MATERIALS AND METHODS

2.1 Design and Fabrication of Two-ply Cross Fiber Stent

The Two-ply cross fiber stent was designed for applications in which vulnerable plaque is present in the coronary blood vessels. The stent was designed to incorporate features like complete expansion and deployment at low balloon inflation pressure, good flexibility and compliance with the vessel wall, high hoop strength, reduced wall stresses from the stent struts and as a substrate for loading significant amounts of anti-inflammatory drugs. The basic framework of the Two-ply cross fiber stent design resembles a coil with multiple rotations, with each rotation manually woven in a specific pattern using two Poly (L-Lactic Acid) (PLLA) fibers. While two long PLLA fibers formed the body of the stent three other short PLLA fibers were used as longitudinal fibers, at 120^0 intervals on the central loop, to hold the whole structure together. While winding each rotation of the stent, the two PLLA fibers were wound to form three small peripheral loops inside a large central loop in the cross section and three crosses on the periphery, figure 2.1. The following section describes the fabrication procedure of the Two-ply cross fiber stent.

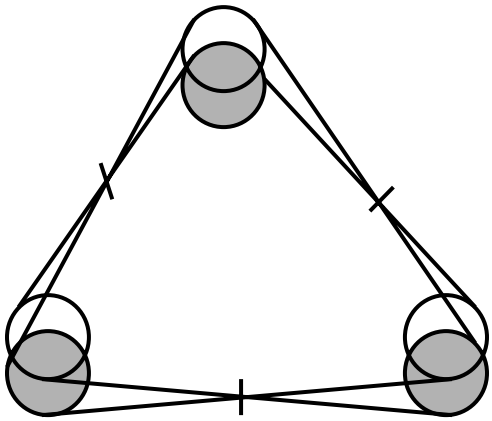

Figure 2.1 Structure of a typical rotation on the coil type Two-ply cross fiber stent

2.1.1 Materials

The stents were fabricated using thin fibers produced by the melt extrusion of PLLA resin (RESOMER® L210, MW 380kD, Boehringer Ingelheim, Germany) in a batch extruder (Alex James & Associates, Inc, Greenville, SC) followed by manual drawing on a heat plate (Nuova II, Sybron/Thermolyne Corporation, Dubuque, IW). The equipment used for winding stents consisted of four Stainless steel rods (Small Parts Inc., Miami, FL) and an acrylic holder (Bio-Instrumentation Laboratory, University of Texas Southwestern Medical Center at Dallas). The gluing procedure involved the use of a viscous solution of 8.0% w/v of PLLA resin in Chloroform (HPLC grade, Aldrich, Milwaukee, WI), a micro-injector and glass capillaries (Nanoject II, Drummond Scientific, Philadelphia, PA) and a stereo microscope (MBC-10, LOMO America Inc, IL).

2.1.2 Methods

The process of fabrication of the Two-ply cross fiber stent from scratch to finish consists of three different stages. The various actions performed at each stage of the process are listed in figure 2.2 and described in the following sections.

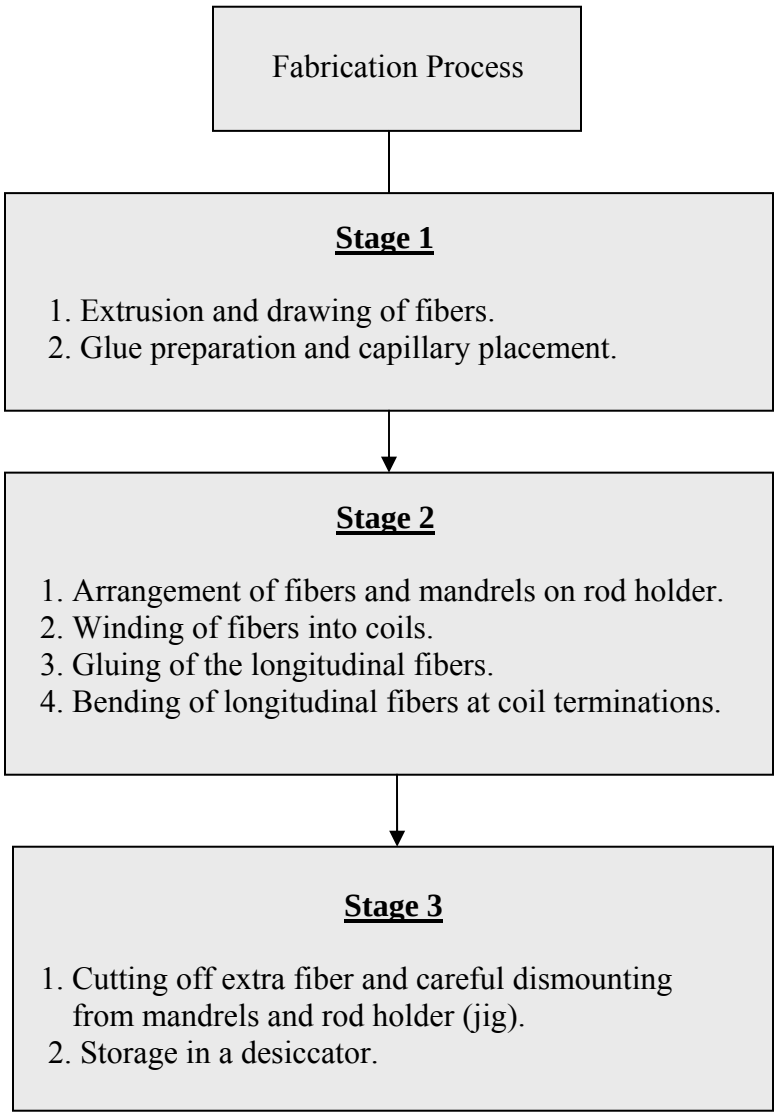

Figure 2.2 Fabrication procedure for a Two-ply cross fiber stent

2.1.2.1 Preparation of Fibers from PLLA Resin

The PLLA fiber required for the fabrication of stents was produced from the resin Resomer L210 by melt extrusion followed by manual drawing on a hot plate. For the extrusion process 10-12 gm of the polymer resin was packed into the cylinder/piston assembly of the extruder and melted completely at a temperature of 190-192 ^{o}C. The molten polymer was then pushed down through a spinneret of 0.016" diameter to obtain translucent fibers. These fibers were stored in a desiccator until used.

The fibers obtained from the extrusion process were brittle, thick and weren't strong enough to be used for the winding process. A manual drawing procedure was employed in order to increase the flexibility and strength and reduce the thickness of the PLLA fibers. For the drawing process the surface of a hot plate was cleaned and covered with aluminum foil and the heater turned on to reach a temperature of 60 ^{o}C. Based on the diameter of the extruded fibers a draw ratio of 1 to 5 or 1 to 6 was used to draw the fibers to a final diameter of 0.10 $\pm$ 0.02 mm. About 10 cm of the extruded fiber was taken and checked for uniformity in its diameter using a screw gauge at 1" intervals. One end of the fiber was then taped to one end of the hot plate and the other end was held tight with tweezers (figure 2.3a) until the section of the fiber on the center of the hot plate appeared to have reached a visco-elastic state (figure 2.3b). The fiber was then pulled slowly on one side till the translucent fiber turned opaque white. This process was repeated for all sections of the fiber (figure 2.3c). At the end of the process the fiber was trimmed off to an inch on both ends, inspected visually for opacity, checked for uniformity in diameter and stored in a desiccator.

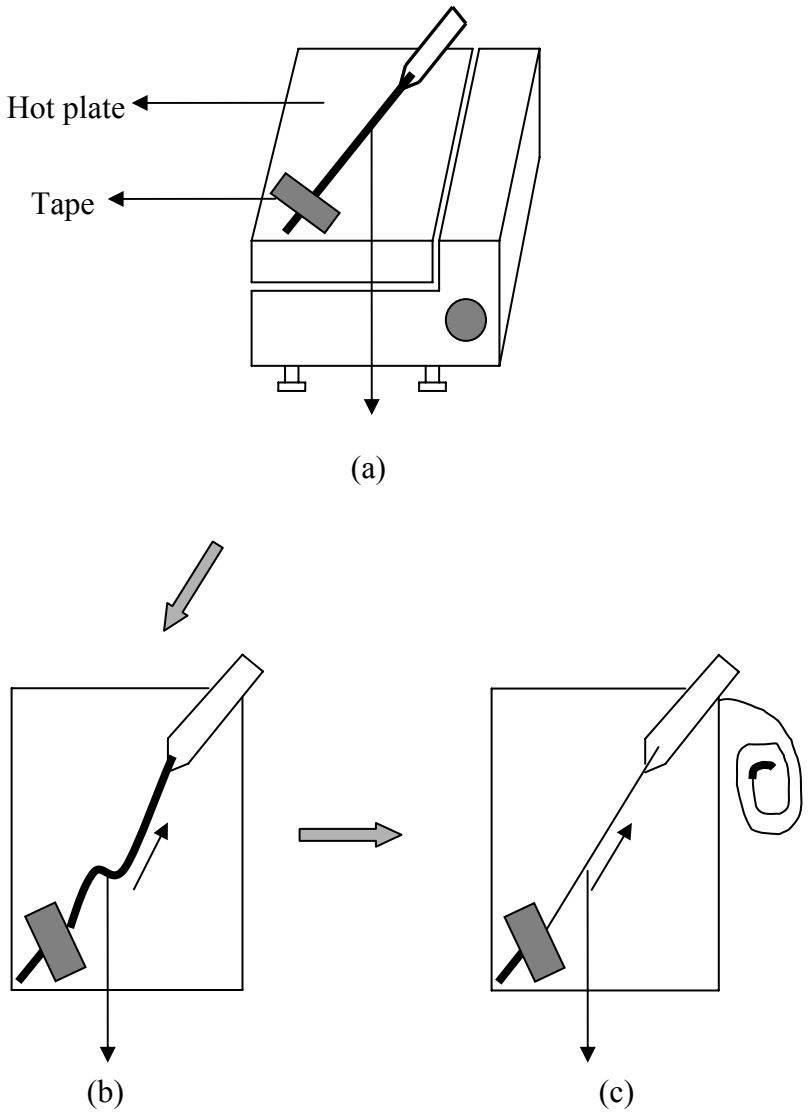

Figure 2.3 Drawing of PLLA fiber on a hot plate. (a) Thick undrawn fiber, (b) Distorted visci-elastic fiber, (c) Drawn fiber.

2.1.2.2 Glue Preparation and Capillary Placement

The fabrication process required the attachment of three short fibers at 120^{o} intervals in the axial direction of the stent. For this purpose a viscous solution of PLLA in Chloroform called "glue" was prepared at least two days before the initiation of the winding process. One gm of PLLA resin and 12.5 ml of Chloroform were mixed in a small clean bottle by shaking intermittently for 12 hours. The solution was then left overnight to allow the entire polymer to dissolve and wash down the walls of the bottle. Glass capillaries with a very fine tip were then added vertically to the glue for 24 hours to allow sufficient time for them to be filled with glue.

2.1.2.3 Arrangement of Fibers and Mandrels on the Rod Holder

The equipment used for winding stents consisted of three peripheral mandrels (0.35 mm OD), a central mandrel (0.64 mm OD) and a custom designed rod holder. All the mandrels were 10 cm in length and could be passed through the holes provided in the rod holder. Apart from holes for the mandrels the rod holder also had small holes at 120^{o} intervals for holding the longitudinal fibers, figure 2.4. Before beginning the winding process all the mandrels were wiped clean with Kimwipes and inserted through their respective holes on the rod holder. A 15 cm long PLLA fiber was cleaned with 70% ethanol wipes and cut into three equal pieces of 5 cm each. Each fiber (longitudinal fiber) was then passed through the small hole on the rod holder between two peripheral rods such that about 1 cm of the fiber was below the rod holder, figure 2.4. All the mandrels and longitudinal fibers were taped together below the rod holder.

Two PLLA fibers of 15 cm length were wiped with 70% ethanol wipes and taped on top of the rod holder beside the 1st peripheral mandrel, figure 2.4.

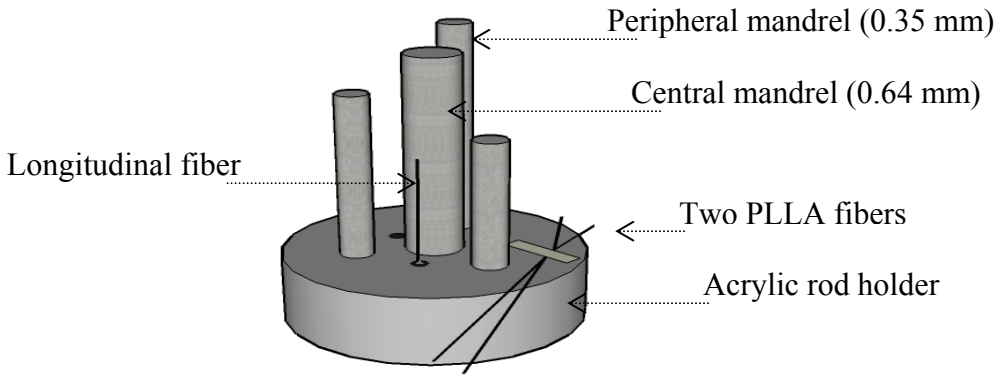

Figure 2.4 Rod holder with the arranged fibers and mandrels

2.1.2.4 Winding of Fibers into Coils

For the winding process the two PLLA fibers taped to the rod holder were held in parallel and close to each other. Together the fibers were passed over the 1st peripheral mandrel and circled around it in clockwise direction. The fibers were then advanced over the 1st peripheral mandrel, over the longitudinal fiber towards the 2nd peripheral mandrel and wound around it (figure 2.5a). At this point the fibers were no longer held together and in parallel to each other. Of the two fibers, the one on top was taken over the 2nd peripheral mandrel, below the longitudinal fiber and wound around the 3rd peripheral mandrel in a clockwise direction and anchored there. At this point the fiber on the bottom of the 2nd peripheral mandrel was taken over the 2nd peripheral mandrel, over the longitudinal fiber and wound around the 3rd peripheral mandrel. The

two fibers were then pulled together on the 3rd peripheral mandrel to tighten the grip (figure 2.5b). The two fibers looked like a cross in the horizontal direction with the longitudinal fiber in between them in the axial direction. Hence the name Two-ply cross fiber stent. The two fibers were then advanced from one peripheral mandrel to another in this fashion with the top fiber going below the longitudinal fiber and the bottom fiber going above the longitudinal fiber followed by tightening of the grip on the mandrels. After winding around all the three peripheral mandrels, the fibers were then advanced 1.2 mm in the axial direction per each turn (figures 2.5c, 2.5d). One coil rotation was completed when the fibers were wound on all the three peripheral mandrels and back on the 1st peripheral mandrel. In order to fabricate a stent of 10 coils, this process of winding the fibers from one peripheral mandrel to another in the circumferential direction while advancing about 1.2 mm in the axial direction per each turn was repeated 10 times. After the 10th coil rotation the two fibers were held together in parallel with each other and advanced over the longitudinal fiber and wound around the 2nd peripheral mandrel in a clockwise direction, pulled together and anchored to the base of the rod holder using a tape. This winding process resulted in a 12 mm stent with 10 coil rotations.

2.1.2.5 Gluing of the Longitudinal Fibers

The stent fabricated by the above winding process was not mechanically stable enough to allow its removal from the mandrels. In order to increase the stability and maintain the integrity of the design, the longitudinal and helical fibers were attached to each other (bonded) using the PLLA glue prepared as described above.

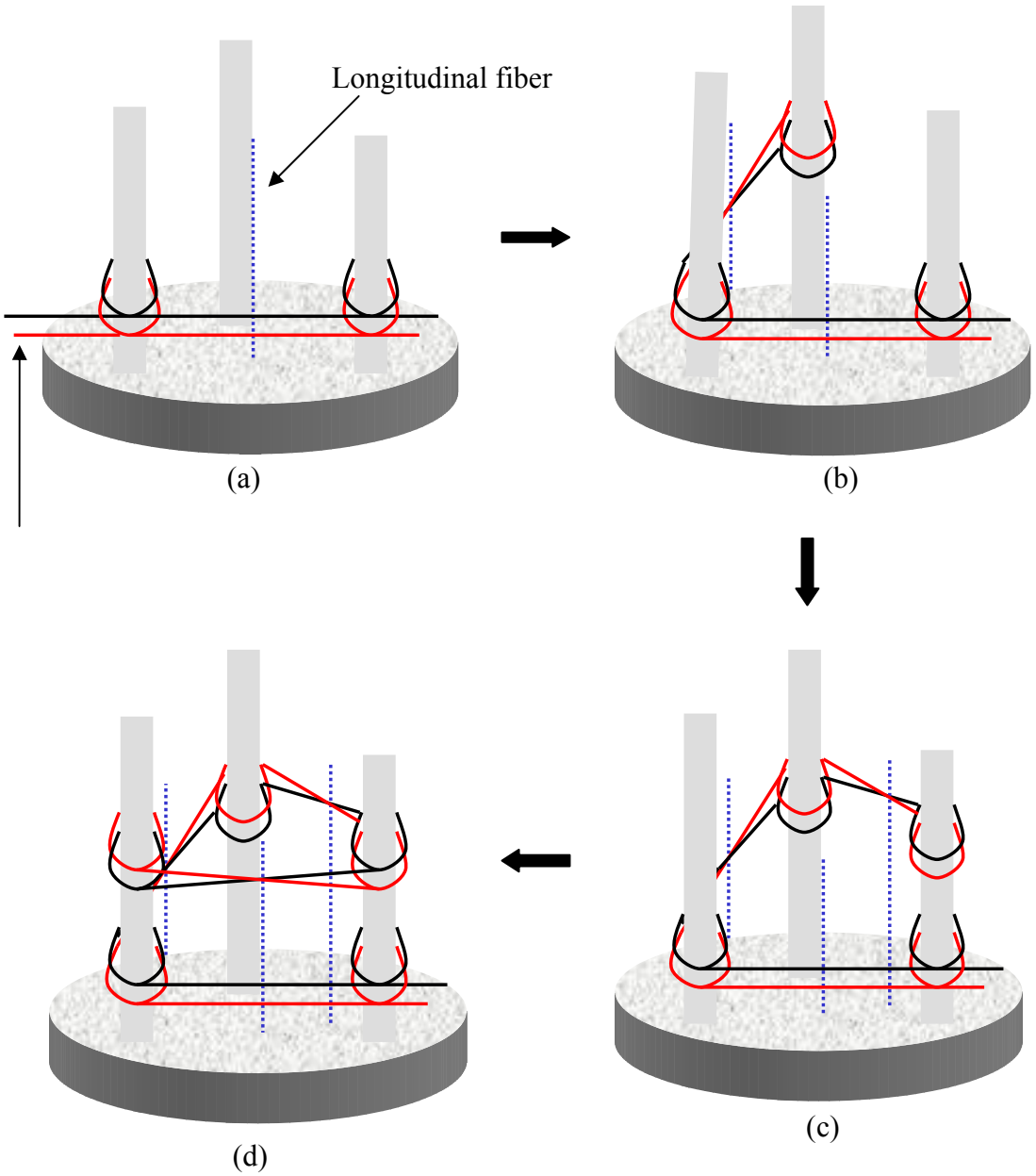

Figure 2.5 Winding of the Two- ply cross fiber stent. The peripheral mandrels are denoted in increasing order of their height, the shortest being the 1st peripheral mandrel. Central mandrel has been omitted for clarity. (a) Stage 1 (b) Stage 2 (c) Stage 3, (d) Stage 4.

Before beginning the gluing process, the glass capillary loaded with PLLA glue was cleaned on the outside using tweezers to remove residual PLLA and mounted onto

the injecting tip of a micro-injector. The stent was then observed under the microscope (8X * 2X) to ensure that the longitudinal fibers were located at the crossing points of the two helical fibers (figure 2.6) and also that all the three fibers were touching each other both at the cross-fiber points as well as at the coil terminations, figure 2.7.

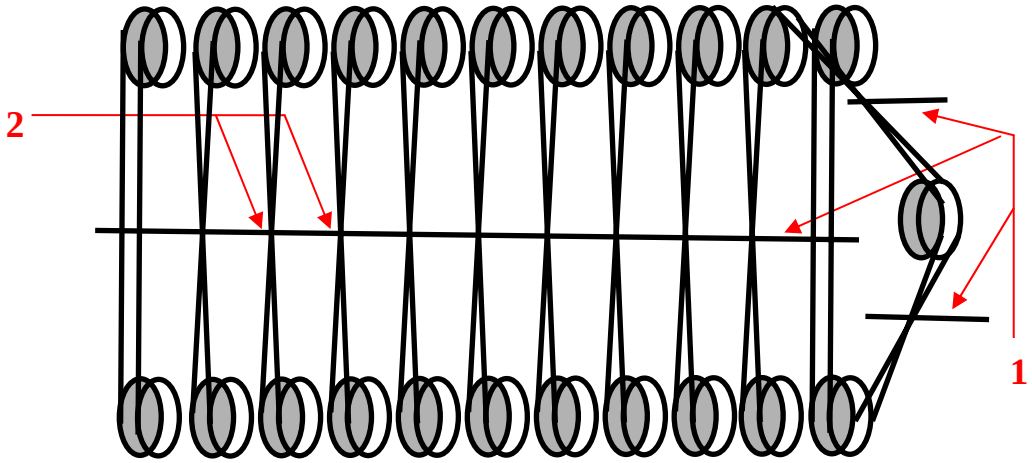

1. Longitudinal fibers 2. Crossing points of two helical fibers

Figure 2.6 Top view of the stent showing the longitudinal fiber located at the fiber cross over points of the two helical fibers.

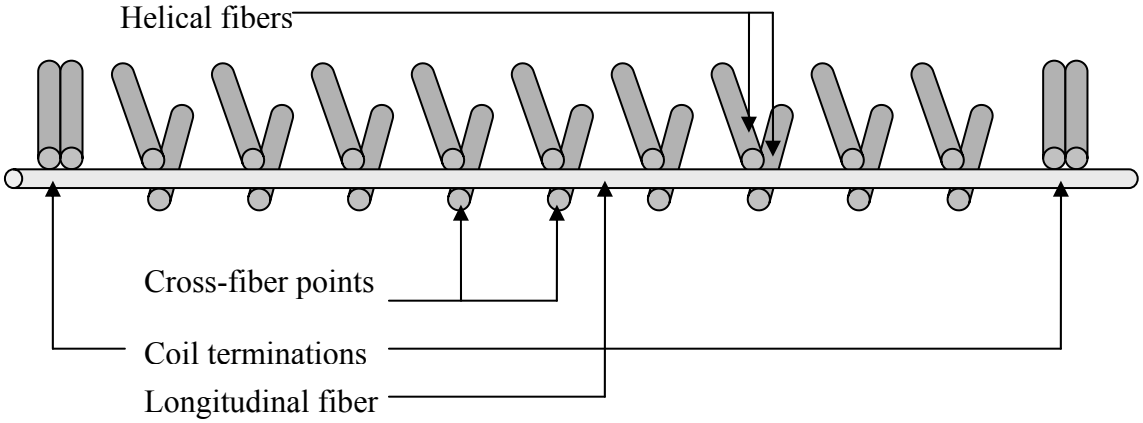

Figure 2.7 Longitudinal and helical fibers touch each other.

The tip of the capillary was arranged under the microscope and set to deliver 4.6 nL of glue for every click on the micro-injector. The stent was then positioned at the capillary tip so that the glue drop could be delivered directly onto the longitudinal fiber between the two helical fibers resulting in the attachment of all three fibers, figure 2.8a. Following this, the stent was advanced in increments of 1.2 mm in the axial direction to glue and secure all the attachment points on one side of a longitudinal fiber and later rotated 180^{o} axially to glue on the other side of that longitudinal fiber. This approach was followed for securing all the three longitudinal fibers to the helical fibers at the fiber crossing points.

The fibers at the end coils and coil terminations were glued differently, to withstand the higher stresses imposed during mounting and expansion on a catheter balloon. On the end coils, where the longitudinal fiber passed between the two helical fibers, glue was applied at two points on each side of the longitudinal fiber instead of one point. These four glue points helped hold the longitudinal fiber firmly in position on the end coils, figure 2.8b. At the coil terminations the longitudinal fiber was passed below the two helical fibers. Here glue was applied to the longitudinal fiber on either side of the two parallel fibers, figure 2.8c. These two glue points helped to hold the two fibers in position and attached to the longitudinal fiber. As the PLLA glue contains Chloroform, a solvent for PLLA and thus capable of eroding the fibers, care must be taken to avoid delivering excess glue and to minimize the gluing time.

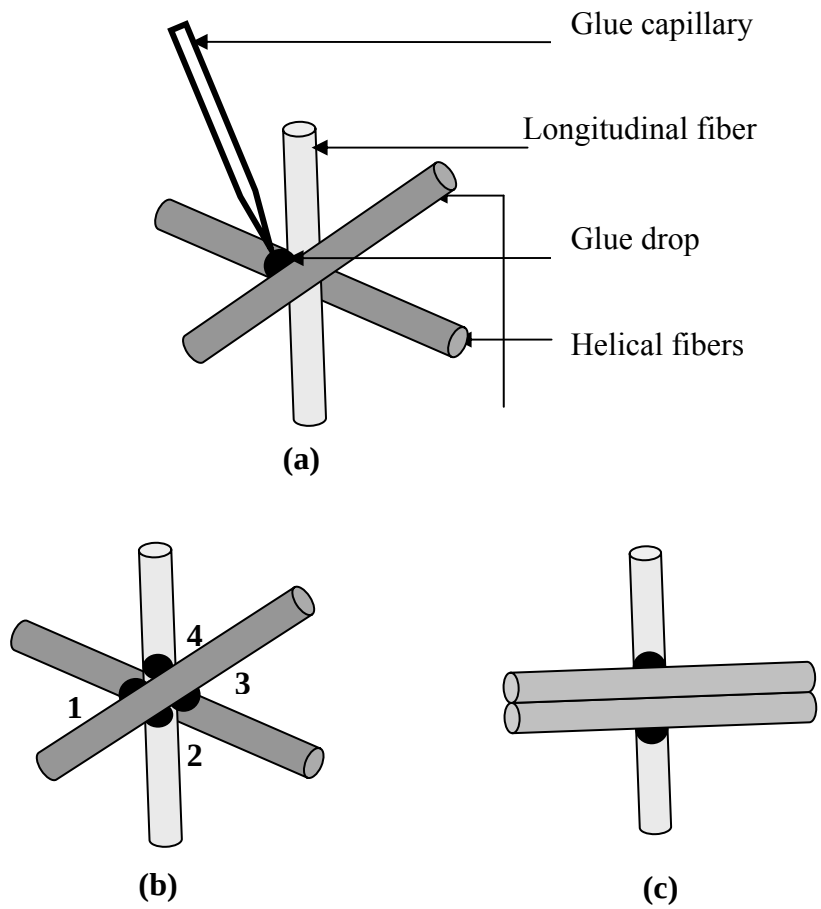

Figure 2.8 Glue delivery to the fiber attachment points on different sections of the stent. (a) On the main body of the stent, (b) end coils and (c) coil terminations.

2.1.2.6 Bending of the Longitudinal Fibers at Coil Terminations

The end coils and coil terminations of the stent must be strong enough to sustain the stresses imposed on them during mounting and expansion on a balloon catheter. Apart from adopting different winding and gluing strategies at these sections additional reinforcement was provided to the coil terminations by bending and attaching the nearby longitudinal fiber in a U configuration to serve as a second longitudinal fiber. At

the coil termination point the longitudinal fiber was passed below the two helical fibers arranged in parallel to each other. Using tweezers the end of this longitudinal fiber was bent over the two helical fibers in a U configuration and passed below the first coil and above the second coil rotation beside it, figure 2.9. PLLA glue was then applied on either side of the longitudinal fiber to attach it to the two helical fibers of the end coil and the first coil beside it as shown in figure 2.9. The termination point on the other side of the stent coil assembly was also reinforced in a similar fashion.

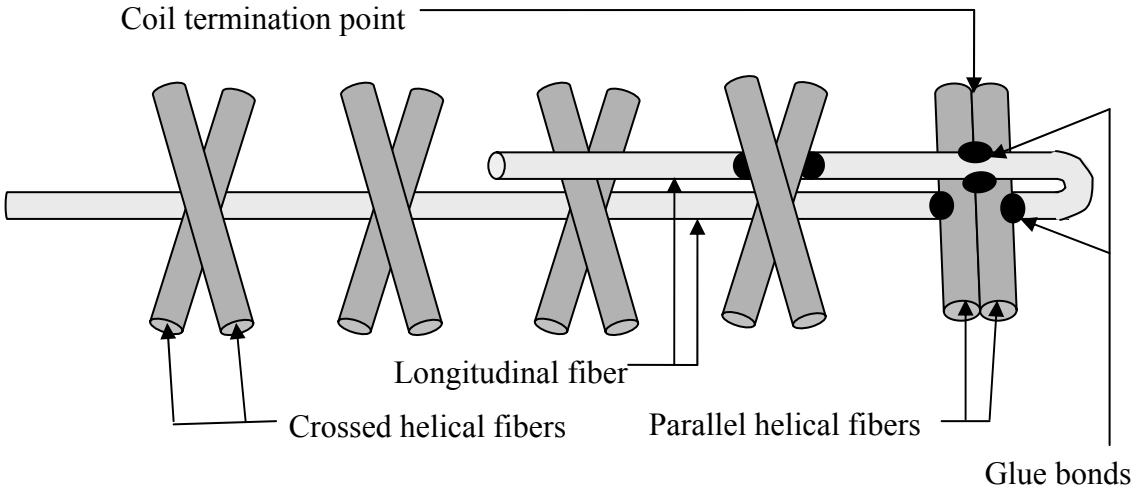

Figure 2.9 Bending and attachment of the longitudinal fiber at coil terminations

2.1.2.7 Fiber Trimming and Stent Dismounting Process

After attaching the longitudinal fibers to the helical fibers and reinforcing the coil terminations, the tapes and the rod holder were removed and the extra fibers extending beyond the desired end points were carefully cut off with a micro scissors while viewing the stent under a magnifying glass. The assembly of the mandrels was dismantled slowly and carefully and the stent was air dried overnight at room

temperature to remove any residual Chloroform from the glue points. The stent was then placed in an Eppendorf tube, sealed with parafilm and stored in a desiccator to avoid degradation due to hydrolysis. A schematic of the completed stent design is shown in figure 2.10.

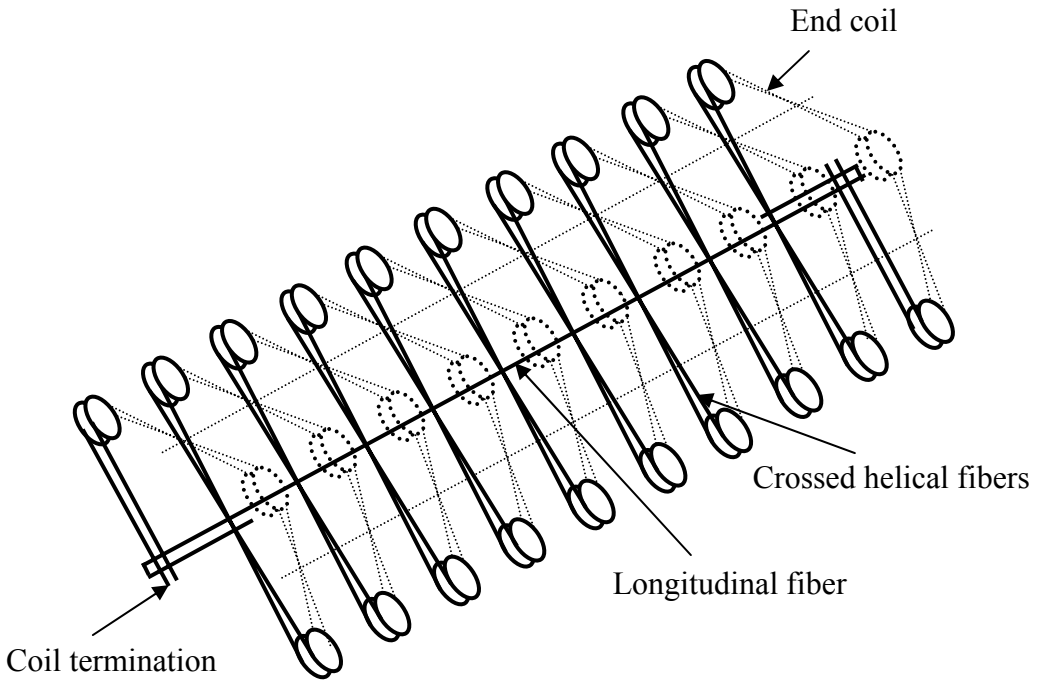

Figure 2.10 Design of a Two-ply cross fiber stent

2.2 Design Integrity

The integrity of the Two-ply cross fiber stent design was tested using three sets of experiments which address 1) the strength of the glue point in clamping the fibers together, 2) spreading of the two helical fibers upon stent expansion and 3) axial shortening of the stent upon expansion.

2.2.1 Strength of Adhesion of Glued Bonds

The glued bonds should be strong enough to attach the longitudinal fibers and the two helical fibers during mounting and expansion on an angioplasty balloon. This helps to provide stability to the stent design while distributing the load evenly throughout the stent coils. The winding pattern chosen for the Two-ply cross fiber stent allowed two different ways to attach the longitudinal and helical fibers together. At each fiber-fiber junction 4 points were accessible for gluing. Type-1 gluing, figure 2.11, where the glue drop could be delivered only onto the longitudinal fiber between the two helical fibers crossing each other and type-2 gluing, figure 2.11, where the glue was aimed to attach each of the two helical fibers separately to the longitudinal fiber at their respective cross-over points to the longitudinal fiber. Though type-2 gluing seems to be stronger than type-1 it requires double the amount of glue of type-1. The following test was done to determine the adhesive strength of the two types of glued bonds.

2.2.1.1 Materials

Twenty Two-ply cross fiber stents were fabricated with both type-1 and type-2 gluing. Ninja^{TM} balloon catheter (3.5 mm x 20 mm, Cordis Corporation, Warren, NJ) and the Encore 26 inflation device (Boston Scientific/ Medi-tech, Boston, MA) were used to expand all the stents. Glued bonds were observed under a light microscope (MBC-10, LOMO America Inc, IL).

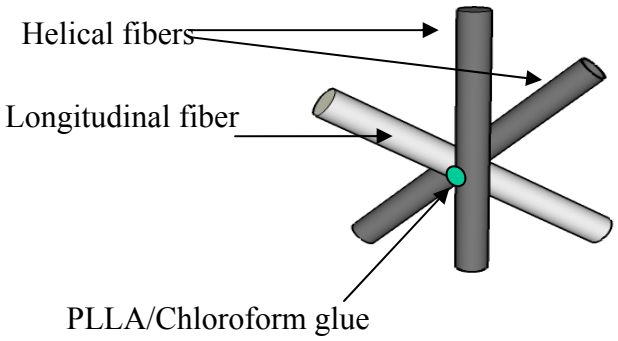

Type-1 gluing

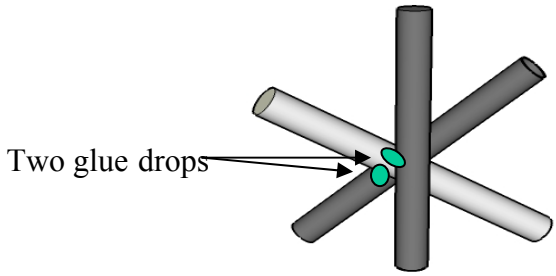

Type-2 gluing

2.2.1.2 Methods

The stents were mounted over an 18G, $1^1/_2$" needle and observed under the microscope to check if the glued bonds at the attachment points were intact. These stents were then mounted slowly and carefully onto the balloon catheter and expanded by inflating the balloon at a pressure of 6 atm applied for 25 seconds. All the stents

were expanded in the same way using the same balloon catheter. After expansion, each stent was again mounted over the 18G, $1^1/_2$" needle and observed under the microscope to note the number and location, if any, of failed bonds. The percentage of glue points that remained intact after expansion was determined for each type of gluing.

2.2.2 Spreading of Helical Fibers between the Longitudinal Fibers

Spreading of the helical fibers between any two longitudinal fibers upon expansion by an angioplasty balloon would help to reduce the compressive forces transmitted from the balloon onto the fibrous cap of the atheromatous plaque. The stent design was developed in a way to allow the spreading of fibers by crossing the helical fibers at the longitudinal fibers and attaching them to the longitudinal fibers.

2.2.2.1 Materials

Six Two-ply cross fiber stents were fabricated with 10 coil rotations using 0.64 mm and 0.35 mm mandrels. Cypher^{TM} balloon catheter (3.0 mm x 15 mm, Cordis Corporation, NJ) and the Encore 26 inflation device (Boston Scientific/ Medi-tech, Boston, MA) were used to expand the stents. Silicone rubber tubes of 3 mm ID were used to mimic a blood vessel. Fiber spreading upon stent expansion within the tube was observed under a light microscope (MBC-10, LOMO America Inc, IL).

2.2.2.2 Methods

All the stents were mounted onto the angioplasty balloon and expanded for 25 seconds at 6 atm inflation pressure. Three of the stents were expanded inside a silicone rubber tube and three were expanded without the tube. All the expanded stents were

then observed under the microscope for lateral spreading of the helical fibers between the longitudinal fibers.

2.2.3 Percentage Foreshortening of the Stent Upon Expansion

The decrease in the length of a stent upon expansion from its furled state is defined as foreshortening. Minimization of foreshortening is necessary to obtain better accuracy in stent positioning and placement inside a stenotic vessel.

2.2.3.1 Materials

Five Two-ply cross fiber stents were fabricated as described above in section 2.1. A digital caliper gauge (Cole-Parmer Instrument Company, Vernon Hills, IL) was used to measure the lengths of the stents. All the stents were expanded using Cypher^{TM} balloon catheter (3.0 mm x 15 mm, Cordis Corporation, NJ) and the Encore 26 inflation device (Boston Scientific/Medi-tech, Boston, MA).

2.2.3.2 Methods

The lengths of all the stents were measured in their furled state. The stents were then expanded one by one on the angioplasty balloon at an inflation pressure of 6 atm applied for 25 seconds. The lengths of the stents in their expanded state were measured immediately after the deflation and removal of the angioplasty balloon. Percentage foreshortening of the stent is calculated as:

$$\% \text{ Foreshortening} = \frac{(\text{Length before expansion} - \text{Length after expansion})}{\text{Length before expansion}} * 100 \quad (2.1)$$

2.3 Pressure Required for the Expansion of the Stent

The pressure at which the stent is fully expanded plays a critical role in endovascular stenting, especially for applications in the vicinity of vulnerable lesion sites. The inflation pressure is defined as that pressure required for expanding the balloon-mounted stent to the desired diameter.

2.3.1 Materials

Six Two-ply cross fiber stents and six single-ply inner coil stents [40] were fabricated using 0.1 $\pm$ 0.02 mm diameter PLLA fibers. Stents were expanded on the Cypher^{TM} balloon catheter (3.0 mm x 15 mm, Cordis Corporation, NJ) using the Encore 26 inflation device (Boston Scientific/ Medi-tech, Boston, MA). A digital caliper (Cole-Parmer Instrument Company, Vernon Hills, IL) was used to measure the diameter of the stents.

2.3.2 Methods

The diameter of the furled stents was carefully measured before mounting each stent on the angioplasty balloon. Balloon was then inflated slowly by applying pressure in increments of 1 atm, applied for 1 minute. At each pressure point the diameter of the stent mounted on the balloon was noted upto an increase in the inflation pressure to 8 atm. The same balloon catheter was used to expand both the single-ply and Two-ply cross fiber stents. Figure 2.12 shows the change in cross section of the Two-ply cross fiber stent due to the action of the applied inflation pressure.

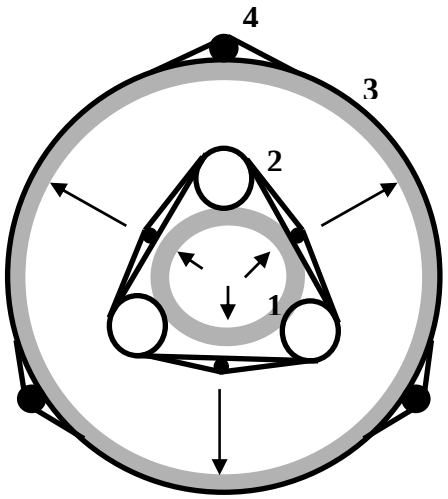

1. Angioplasty balloon
2. Furled Two-ply cross fiber stent
3. Expanded stent
4. Longitudinal fiber

Figure 2.12 Pressure required for the expansion of the stent. The arrows show the direction of action of inflation pressure during stent expansion.

2.4 Measurement of Expansion Ratio

It is important for a stent to have a low profile in the furled state to allow its deployment in the narrowed lumen of the vessels with plaque accumulations. The outer diameter of the stent in this furled state is defined as the "furled diameter", figure 2.13a. Upon expansion, due to the pressure from the angioplasty balloon, fiber from the peripheral lobes would be transferred to the central lobes changing the stent configuration to a single helical coil. It is important for a stent to expand sufficiently to match the vessel lumen and provide good apposition and support to the vessel wall. The outer diameter of the stent in this expanded configuration is defined as the "expanded diameter", figure 2.13b.

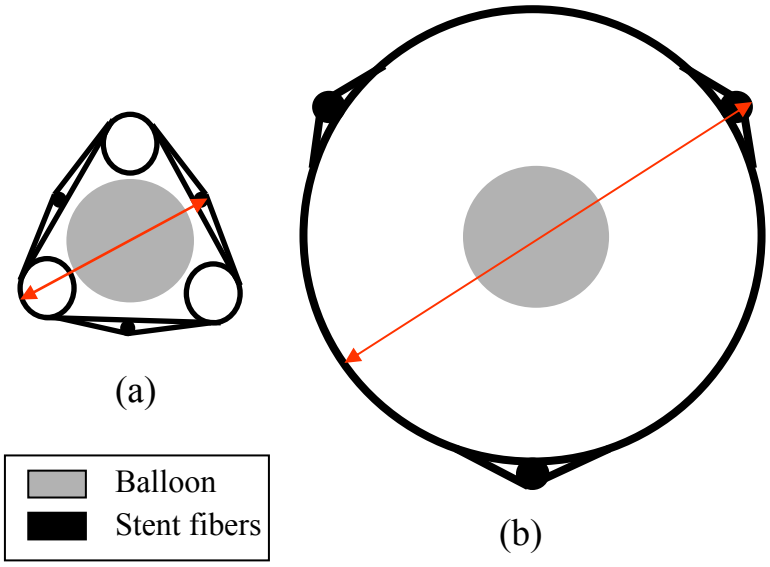

Figure 2.13 Cross sectional view of the Two-ply cross fiber stent (a) furled and (b) expanded configuration. Furled and expanded diameters are represented by arrows.

2.4.1 Materials

Five Two-ply cross fiber stents were fabricated using 0.1 $\pm$ 0.02 mm PLLA fibers. Cypher^{TM} balloon catheter (3.0 mm x 15 mm, Cordis Corporation, NJ) and the Encore 26 inflation device (Boston Scientific/ Medi-tech, Boston, MA) were used for stent expansion. A digital caliper (Cole-Parmer Instrument Company, Vernon Hills, IL) was used to measure the diameter of the stents.

2.4.2 Methods

The furled diameter of the five stents was carefully measured at three equally spaced coils along the stents axes by turning the stent 90^{o} at each measurement point. The average of all three measurements was reported as the furled diameter. Each stent was then carefully mounted onto the balloon catheter and an inflation pressure of 6 atm

was applied for 25 seconds thereby expanding the stent. However it was observed that the expansion of the balloon was not uniform axially and there was the formation of a "dogbone" shape before expanding completely into a uniform configuration. The expanded diameter of the stent was measured and noted in the same way as the furled diameter.

2.5 Elastic Recoil of the Stent After Balloon Deflation

Almost all balloon-expandable stents experience elastic recoil and undergo slight reduction in their expanded diameters as soon as the balloon is deflated and no longer supports the stent. This elastic recoil is an inherent property of the stent and depends on the specific material and structure of the stent. Low stent recoil helps to maintain a larger vessel lumen and minimize arterial flow perturbation.

2.5.1 Materials

Five Two-ply cross fiber stents were fabricated with 0.1 $\pm$ 0.02 mm PLLA fibers. The Cypher^{TM} balloon catheter (3.0 mm x 15 mm, Cordis Corporation, NJ) and the Encore 26 inflation device (Boston Scientific/ Medi-tech, Boston, MA) were used for the expansion of these stents. A digital caliper (Cole-Parmer Instrument Company, Vernon Hills, IL) was used to measure the diameter of the stents.

2.5.2 Methods

Each stent was carefully mounted onto the balloon catheter and an inflation pressure of 6 atm was applied for 25 to 30 seconds thereby expanding the stent. The diameter of the stents was measured at three equally spaced coils while it was on the

inflated balloon and also immediately after the balloon was deflated. The percent recoil is calculated as:

$$\% \text{ Recoil} = \frac{(\text{diameter on inflated balloon} - \text{diameter on deflated balloon})}{\text{Stent diameter on inflated balloon}} * 100 \qquad (2.2)$$

2.6 Hoop Strength of the Two-ply Cross Fiber Stent

An intravascular stent deployed after percutaneous transluminal angioplasty is intended to prevent the elastic recoil of the dilated vessel wall and improve its lumen patency by serving as a scaffold. Vessel walls in the vicinity of the stenotic lesion site are subjected to a complex interplay of compressive forces (from wall- and surrounding tissue elements in tension) and expansion forces (from the blood pressure). It is critical for the stent to withstand these forces in order to buttress the arterial wall from inside. The ability of the stent to withstand the constant radial compressive force from the vessel wall is described as the hoop strength of the stent. In this thesis the hoop strength is measured in terms of the compressive pressure required to cause irreversible plastic deformation of a stent in its expanded configuration.

2.6.1 Materials

All the stents were fabricated with 10 coil rotations using the PLLA fibers with 0.1 ± 0.02 mm diameter. These were expanded using the Cypher^{TM} balloon catheter (3.0 mm x 15 mm, Cordis Corporation, NJ) and the Encore 26 inflation device (Boston Scientific/ Medi-tech, Boston, MA). The equipment used for determining the hoop strength of the Two-ply cross fiber stents consisted of an acrylic pressure chamber (Bio-Instrumentation Laboratory, The University of Texas Southwestern Medical Center at

Dallas, TX) connected to a pressure gauge (PSI-TRONIX, Tulare, CA) and an air pump (Microflex, Cole-Parmer Instruments Inc., Chicago, IL), figure 2.14.

2.6.2 Methods

All the stents were expanded as described in the above sections. Each expanded stent was then mounted over the rubber tip of a nozzle present at the base of the pressure chamber and carefully covered with a flexible and transparent plastic sleeve. The sleeve was sealed airtight near the bottom of the rubber tip and the acrylic chamber reassembled. Then the tube connected to the base of the nozzle was opened to atmosphere and the air-pump switched on to pump air into the chamber. The airtight seal at the bottom of the rubber tip helps to maintain a pressure gradient across the plastic sleeve and the air pumped into the chamber applies radial compressive forces over the stent, figure 2.14. Compressive pressure was allowed to increase till a structural deformation of the stent was noticed. At this point pressure in the chamber was recorded and then released to allow the complete recovery of the stent structure. As long as the compressive forces are low the stent would undergo reversible elastic deformation, but once the compressive forces exceed the maximum hoop strength the stent undergoes irreversible plastic deformation. Each stent was subjected to several pressure compression-release cycles in the chamber until the stent lost its capability to recover back to its original structure upon release of the pressure. The pressure causing the permanent deformation of the stent was noted as the pneumatic hoop strength of the stent. All the stents were later observed under a light microscope to check for damage of both the fibers and the glue points.

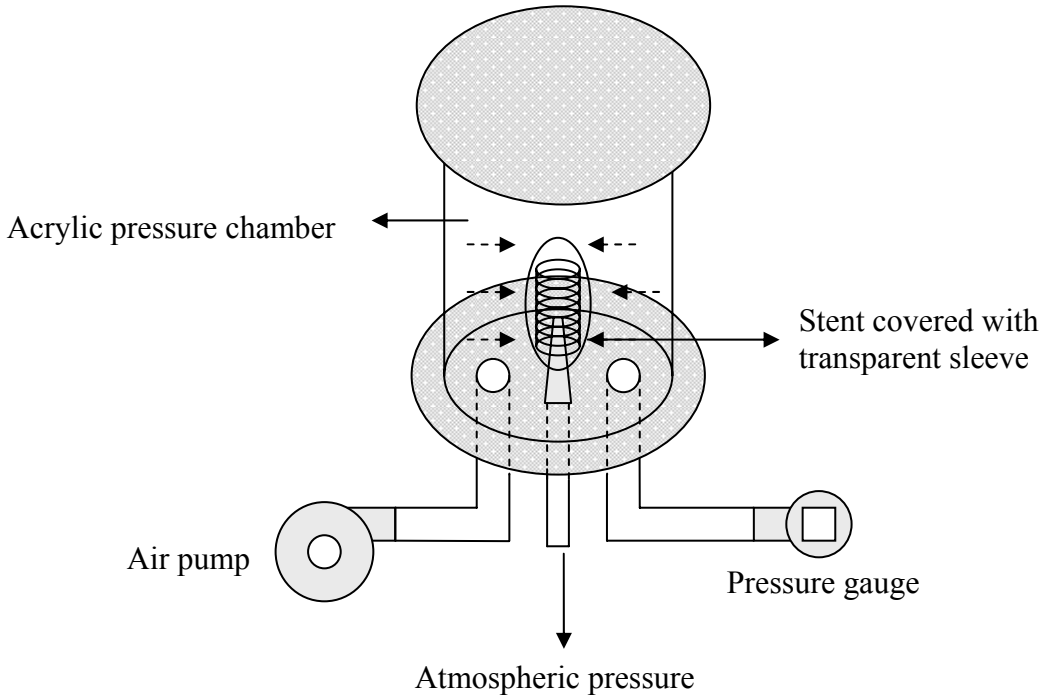

Figure 2.14 Compression chamber and the radial compressive forces on the stent

2.7 Determination of Stent Flexibility

Longitudinal flexibility of a stent is important both in the furled and expanded configurations. Good flexibility in the furled state helps stent to pass easily through tortuous vessels during deployment and in the expanded state helps it to conform sufficiently to vessel contour and minimize distortion at the stent/vessel junction. In either case flexibility helps to minimize the irritation on the vessel wall during delivery and deployment at a lesion site. Here a three point bend test technique described by Ormiston et al [39] is adopted to measure the stiffness (reciprocal of flexibility) of both the Two-ply cross fiber and single-ply inner coil stents. The three point bending test is more appropriate for relatively short structures like vascular stents employed in this

work and the Ormiston study, rather than the four point bending test. The effect of various design parameters like the fiber ply, fiber diameter, coil pitch and configuration (furled vs expanded) on the stent flexibility were studied in this test.

2.7.1 Materials

Stents that are 26mm long were fabricated using 35mm long PLLA fibers and 0.64mm and 0.35mm mandrels. A sample size of 3 was used for each design parameter tested. Details of the stent types and various parameters studied in the flexibility test are shown in table 2.1. Except for the effect of fiber ply and stent configuration all other stents were fabricated using the single-ply inner coil design.

Table 2.1 Parameters and Stents Studied in the Flexibility Test.

Design parameter	**Parameter values**	**Stent type**	**Stent configuration**
Fiber ply	One, Two	Single-ply inner coil, Two-ply cross fiber	Furled, Expanded
Fiber diameter	0.1 mm, 0.13 mm	Single-ply inner coil stent	Furled
Coil pitch	1.0mm, 1.2mm, 1.4mm	Single-ply inner coil stent	Furled
Stent configuration	Furled, Expanded	Single-ply inner coil, Two-ply cross fiber	Furled, Expanded

All the stents being tested in the expanded configuration were expanded with the Ninja^{TM} balloon catheter (3.5 mm x 30 mm, Cordis Corporation, NJ) and the Encore 26 inflation device (Boston Scientific/Medi-tech, Boston, MA) at an inflation pressure of 6 atm. Pictures of the stents were taken both before and after the flexibility test using a

digital camera (Olympus C-740 Ultrazoom, Olympus America Inc., Melville, NY).The equipment used for conducting the three point bend test consisted of two custom designed aluminum fixtures, figure 2.15 (Machine shop, University of Texas at Arlington) and an MTS Q Test/150 system (MTS System Inc, MN) equipped with a 75 g miniature load cell (Model 31, Honeywell Sensotec, Columbus, Ohio). All the stents were observed under a stereo microscope (MBC-10, LOMO America Inc, IL).

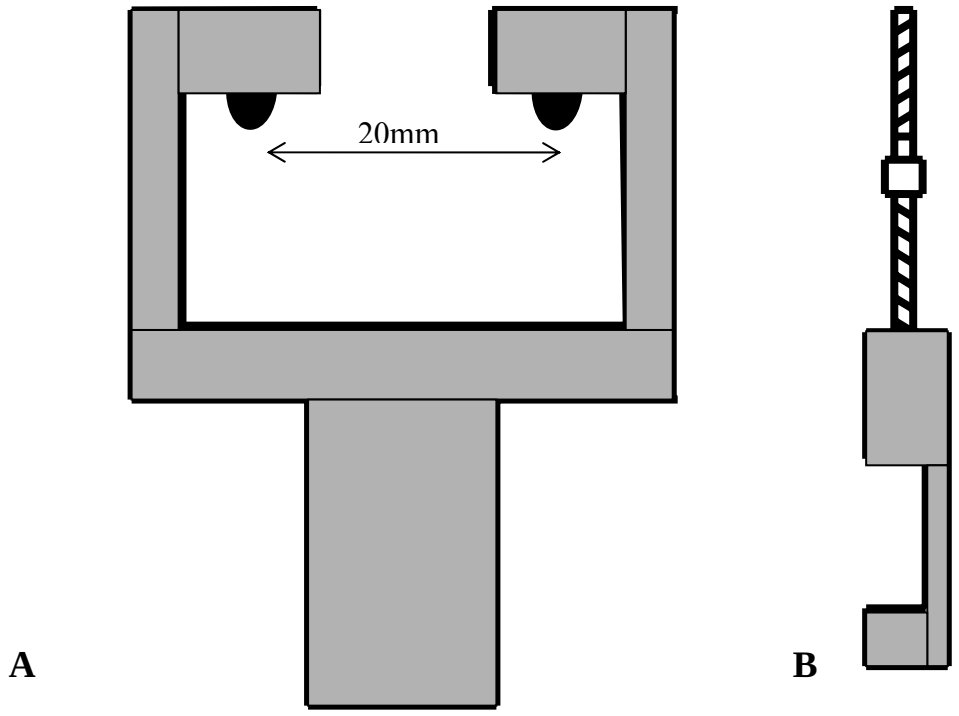

Figure 2.15 Fixtures for conducting the three point bend test. (A) Y-fixture for holding the stent (B) J-hook for pulling the stent.

2.7.2 Methods

Before beginning the three-point bend test, all the stents were carefully marked at their midpoint using a black permanent marker pen. Care was taken not to apply

much pressure while doing so. Digital pictures of all the stents were captured with the stents placed beside a straight edge. The Y-shaped fixture was fitted to the base of the MTS machine and the J-hook to the load cell. The stent was positioned carefully as shown in Figure 2.16 such that the marked midpoint was on the J-hook. The two spherical rods on the Y-fixture provided the two end points and the J-hook provided the third point for the three point bend test. Force was slowly applied to the stent by pulling the J-hook at a cross head speed of 5 mm/min at room temperature. Pulling was stopped when the extension of the stent reached 3 mm. In order to determine if the loading rate applied to the stents was in their elastic limit a test run was made with two single-ply and two two-ply stents under above conditions. Pictures of the stents taken before and after the test were compared to see if there was any longitudinal deformation. No deformation or sliding during flexion could be observed, based on those pictures. The stents were also observed under the microscope to check for local damage to the fibers or the glue points. After determining that the loading rate was within the elastic limit of the stents similar procedure was repeated for all the other test stents. From the data Force (g) Vs displacement (mm) curves were constructed up to a displacement of 2 mm and the slope of the best-fit straight line was recorded as the stiffness of that particular stent.

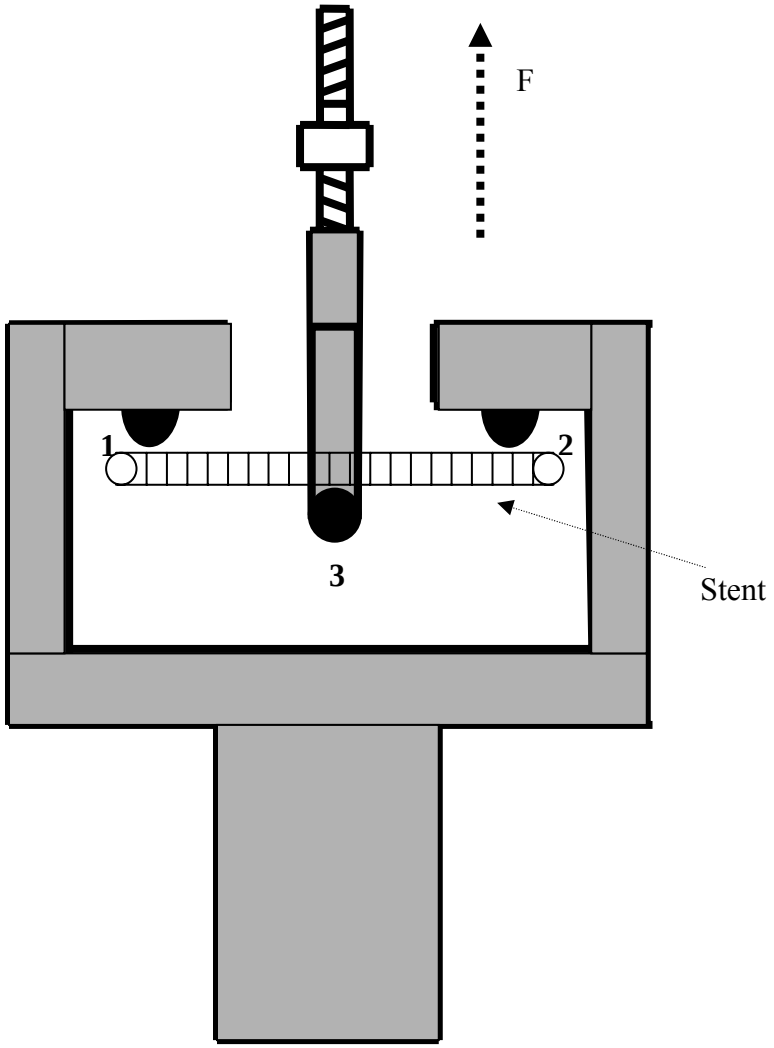

Figure 2.16 Experimental setup for the three-point bend test. The numbers show the three points where force is applied on the stent.

2.8 Binary Blends of High, Intermediate and Low Molecular Weight PLLA

There is an increased research interest in the development of stents loaded with drugs, due to their ability to provide localized drug delivery. In this regard we tried to incorporate an anti-inflammatory drug Curcumin into the bulk of the PLLA fiber (Resomer L210) used for the fabrication of stents. When an attempt was made to load

Curcumin into PLLA fibers by melt extrusion no fibers could be obtained due to the thermal degradation of the drug. High molecular weight PLLA was used for the fabrication of the stents to provide good mechanical properties. Blending of this PLLA with lower molecular weight PLLA may help to modulate the thermal properties and thereby, improve the loading, by melt extrusion technique, of Curcumin into the bulk of the fiber. For this purpose two PLLA resins with average molecular weights lower than that of the PLLA resin used for stent fabrication were chosen. The following section describes the preparation of the binary blends of these PLLA resins. Following blend preparation, DSC was used to determine the thermal transitions of the blended PLLA films. Feasibility to melt extrude fibers from the blended films was demonstrated and the fibers were tested for their mechanical strength. Stents were fabricated using blended fiber and were tested for expansion ratio, intrinsic elastic recoil and hoop strength.

2.8.1 Materials

Three PLLA resins of molecular weights ~380 kD (RESOMER® L210 (i.v. = 3.6 dl/g in $CHCl_3$ at 30 ^{0}C), Boehringer Ingelheim, Germany), 300 kD (Polysciences Inc, Warrington, PA) and ~100 kD (0.96 dL/g in $CHCl_3$, Absorbable Polymers International, Pelham, AL) were used for the preparation of blends. The three polymers are referred as H-PLLA, I-PLLA and L-PLLA (H-High, I-Intermediate, L-Low) respectively in the order of their molecular weights [41]. Required amounts of polymers weighed on an electronic balance (HR-202 mass balance, A & D company Ltd, Tokyo, Japan) were dissolved in Chloroform (GRACS, EMD Chemicals Inc, Gibbstown, NJ)

over a stir plate (Nuova II, Sybron/Thermolyne Corporation, Dubuque, IW) and final films were dried in a vacuum oven (PRECISION, GCA Corporation).

2.8.2 Methods

Binary blends of H-PLLA/I-PLLA and H-PLLA/L-PLLA were prepared with w/w ratios of 100:0, 60:40, 50:50, 40:60 and 0:100 respectively. Based on the blend composition appropriate amounts of the two polymer pellets were weighed to make up a mixture of 5 gm total weight. 200 ml of Chloroform was then added to this resin mixture and the solution stirred overnight to dissolve the two polymers. The polymer solution was then used to cast films in pyrex glass dishes, which were air-dried inside a chemical hood at room temperature for 12 hrs for evaporation of the solvent. The resulting blended polymer film was dried inside a vacuum oven at room temperature for 12 more hours in order to remove traces of the residual solvent. All the films were sealed in air-tight covers at room temperature and stored inside a desiccator.

2.9 Thermal Analysis Using DSC

Differential scanning calorimetry (DSC) allows the determination of thermal transitions in polymers like the glass transition, melting and crystallization. The principle of DSC is that both the sample and the reference furnaces are always maintained at the same temperature by varying the amount of heat flow. This heat flow between the two furnaces remains the same, unless there is a thermal transition in the sample and thus can be used to determine the thermal properties of the sample.

2.9.1 Materials

Thermal analysis was performed using the Pyris 6 Diamond DSC (Perkin Elmer Instruments, Norwalk, CT) system. The PLLA samples were weighed carefully on a microbalance (UMX2, Mettler-Toledo Inc, Columbus, OH), placed into 50 µl aluminium pans and sealed using a 10 µl aluminium lid (Perkin-Elmer Instruments, Norwalk, CT) and a crimper (Perkin-Elmer Instruments, Norwalk, CT). Pyris 6 Diamond Software (Perkin Elmer Instruments, Norwalk, CT) was used to control the DSC system and also to collect and analyze data.

2.9.2 Methods

Both the aluminum pans and lids were carefully washed with isopropanol; the samples were cleaned with 70 % ethanol wipes and air-dried. About 5-9 mg of each sample was weighed out and sealed into aluminum pans and stored in disposable scintillation vials until use, to avoid contamination. Before beginning the DSC scanning process the two furnaces of the calorimeter were cleaned by heating the system for about 30 min at 600 ^{o}C and then cooling back to 30 ^{o}C. This cleaning cycle was repeated until a uniform heat flow path was obtained. Two empty sealed pans were carefully placed in the reference and sample furnaces and allowed to equilibrate at 30 ^{o}C for 5 min before beginning the heating cycle. The two pans were heated from 30 ^{o}C to 210 ^{o}C, maintained at 210 ^{o}C for 2 minutes and then cooled back to 30 ^{o}C at a temperature ramping rate of 15 ^{o}C/min with Nitrogen as purge gas. The heat flow-temperature curve obtained with the two empty pans was recorded as the baseline. After obtaining the baseline heat flow data samples were scanned one after the other by replacing the

empty pan in the sample furnace and following the same heating/cooling cycles used to obtain the base line. During all the DSC scans an empty sealed pan remained in the reference furnace. All the samples were subjected to two heating/cooling cycles. The first cycle removes differences in the thermal history of the samples. So the data from the second cycle can be used for appropriate comparison of the various samples with baseline subtraction. The glass transition temperature (T_g) and the melting point temperature (T_m) were determined for all the blend films from their respective DSC curves. For the fibers produced by melt extrusion of H-PLLA/L-PLLA blends, the degree of crystallinity was determined from the respective enthalpy of crystallization (ΔH_c) and the enthalpy of fusion (ΔH_f) using the relationship:

$$\% \text{ Crystallinity} = \left(\frac{\Delta H_f - \Delta H_c}{\Delta H_f'}\right) \times 100 \qquad (2.3)$$

where $\Delta H_f'$=93.7 J/g is the enthapy of fusion of 100 % crystalline sample of PLLA [42].

2.10 Characterization of Fibers and Stents Made with Blended Polymers

Blends of H-PLLA and L-PLLA prepared in w/w ratios of 100:0, 60:40, 50:50, 40:60 and 0:100 respectively were selected to check the feasibility of fiber extrusion and stent fabrication. In order to melt extrude the blended polymer, films were cleaned with 70 % ethanol wipes and finely cut into small pieces of approximately 2 mm x 1 mm before loading them into the extruder as described in section 2.1.2.1. Because of the strenuous process involved in preparing particulates and extrusion into fibers only H-

PLLA/L-PLLA blends were selected for fiber production. Thus no studies of High//Intermediate PLLA blends were performed.

2.10.1 Mechanical strength of the blended fibers

2.10.1.1 Materials

The mechanical properties of the drawn fibers were measured using a tensile testing apparatus (INSTRON 5848 Microtester) equipped with a 1kN static load cell (Instron Corp., Canton, MA). Five samples of each fiber were tested at room temperature in unidirectional tension at an extension rate of 10 mm/min.

2.10.1.2 Methods

Each fiber was carefully mounted onto the magnetic clamps of the tensile testing machine using a hydraulic press and slowly tightened using the fine adjustment setting on the machine such that the length between the clamps was approximately 1 inch. The test specimen was then subjected to a constant strain rate of 10 mm/min until the specimen was broken. From the stress-strain curves the maximum strength was noted as the tensile strength of the fibers, the slope of the elastic region was noted as the Young's modulus and the maximal strain at which the fiber broke was noted as the breaking strain.

2.10.2 Fabrication and testing of stents

The feasibility of stent fabrication from blended fibers was tested by constructing stents using the Single-ply inner coil design: the Single ply design rather than the Two ply cross over design was chosen due to the limitation in the length of fiber available for fabrication. Some stent characteristics, like the expansion ratio,

intrinsic elastic recoil and hoop strength were determined using the same procedures described in sections 2.4, 2.5 and 2.6, with a sample size of 3.

2.11 Molecular Weight Determination

The molecular weight distribution of the PLLA blends was studied using the Size Exclusion Chromatography (SEC) technique. In SEC, the polymer being investigated is dissolved into a solvent and injected into a column containing porous packing material. The polymer molecules that are smaller than the pore size can selectively permeate into the particles in the column and take longer paths and longer times to elute than the long polymer chains that cannot enter into the particles. Thus the eluted fractions collected at different time points represent the quantities of the different sized polymer chains present in the synthetic polymer.

2.11.1 Materials

SEC was performed on a DX 500 High Performance Liquid chromatography (HPLC) system equipped with GP50 Gradient Pump, AD-20 UV-Vis absorbance detector and an auto sampling system (Dionex Corporation, Sunnyvale, CA). Chromeleon Chromatography Management System (Dionex Corporation, Sunnyvale, CA) was used to control the HPLC machine and to collect and analyse the data. Polystyrene standards (Supelco, Bellefonte, PA) were used to calibrate the JORDI GPC Mixed Bed Column (Altech Associates Inc., Deerfield, IL) with HPLC grade Chloroform as the mobile phase.

2.11.2 Methods

Choloroform was degasified by purging nitrogen for 40-50 min before using it as the mobile phase in the HPLC system. Immediately after degasifying the choloform bottle lid was sealed under pressure so as to prevent any air from mixing into the solvent. At every stage of the SEC process care must be taken to avoid air bubbles in the system tubing. The flow rate of the solvent was then set to 0.4 ml/min and the valve before the column was toggled so that the solvent flowing through the system is drained to the disposal container. This process was done to drain off any solvents and deposits from the previous use. After about 30 min the flow rate was reduced to 0.2 ml/min and the valve toggled so that the solvent was now flowing through the column and other tubing beyond the column. The solvent was allowed to flow through the system at this flow rate for about 2 hrs before increasing it to 0.5 ml/min. All the samples to be analyzed were prepared a day ahead at a polymer concentration of 1 mg/1 ml of chloroform with little shaking, in order to avoid shearing of the polymer molecules. The samples were carefully transferred to HPLC vials and arranged into the carousel of the auto-sampler; the Chromeleon program was then turned on. For SEC the mobile phase flow rate was set at 0.8 ml/min, the sample injection volume at 100 μL and the UV detector absorbance wavelength at 254 nm. The absorbance readings were recorded for 40 min for each sample starting from its injection time so as to allow sufficient time for the samples to come out of the column and not mix with the next sample. For each sample the absorbance (mAU) vs elution time (min) was recorded and later used to calculate number average (Mn) and weight average (Mw) molecular weights of the

samples relative to the molecular weights of polystyrene standards. In order to create a calibration curve, polystyrene standards of known molecular weights were prepared and run through the column in the same way as were the samples. A calibration curve was then obtained by plotting log molecular weight vs. elution volumes (molecular weight and molecular size relationship) using polystyrene samples data. The chromatograms of the samples were then edited so as to obtain just the absorbance peak and these peaks were converted to mAU vs molecular weight using the calibration equation and the average molecular weights of the samples were calculated using the relations:

$$Mn = \Sigma N_i M_i / \Sigma N_i = \Sigma W_i / \Sigma (W_i/M_i) = \Sigma h_i / \Sigma (h_i/M_i) \quad (2.4)$$

$$Mw = \Sigma N_i M_i^2 / \Sigma N_i M_i = \Sigma W_i M_i / \Sigma W_i = \Sigma (h_i M_i)/ \Sigma h_i \quad (2.5)$$

where W_i and N_i are the weight and number of molecules of molecular weight M_i , respectively, and i is an incrementing index over all molecular weights present. The last equation was actually used to calculate Mn and Mw from SEC chromatograms. Here h_i is the absorbance peak height at the ith volume increment and M_i the molecular weight of the species eluted at the i^{th} retention volume [43].

CHAPTER 3

RESULTS

3.1 Fabrication of the Two-ply Cross Fiber Stent

Figure 3.1 shows the picture of a typical Two-ply cross fiber stent manufactured using the fabrication technique described in the materials and methods section. A ruler with centimeters as major units and millimeters as minor units has been placed beside the stent to illustrate the small size of the Two-ply cross fiber stent. A typical Two-ply cross fiber stent was 12 mm in length with a total of 10 coil turns and had a diameter of 1.54 $\pm$ 0.02 mm (mean $\pm$ SD, n=5) in its unexpanded configuration. An enlarged view of the area circled in white is shown in figure 3.2 along with the identification of the different parts of the stent.

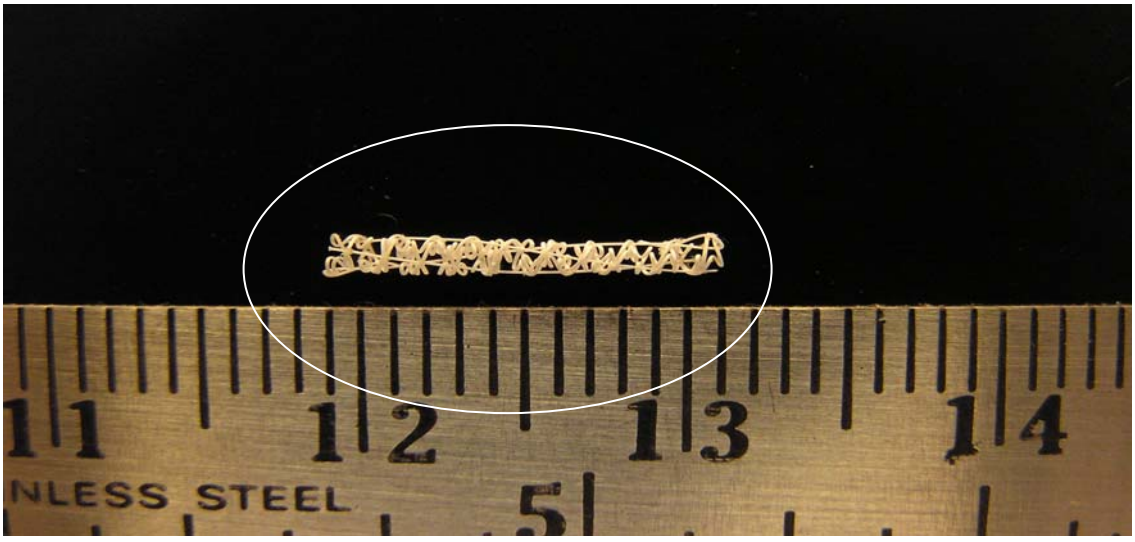

Figure 3.1 Two-ply cross fiber stent placed beside a ruler with millimeter markings

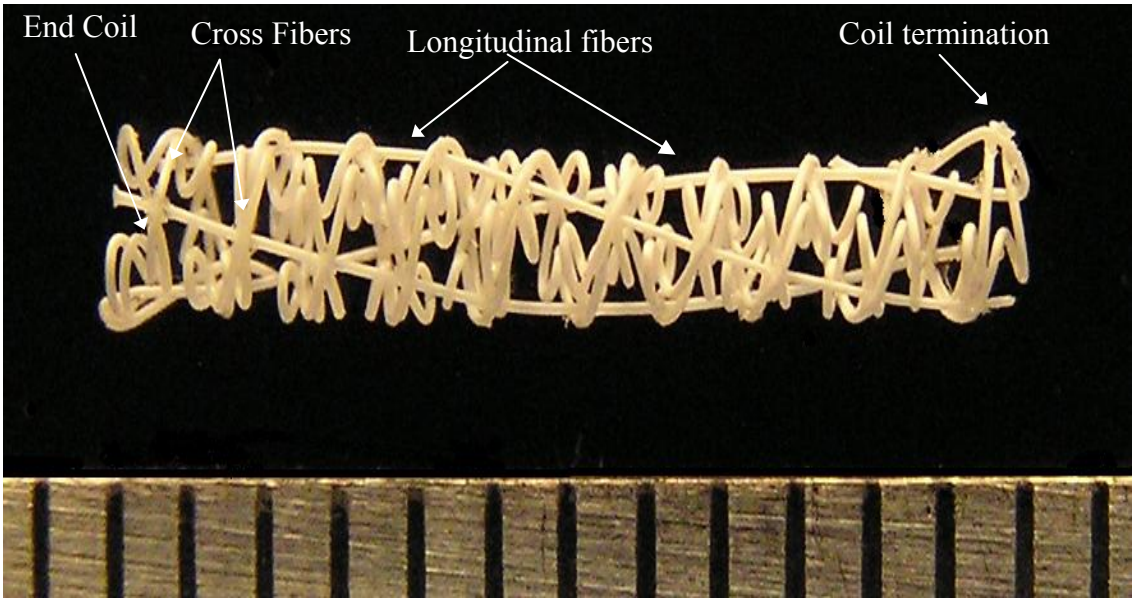

Figure 3.2 Two-ply cross fiber stent with identification of different parts

3.2 Design Integrity

3.2.1 Percentage Adhesion of Type-1 and Type-2 Glued Bonds

The glue bonds that help to adhere the longitudinal fibers to the helical fibers will be under stress during the process of balloon mounting of the furled stent as well as during its expansion. If these bonds are weak there is a chance that they may break, thereby risking the integrity of the stent. In order to test the adhesive strength of type-1 and type-2 glue bonds the stents were divided into two groups of 10 stents each. Each group had equal number of stents with type-1 and type-2 gluing.

Figure 3.3 shows a type-1 glue bond with a single glue fillet for bonding the two helical fibers onto the longitudinal fiber at the fiber cross-over point. Figure 3.4 shows a type-2 glue bond with two glue fillets to do the same.

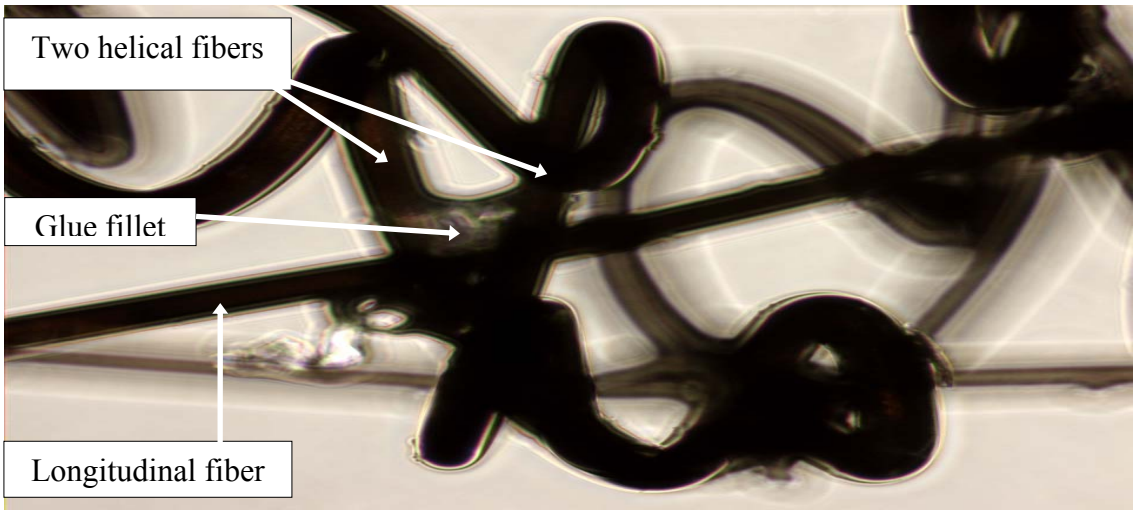

Figure 3.3 Type-1 glue bond with a single glue fillet

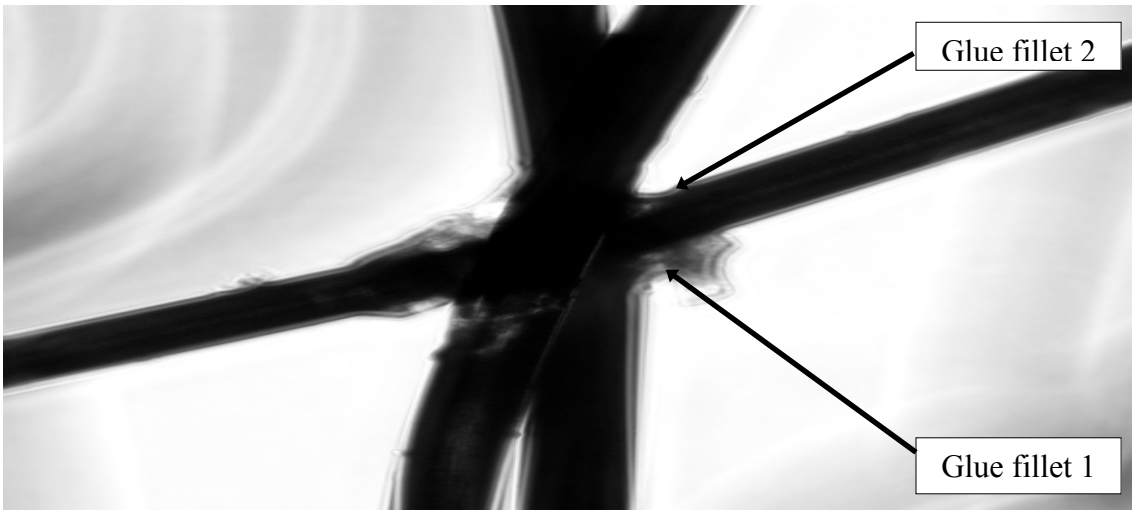

Figure 3.4 Type-2 glue bond with two glue fillets

In the unexpanded configuration it was observed that all the glued bonds were intact, irrespective of the type of gluing. After expansion, the percentage of glued bonds that remained intact was calculated as

$$\% \text{ Intact} = \frac{(\text{Total number of glued bonds} - \text{number of detached glued bonds})}{\text{Total number of glued bonds}} * 100 \quad (3.1)$$

It was observed that the stents in group 1, with type-1 gluing, had the lowest percentage of glued bonds that remained intact after expansion with a balloon catheter, 97.43%, Table 3.1. But this was not significantly different ($p>0.05$) from the 100% adhesion achieved with type-2 gluing in the same group. These were the very first stents fabricated after designing the two-ply cross fiber stent. Both type-1 and type-2 glue bonds were 100% intact in group 2. Since there was no significant difference between the two types of gluing techniques, type-1 gluing which uses a lesser amount of PLLA/Chloroform glue was chosen to fabricate all the Two-ply cross fiber stents used in the following experiments.

Table 3.1 Percentage of Intact Glue Bonds after Stent Expansion

Group	**Type of gluing**	**% Intact**
1	1	97.43
	2	100
2	1	100
	2	100

3.2.2 Lateral Spreading of Fibers

Figures 3.5 and 3.6 show the lateral spreading of the helical fibers upon expansion of the stent in air and inside a silicone rubber tube of slightly smaller diameter than the stent, respectively. All six stents used to study the lateral spreading of the helical fibers showed the same behavior. Since the vulnerable plaque lesions in the

arterial wall often have a thin fibrotic cap and are therefore prone to rupture, it is very important to reduce the compressive forces transferred from the expanding balloon onto vulnerable plaque during stent deployment. Lateral spreading of the stent helical fibers provides an axial gripping force, parallel to the vessel wall, that may reduce the compressive force necessary to secure the stent to the wall.

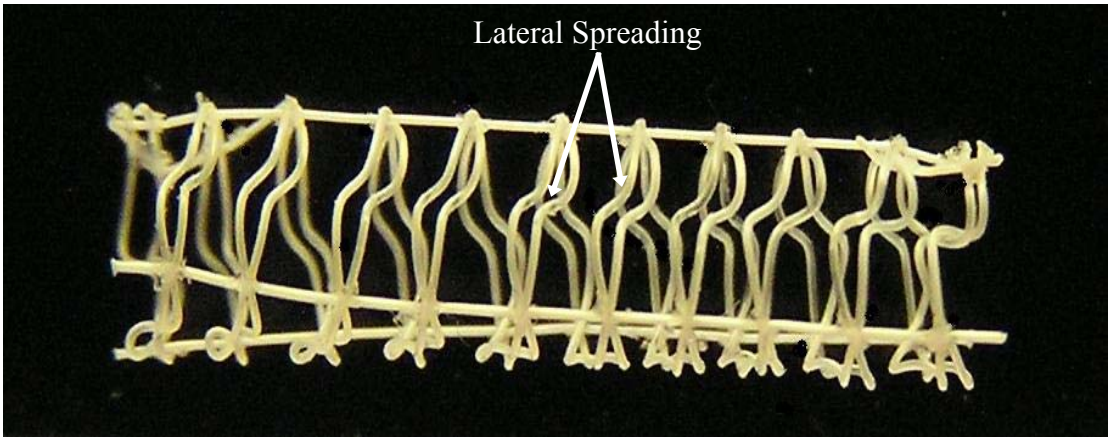

Figure 3.5 Lateral spreading of the helical fibers upon stent expansion

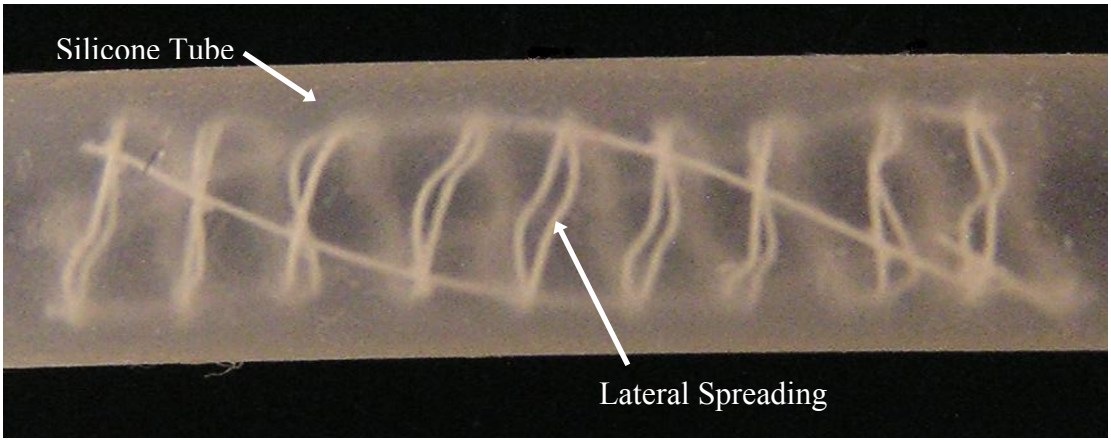

Figure 3.6 Lateral spreading of the helical fibers upon expansion inside a silicone tube

3.2.3 Percentage Foreshortening of the Two-ply Cross Fiber Stent

There was no change in the length, i.e, 0% foreshortening, of the stents after expansion from their furled state. The anchoring of the helical fibers to the longitudinal fibers using PLLA/Chloroform glue helped to prevent any possible change in length of the stent after expansion with an angioplasty balloon. Elimination of stent foreshortening for precise stent deployment is clinically important, especially near vessel intersections.

3.3 Pressure Required for the Expansion of the Stent

This study compared the changes in diameters of the Two-ply cross fiber stents and Single-ply inner coil stents with regular increments in inflation pressure. Both the Single and Two-ply stents follow the same pattern in their expansion with increasing inflation pressure, figure 3.7. The diameters of the two stents increased rapidly up to 3 atm inflation pressure, achieving about 96% of the total expansion, followed by very little changes upto 8 atm inflation pressures. Though they follow a similar trend in their expansion processes, the rate of expansion of the Single-ply inner coil stent is much higher than the Two-ply cross fiber stent. This difference may be attributed to the additional strain release required from the use of two PLLA fibers in the Two-ply cross fiber stent as compared to one in inner coil stents [49].

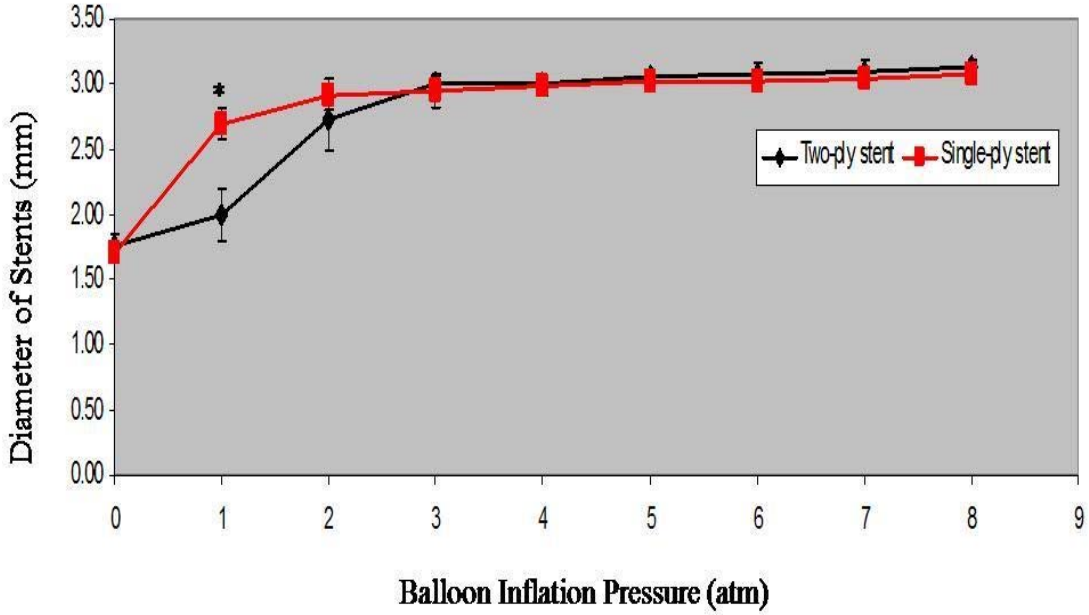

Figure 3.7 Changes in stent diameter with increasing balloon inflation pressure, n=6, mean ± SD, *p < 0.05

3.4 Expansion Ratios of the Stents

Optimal stent deployment requires complete apposition, e.g., that the stent/artery diameter ratio be equal to one. The inner coil design of the stent allows incorporation of extra fiber in the three peripheral lobes. Upon expansion of the stent using an angioplasty balloon the fiber will be gradually transferred from the peripheral lobes into the central lobe resulting in the formation of a single helical coil of a bigger diameter. Figure 3.8 shows the longitudinal views of furled and expanded Two-ply cross fiber stents placed beside each other.

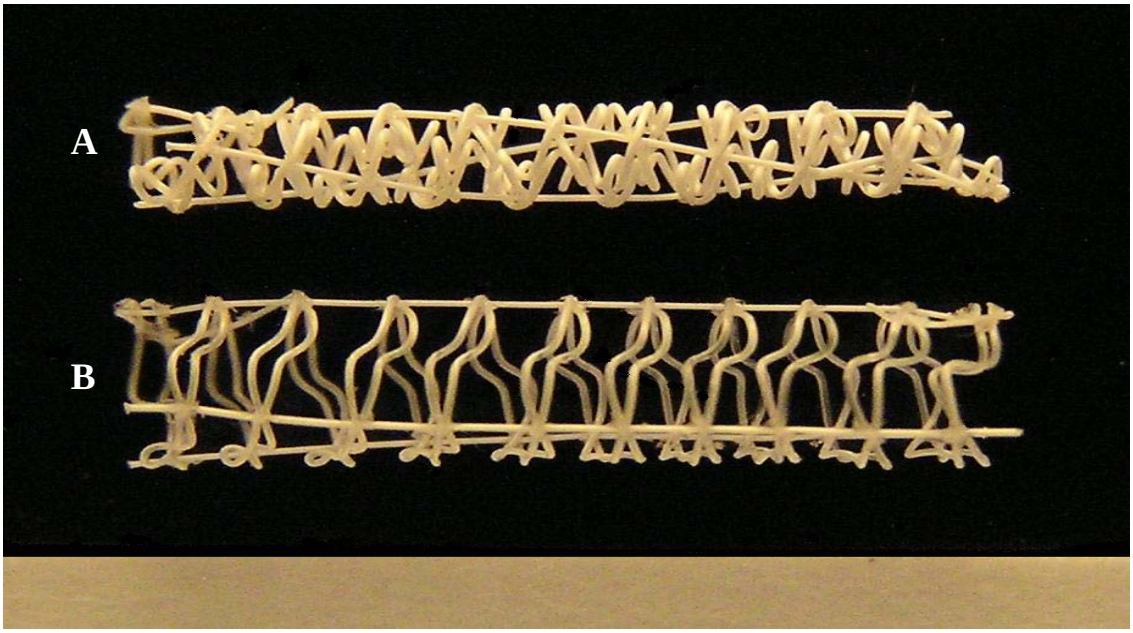

Figure 3.8 Longitudinal view of the Two-ply cross fiber stents (A) Furled stent (B) Expanded stent.

The diameter of the Two-ply cross fiber stent nearly doubled in size when the stent was expanded at a balloon pressure of 6 atm. The diameter of the stent increased on average from 1.54 $\pm$ 0.02 mm to 3.06 $\pm$ 0.08 mm (mean $\pm$ SD, n=5) after expansion. The stent expansion ratio, calculated as the ratio of the expanded diameter to the furled diameter, is 1.99 $\pm$ 0.06 (mean $\pm$ SD, n=5) for the Two-ply cross fiber stent.

The corresponding expansion ratio of the Single-ply inner coil stent is 1.90 $\pm$ 0.05 (mean $\pm$ SD, n=3). Though it is slightly lower than the expansion ratio of the Two-ply cross fiber stent, figure 3.9, it is not significantly different ($p>0.05$). Though the two designs differ in many ways, both of them use the coil-within-coil configuration to provide the length of extra fiber for expansion from the furled state.

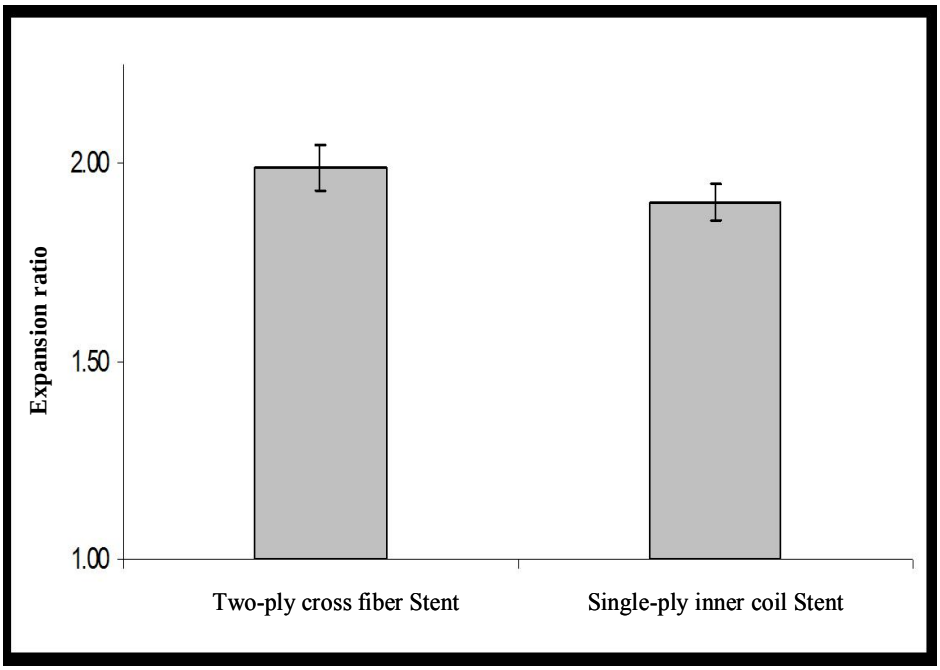

Figure 3.9 Expansion ratios of the Two-ply cross fiber stent (1.99 ± 0.06, n=5) and Single-ply inner coil stent (1.90 ± 0.05, n=3).

The expansion ratios of Single-ply inner coil stents fabricated with the fibers extruded from the different blends of high and low molecular weight PLLA are given in table 3.2. There is a slight, nonsignificant decrease in the expansion ratio, as the amount of high molecular weight polymer decreases and the amount of low molecular weight polymer increases, in the fiber used for stent fabrication.

Table 3.2 Expansion Ratios of the Stents Made With PLLA Blends, n=3.

Stent fiber composition High MW/ Low MW	**Expansion ratio (mean ± SD)**
100 / 0	1.90 ± 0.05
60 / 40	1.86 ± 0.06
50 / 50	1.85 ± 0.17

3.5 Intrinsic Elastic Recoil

During the process of expansion of the Two-ply cross fiber stents using an angioplasty balloon catheter it was observed that the stents had an average expanded diameter of 3.14 ± 0.09 mm (mean ± SD, n=5) as long as the balloon was held inflated. As soon as the balloon was deflated, the expanded stent diameter decreased, slightly, on average 3.06 ± 0.09 mm (mean ± SD, n=5). This reduction in the diameter of the stent immediately following deflation and removal of the angioplasty balloon is called the intrinsic recoil of the stent and is shown, exaggerated, in figure 3.10. It is supposed to be caused by to the elastic recoil of the material of the stent as well as the structural design of the stent. The percent recoil of the Two-ply cross fiber stent is 2.5 % and it is not significant ($p>0.05$) compared to the diameter of the stent over the balloon.

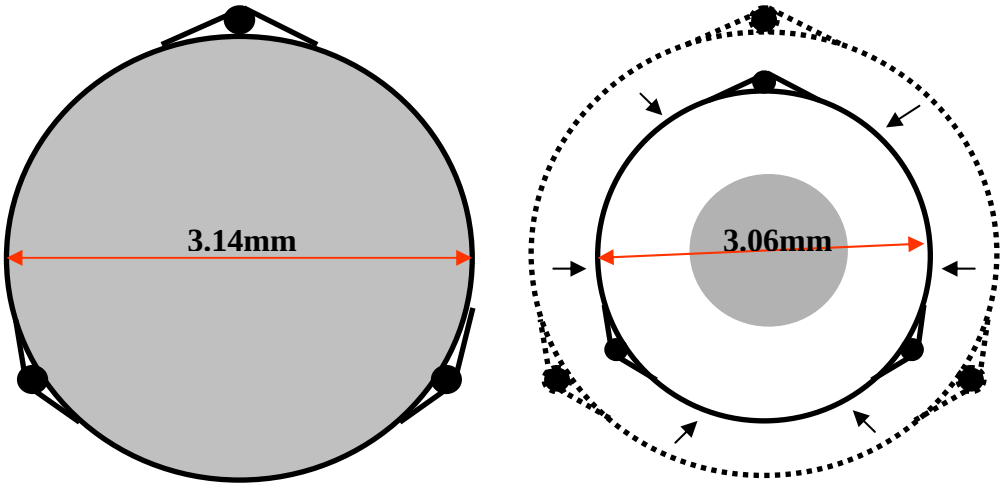

Figure 3.10. Intrinsic elastic recoil of the Two-ply cross fiber stent. (a) Maximum expanded diameter of the stent on inflated balloon. (b) Elastic recoil (enlarged) on deflation of the balloon

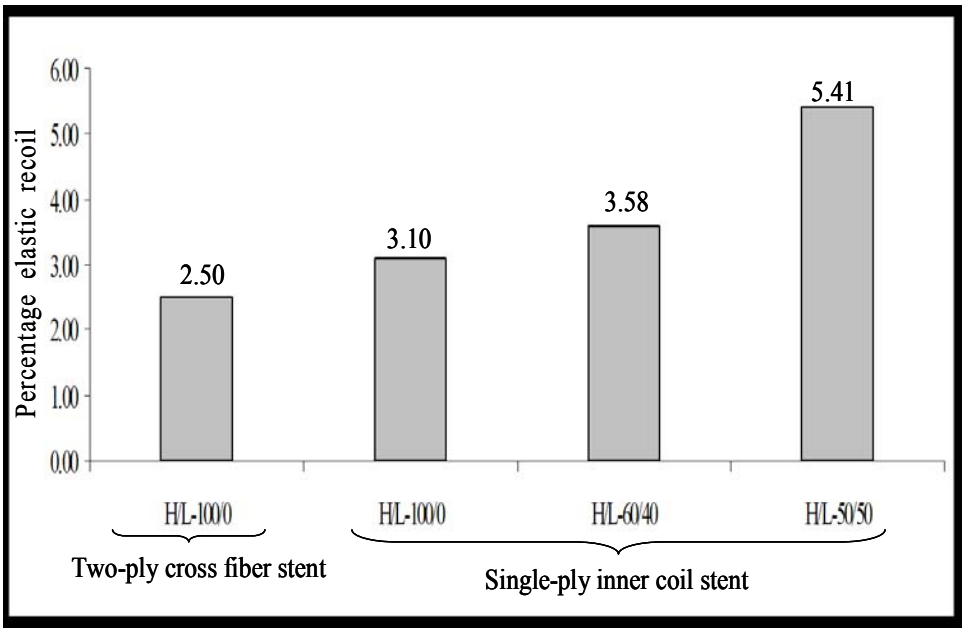

Figure 3.11 Percentage elastic recoil of the Two-ply cross fiber stent (H/L-100/0, n=5) and Single-ply inner coil stents of PLLA blends (H/L-100/0, H/L-60/40, H/L-50/50, n=3). H-high molecular weight PLLA; L-low molecular weight PLLA.

Figure 3.11 shows a comparison of the percentage elastic recoil of the Two-ply cross fiber stent and the Single-ply inner coil stents fabricated using fibers of H-PLLA and L-PLLA blends. The percentage elastic recoil of the Two-ply cross fiber stent (2.5 %) is lower than that of the Single-ply inner coil stent (3.10 %) made with the same high molecular weight PLLA fiber. Also the percentage elastic recoil of the Two-ply cross fiber stent is the lowest of all the stents compared in figure 3.11. Among the Single-ply inner coil stents fabricated using fibers of H-PLLA/L-PLLA blends the percentage elastic recoil of the stent with 100 % H-PLLA fiber is 3.10 %. As the percentage of H-PLLA decreases or conversely as the percentage of L-PLLA increases in the fiber composition the percentage elastic recoil is observed to increase from 3.10 (H/ L - 100/0) to 5.41 (H/ L - 50/50). The observed difference in the percentage elastic

recoil among the different stent types is not significant ($p>0.05$). Stents with lower elastic recoil would be able to maintain adequate apposition to the lumen without overly high deployment pressures.

3.6 Hoop strength measurements

As described in the methods section of the thesis, the hoop strength of the stent is measured in terms of the compressive pressure (psi) required to cause irreversible plastic deformation and collapse of the expanded stent. The hoop strength of the Two-ply cross fiber stent is 18.78 $\pm$ 2.73 psi (mean $\pm$ SD, n = 5). It is almost 250% higher than the hoop strength of the Single-ply inner coil stent made from similar PLLA fibers, which is 5.40 $\pm$ 0.71 psi (mean $\pm$ SD, n = 3), figure 3.12.

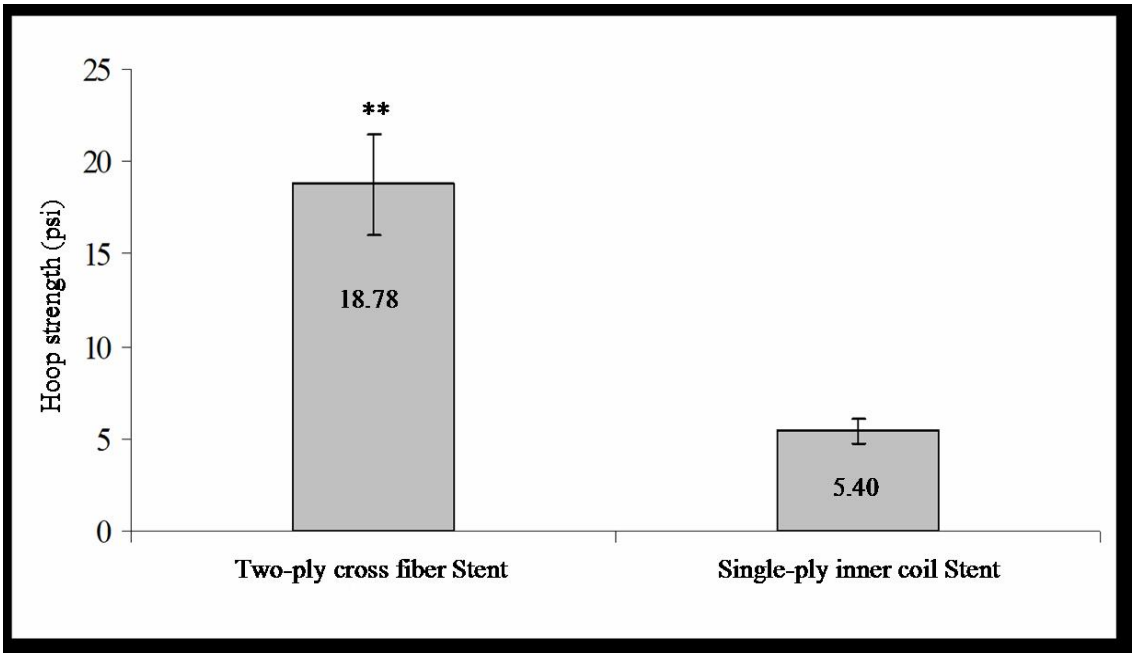

Figure 3.12 Hoop strengths of the Two-ply cross fiber stent and Single-ply inner coil stent. Numbers inside the bars denote mean hoop strength. **P < 0.001.

The hoop strength of the Two-ply cross fiber stent is also compared to that of the stents made from blended fibers of H-PLLA/L-PLLA. Though the fiber compositions were different, these stents were all fabricated using Single-ply inner coil design. The hoop strengths of all the stents fabricated using blended fibers are significantly lower when compared to the hoop strength of the Two-ply cross fiber stent, figure 3.13. Among the Single-ply inner coil stents it is observed that the hoop strength increases significantly, from 5.40 $\pm$ 0.71 psi to 13.77 $\pm$ 1.12 psi, as the amount of L-PLLA increases in the bulk of the polymer fiber.

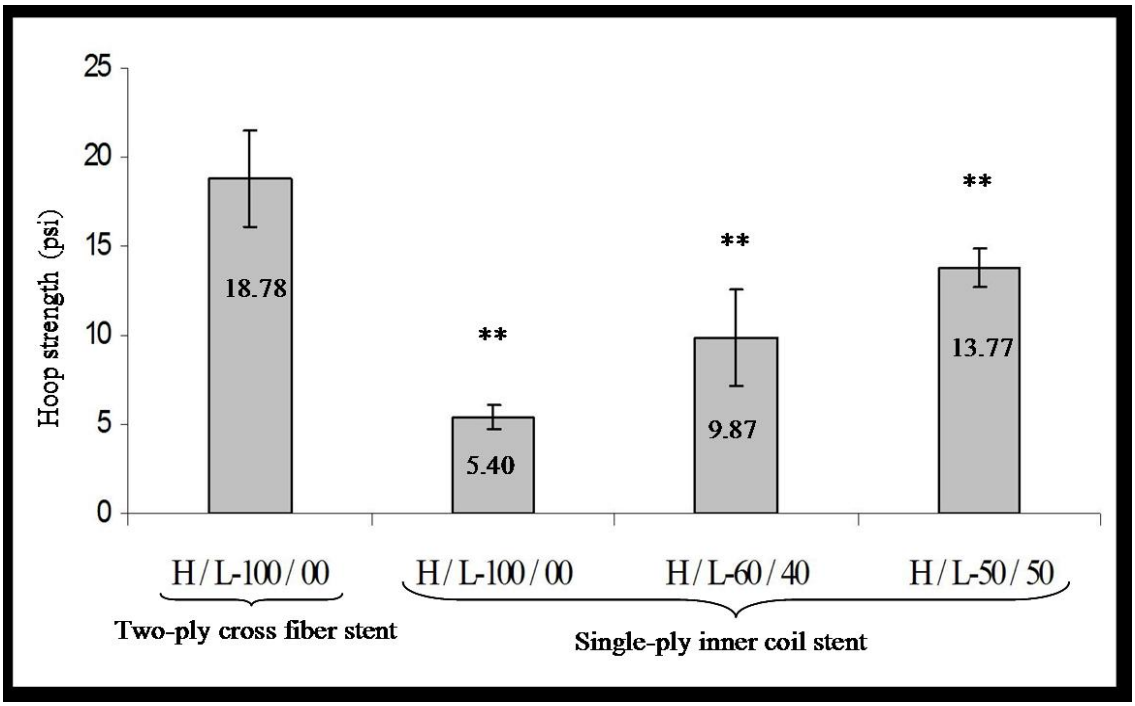

Figure 3.13 Hoop strengths of the Two-ply cross fiber stent (H/L-100/0, n=5) and Single-ply inner coil stents of PLLA blends (H/L-100/0, H/L-60/40, H/L-50/50, n=3). Numbers inside the bars denote mean hoop strength. H-high molecular weight PLLA; L-low molecular weight PLLA. **P < 0.001.

3.7 Longitudinal Flexibility of Stent

Good longitudinal flexibility is very important for navigation of long stents (>10 mm in length) than it is for shorter stents [39]. Hence for the flexibility measurements, all the stents were fabricated with an average length of 26 mm, figures 3.14 and 3.15. The stiffness, reciprocal of flexibility, of the Two-ply cross fiber stent is 1.86 $\pm$ 0.95 and 1.96 $\pm$ 0.92 gforce/mm in the furled and expanded configurations respectively. A typical Two-ply cross fiber stent is fabricated with 0.1 mm diameter fiber and a coil pitch of 1 turn/1.2mm whereas a typical Single-ply inner coil stent is fabricated with 0.1 mm diameter PLLA fiber and coil pitch of 1turn/1mm. Its stiffness is 1.48 $\pm$ 0.16 and 2.01 $\pm$ 0.16 gforce/mm (mean $\pm$ SD) in the furled and expanded configurations respectively. In the furled state the stiffness of the Two-ply cross fiber stent exceeds that of the Single-ply stent design ($p>0.05$). But when the two stent types are expanded to the same final diameter they do not vary in stiffness, figure 3.16.

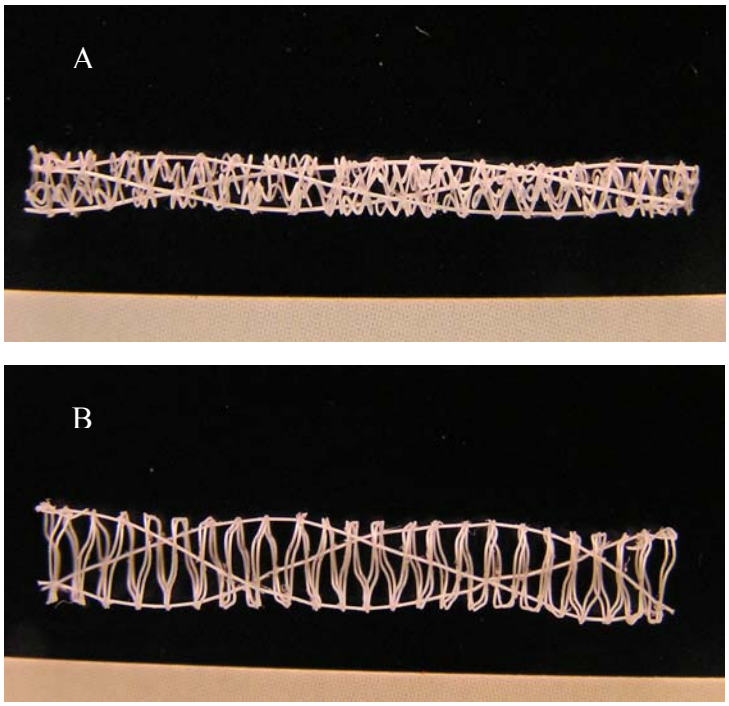

Figure 3.14 Two-ply cross fiber stent of 26 mm length (A) Furled and (B) Expanded in air configuration.

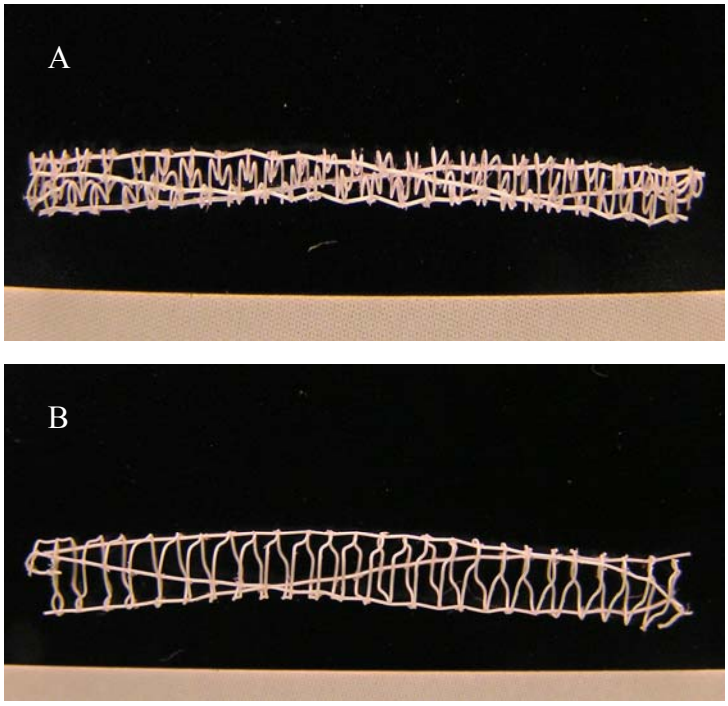

Figure 3.15 Single-ply inner coil stent of 26 mm length (A) Furled and (B) Expanded in air configuration.

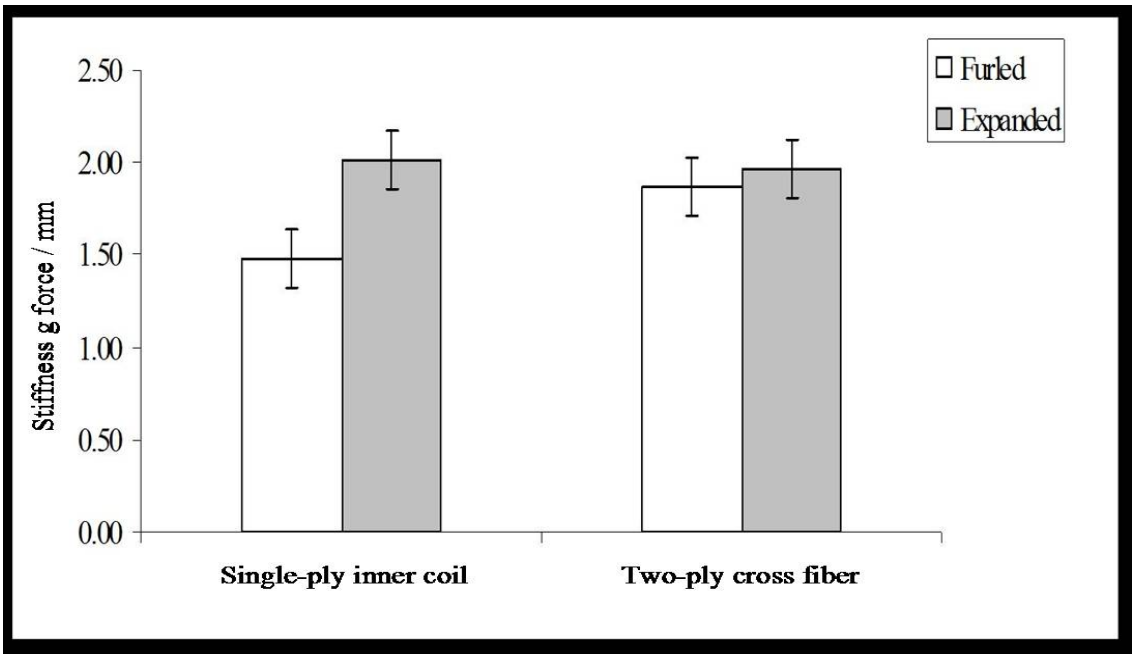

Figure 3.16 Stiffness of Two-ply cross fiber and Single-ply inner coil stent designs.

The effect of the stent configuration on its longitudinal flexibility is evaluated for both designs, figure 3.17. It is observed that the stiffness of the two stent designs is higher in the expanded configuration. This increase is especially significant for the Single-ply inner coil stent design ($p<0.05$) with an increase in the stiffness of about 35 % from furled to expanded state.

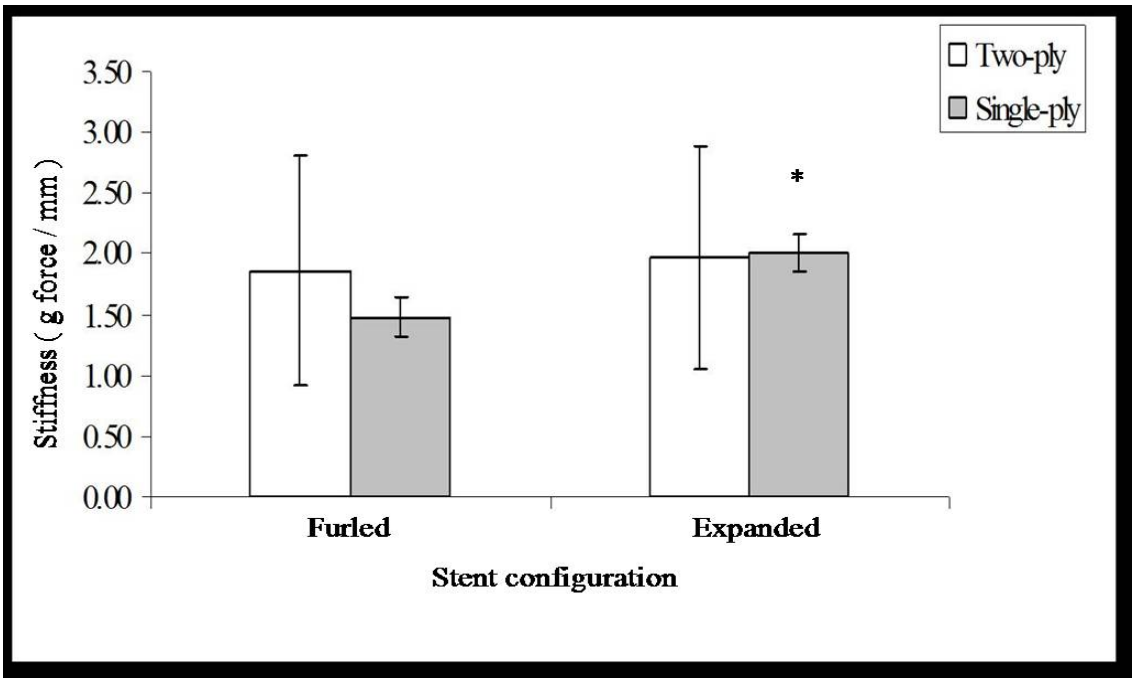

Figure 3.17 Effect of stent configuration on stiffness.*$p<0.05$

Both the Two-ply cross fiber and Single-ply inner coil stent designs allow choice of fiber diameter as well as coil pitch (stent length/number of coil turns) during the fabrication process. The effect of these two parameters on the stent longitudinal flexibility has been studied using Single-ply inner coil stents in the furled configuration.

To study the effect of variation in coil pitch on the longitudinal flexibility Single-ply inner coil stents were fabricated with the distance between coil turns ranging from 1 mm to 1.4 mm using 0.1 mm diameter PLLA fiber. From figure 3.18 it can be observed that as the coil pitch increases from 1turn/1mm to 1turn/1.4mm the stiffness of the stent drastically drops about 28 % from 1.48 $\pm$ 0.16 to 1.06 $\pm$ 0.29 gforce/mm (mean $\pm$ SD, n=3). Regression analysis performed to determine the linear association of stent stiffness and coil pitch yielded a Pearson's correlation coefficient of -0.9245. This

indicates a strong inverse relation between stent stiffness and coil pitch or conversely a strong direct relation between coil pitch and longitudinal flexibility, figure 3.18. When the coil pitch of the Single-ply inner coil stent was matched with that of the Two-ply cross fiber stent (1turn/1.2mm) it is observed that the former is more flexible than the latter, $p>0.05$ (1.12 ± 0.37 Vs 1.86 ± 0.95 gforce/mm) in the furled configuration.

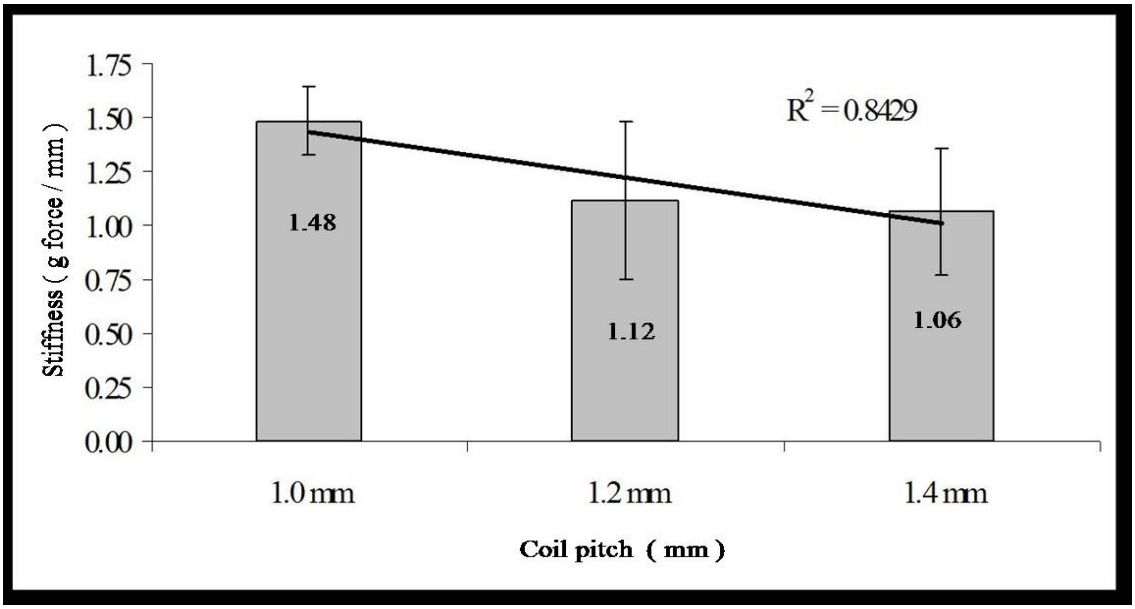

Figure 3.18 Effect of coil pitch on stent stiffness.

To study the effect of variation in fiber diameter on the stents longitudinal flexibility Single-ply inner coil stents were fabricated with PLLA fibers of 0.1 mm and 0.13 mm diameter while keeping a constant coil pitch of 1turn/1mm. It is observed that the stents made with 0.13 mm diameter fiber were significantly stiffer ($p<0.05$) than the stents fabricated with 0.1 mm diameter fiber with a stiffness of 2.23 ± 0.31 gforce/mm, figure 3.19.

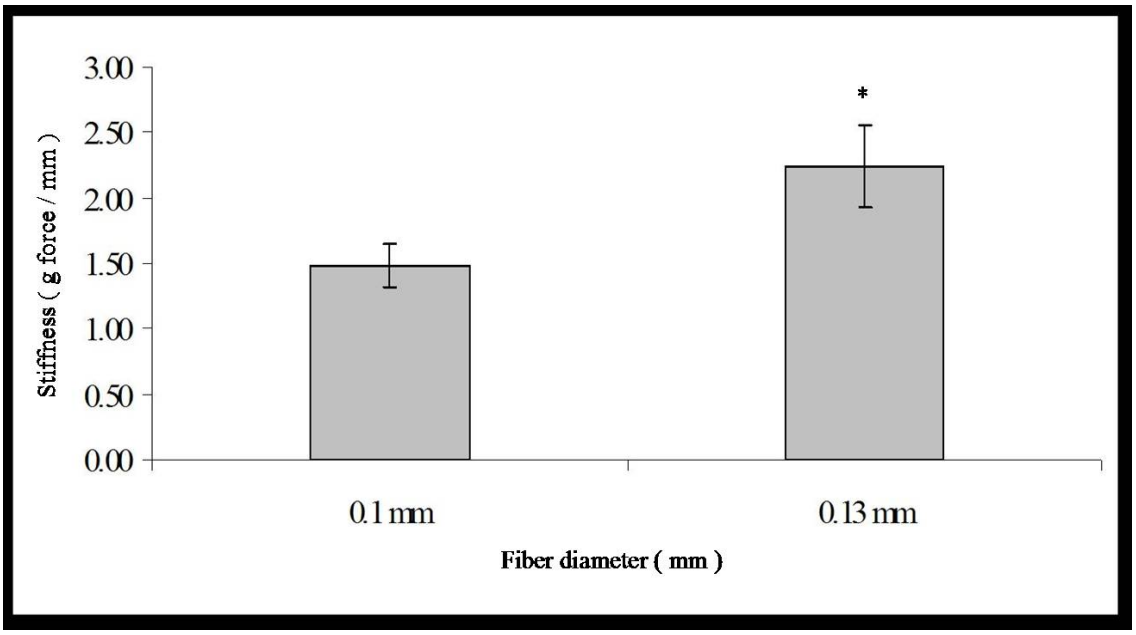

Figure 3.19 Effect of fiber diameter on stent stiffness. *p < 0.05.

Of all the stents tested, the Single-ply inner coil stent fabricated with 0.13 mm diameter fiber had the highest stiffness and the Single-ply inner coil stent with the coil pitch of 1turn/1.4mm had the lowest stiffness value.

3.8 Thermal Analysis of Blends

DSC was used to determine the thermal properties, like the glass transition temperature (Tg) and the melting temperature (Tm), for H-PLLA/I-PLLA and H-PLLA/L-PLLA blends prepared with w/w ratios of 100:0, 60:40, 50:50, 40:60, 0:100. Typical DSC thermograms of H-PLLA/I-PLLA blend films are shown in figure 3.20 and the corresponding thermal data are listed in table 3.3. It can be observed that the shape of the thermograms is similar for all the blend ratios. The spike in the H-PLLA/I-PLLA-0/100 DSC thermogram could be due to accidental addition of oils from the skin or any dust particles during the sample preparation process. A single glass transition

temperature was observed for both the blend types prepared indicating that the amorphous portions of the two polymers were miscible with each other. Both Tg and Tm remained almost constant for the blends prepared from different weight proportions of H-PLLA and I-PLLA, except for the slightly higher melting temperature of the 50/50 blend (183.1 ^{o}C), figures 3.21 and 3.22. The glass transition temperatures ranged from 57.31 ^{o}C to 58.31 ^{o}C and the melting temperatures ranged from 179.14 ^{o}C to 181.91 ^{o}C. However the blends of H-PLLA and L-PLLA demonstrated differences in thermal behavior, with changes in the proportions of high and low molecular weight PLLAs, table 3.4. Though the molecular weights of the two PLLAs differed significantly all the blends prepared with H-PLLA and L-PLLA demonstrated a single glass transition temperature similar to the blends of H-PLLA and I-PLLA. The Tg of pure L-PLLA was 50.48 ^{o}C and that of the H-PLLA was 58.31 ^{o}C. The glass transition temperatures of the blends 60/40, 50/50 and 40/60 however were around 53 ^{o}C, i.e., in between the Tg values of the two pure polymers making up the blend, figure 3.21. The DSC thermograms of H-PLLA/L-PLLA blends showed cold crystallization exotherms before their main melting endotherms, figure 3.23. The melting endotherms of both pure L-PLLA and 60/40, 50/50, 40/60 blends of H-PLLA/L-PLLA were not symmetrical like the melting endotherm for pure H-PLLA. In spite of the asymmetry, the peak melting temperatures decreased from 181.91 ^{o}C to 169.57 ^{o}C as the weight proportion of the H-PLLA decreased in the blend composition, figure 3.22.

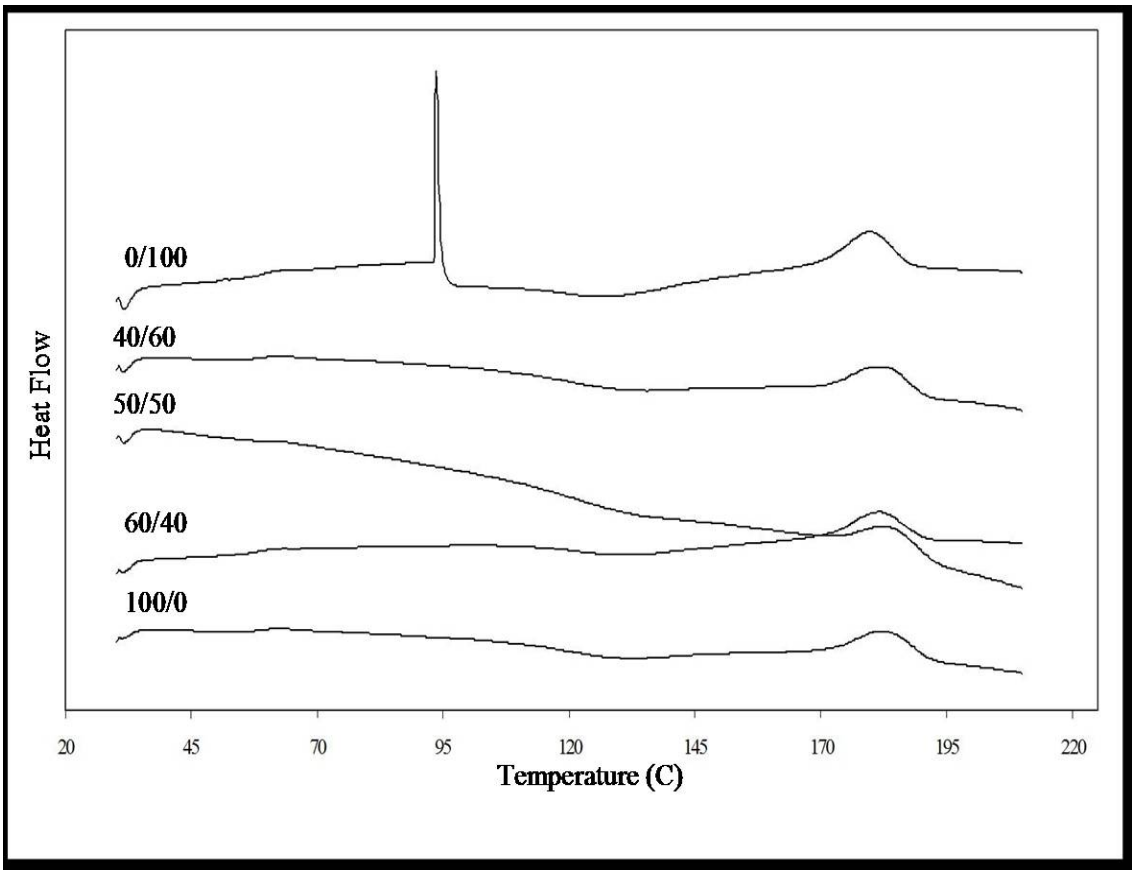

Figure 3.20. DSC thermograms of H-PLLA/I-PLLA blends. The curves are denoted by the w/w ratios of H-PLLA/L-PLLA indicated on the left.

Table 3.3 Thermal Properties of H-PLLA/I-PLLA Blends.

H-PLLA/I-PLLA	Glass transition, Tg (^{o}C)	Melting Temperature, Tm (^{o}C)
100/0	58.31	181.91
60/40	58.05	180.95
50/50	57.5	183.1
40/60	57.31	181.74
0/100	57.5	179.14

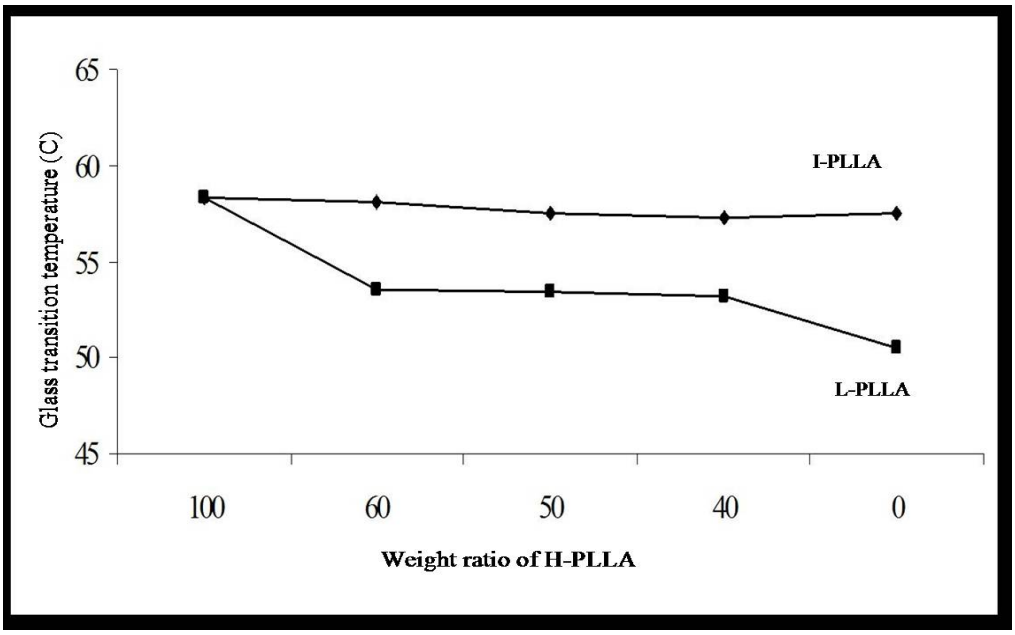

Figure 3.21 Glass transition temperatures of the blends of H-PLLA/I-PLLA and H-PLLA/L-PLLA.

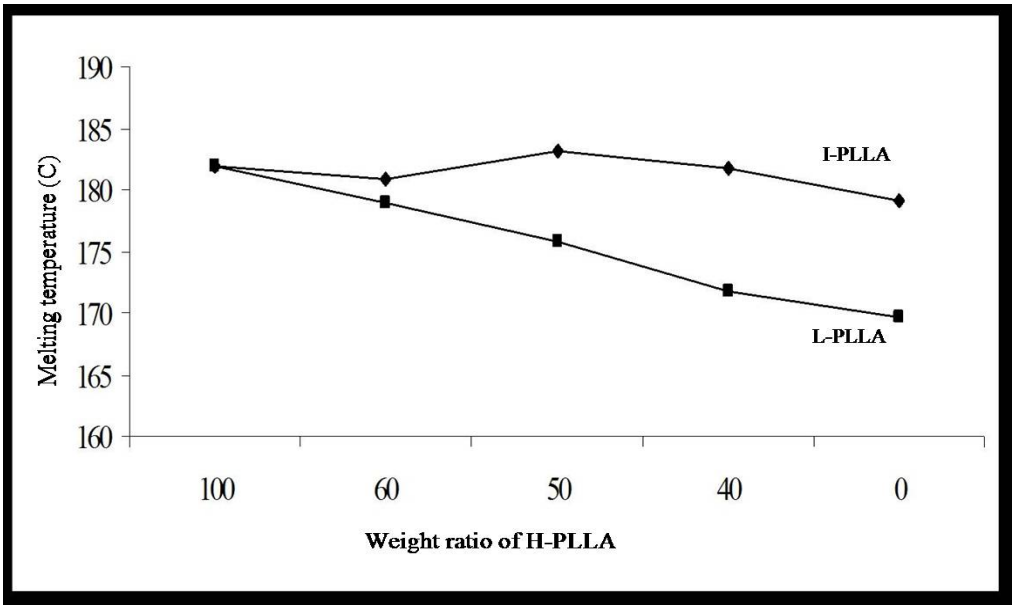

Figure 3.22 Melting temperatures of the blends of H-PLLA/I-PLLA and H-PLLA/L-PLLA.

Table 3.4 Thermal Properties of H-PLLA/L-PLLA Blends.

H-PLLA/L-PLLA	Glass transition, Tg (^{o}C)	Melting temperature, Tm (^{o}C)
100/0	58.31	181.91
60/40	53.52	178.88
50/50	53.4	175.72
40/60	53.13	171.8
0/100	50.48	169.57

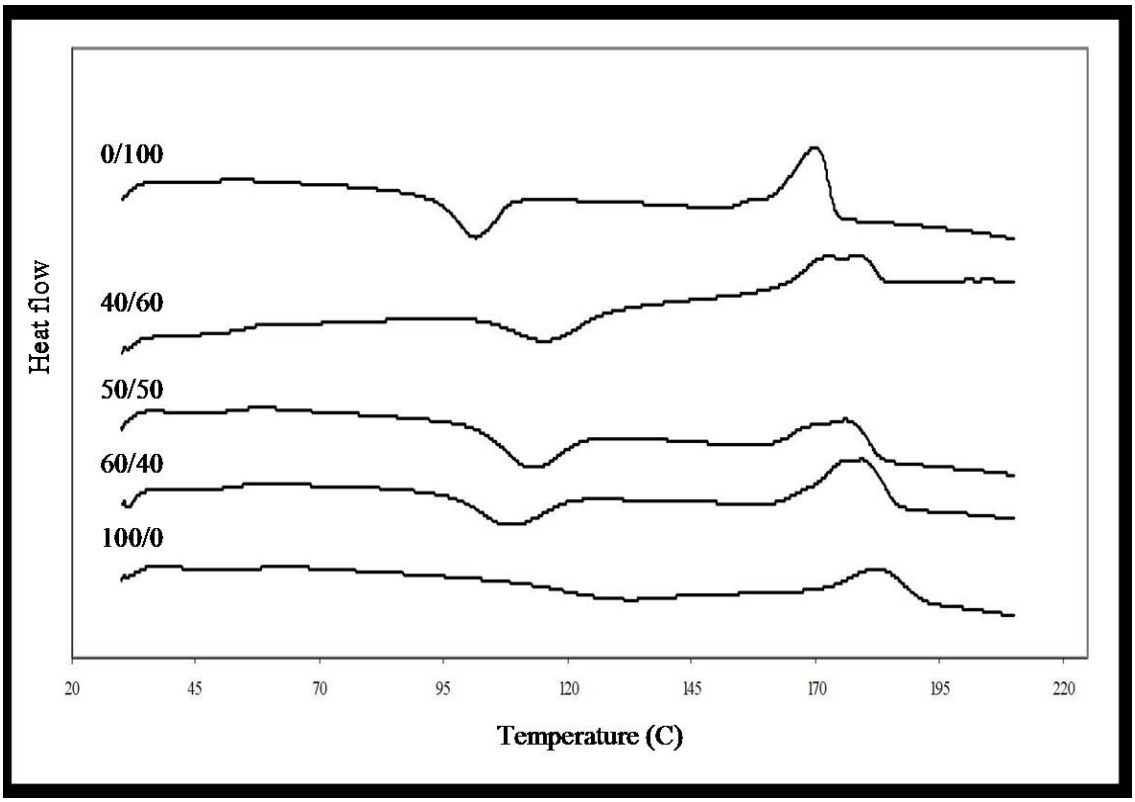

Figure 3.23 DSC thermograms of H-PLLA/L-PLLA blends. The curves are denoted by the w/w ratios of H-PLLA/L-PLLA indicated on the left.

Percentage crystallinities of drawn H-PLLA/L-PLLA fibers of ratios 100/0, 60/40 and 50/50 were also determined to see how the lower molecular weight polymer affects the crystallinity of the blended fiber. It was observed that the crystallinity of the fiber made with a 50/50 ratio of H-PLLA/L-PLLA was higher than the crystallinity of

the fiber made with a 60/40 weight ratio (67.11 % vs 54.37 %), indicating that the lower molecular weight component is helping to increase the % crystallinity of the blended fiber. H-PLLA was observed to have lower crystallinity, compared to the two blended polymers (28.83 %). Unlike the fibers from blends, the thermogram of pure H-PLLA had a cold crystallization exotherm before its melting peak, figure 3.24.

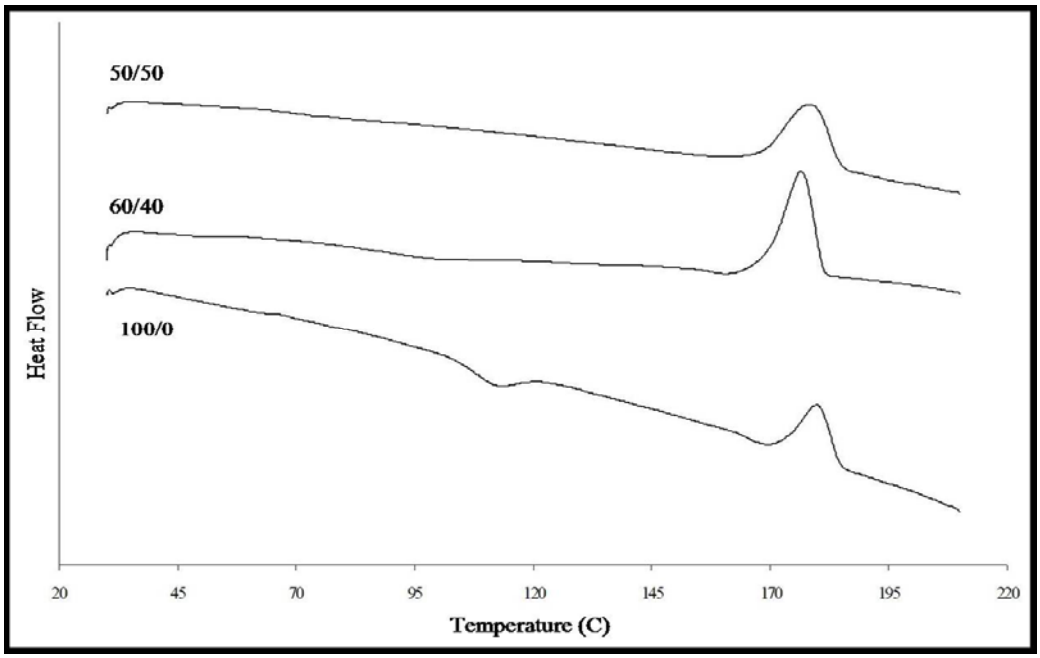

Figure 3.24 DSC thermograms of H-PLLA/L-PLLA fibers. The curves are denoted by the w/w ratios of H-PLLA/L-PLLA depicted on the left.

3.9 Mechanical Characterization of Blend Fibers

Since the DSC data on the melting temperatures of the binary blends was not available during this mechanical test, the feasibility of producing fibers from blends of H-PLLA and L-PLLA was checked using random temperature settings on the extruder. Using this technique, nice fibers could be manufactured from 100/0, 60/40 and 50/50

blends but not from 40/60 and 0/100 blends. Since the L-PLLA control fiber could not be obtained, all the results involving blend fibers are interpreted only with respect to H-PLLA.

During the tensile testing process, one of the 50/50 fibers broke near the clamps. So the data obtained with this sample was not considered in the calculation of the Young's modulus, ultimate tensile strength and percentage strain at break. Hence the sample size was reduced to 4 for the H-PLLA/L-PLLA blend with 50/50 weight ratio. The tensile properties of all the fibers tested are listed in table 3.5. Though not statistically significant, it was observed that the ultimate tensile strength is highest for the H/L-100/0 blend (193.77 $\pm$ 29.30 MPa) and decreased gradually as the amount of H-PLLA decreased in the fiber composition to 148.45 $\pm$ 37.74 MPa for H/L-50/50 fiber. On the other hand, the percentage strain was highest for H/L-50/50 fibers and lowest for the H/L-100/0 fiber indicating higher ductility in the presence of L-PLLA in the fiber composition. The modulus of elasticity of the H/L-60/40 fiber was the highest among all the fibers tested (8046.28 $\pm$ 942.17 MPa). There were significant differences in the modulus of elasticity for the different fiber blends ($p<0.001$).

Table 3.5 Tensile Properties of H-PLLA/L-PLLA Blend Fibers

H-PLLA/L-PLLA	Youngs Modulu's (MPa)	Tensile Strength (MPa)	Strain (%)
100/0	8046 $\pm$ 942	194 $\pm$ 29	10.2 $\pm$ 2.6
60/40	9853 $\pm$ 861	187 $\pm$ 28	13.2 $\pm$ 4.3
50/50	4727 $\pm$ 650	148 $\pm$ 38	13.4 $\pm$ 5.7

The determination of molecular weights using SEC yielded results that were beyond any reasonable interpretation. Since they seemed to contradict the basic size exclusion phenomenon of SEC they have been included in the appendix section.

CHAPTER 4

DISCUSSION

4.1 Design and Dimensions and Material of the Two-ply Cross Fiber Stent

The implantation of stents following percutaneous transluminal coronary angioplasty (PTCA) has become a common practice in hospitals around the world. With increasing evidence showing that the rupture of arterial wall vulnerable plaque is a major cause of ominous cardiac events like myocardial infarction or sudden cardiac death, a lot of effort is being directed towards the development of imaging and treatment modalities focusing on this issue. One postulate is that stabilization and passivation of the vulnerable plaque using appropriate pharmaceutical agents could help in reduction of the ACS [44]. Stent-based local drug delivery systems are attractive in this regard, in theory, because they may provide sufficient luminal patency while also hastening the stabilization process by delivering sufficient amounts of therapeutic agents via constant tissue contact over a prolonged time period. However the current series of drug eluting stents have recently been shown, in intravascular ultrasound (IVUS) studies, to fail to appose the vessel wall, either immediately upon deployment, or gradually to lose contact over a period of months [45, 46]. Apposition failure might be counteracted by applying higher balloon expansion pressure and volume, to force the stent against the arterial wall. However this would act in opposition to the desire to protect the fragile fibrotic cap over vulnerable plaque lesions, the higher compression

force promoting cap rupture. This dilemma may be usefully addressed with the bioresorbable stent design of this thesis, providing a stent with large drug reservoir capacity, lower expansion pressure, lateral fiber spreading to maintain stent grip on the wall and sufficient hoop strength to avoid recoil and collapse.

The Two-ply cross fiber stent design has been developed in order to accommodate these features, including gentle implantation at the fragile vulnerable lesion sites. This is a biodegradable coil type stent fabricated using two PLLA fibers, for sufficient hoop strength, wound in a criss-cross fashion. The design features include the helical coil feature with three peripheral loops and a central loop, as developed by Su [44] with the peripheral loops wound inside the central loop as developed by Satasiya [40].

4.1.1 Profile and Dimensions of the Stent

The Two-ply cross fiber stent design uses the coil-within-coil configuration to wind the peripheral lobes and central lobes, and this helps to obtain a small diameter profile in the furled state, as observed (1.54 $\pm$ 0.02 mm). Though this design varies significantly from the inner coil stent [40] in the fiber weave pattern and fiber ply, the diameters of the two stents are not very different (1.54 $\pm$ 0.02 mm vs 1.51 $\pm$ 0.03 mm) in the furled state. This may be because the two designs use the same diameter fibers (0.10 mm) and both are wound with the peripheral lobes inside the central lobe. Another method of explaining this is possible by considering the weaving pattern of the two designs above and below the longitudinal fibers. In our Two-ply stent design the two fibers go criss-cross above and below the longitudinal fiber, while in the earlier

inner coil design a single fiber goes above and below the longitudinal fiber alternatively; thus the final profile is same in either case. The stent design and fabrication technique allows sufficient flexibility to increase or decrease the stent profile as required, just by changing the size of the central mandrel used during stent fabrication. Winding peripheral coils inside the central coil instead of external to it (as in the outer coil design) also helps indirectly, by these axially inclined coils increasing the grip of the furled stent on the angioplasty balloon catheter, thereby reducing the chance of stent dislodgement during navigation.

The stent length is considered to be an independent predictor of in-stent restenosis [47]. In a study using the Magic Wallstent, the angiographic restenosis rate increased from 22.6 % for a 20 mm stent to 67.5 % for a 43 mm long stent. Multivariate analysis revealed that the stent length was independently associated with greater angiographic restenosis and adverse events [48, 3]. In another study by Dietz et al, short stents (<10 mm) were implanted either directly, or after balloon angioplasty only into that part of the lesion where the residual stenosis was greater than 30%. They found that in nearly 60% of these cases, it was feasible to use shorter stents and that the restenosis rate was low in the shorter stent group (15.6%) compared to the longer stent group (18.9%) [49]. Also, the treatment of in-stent restenosis in long stents is often difficult, and bypass surgery might be the only option in case of severe restenosis [3]. The length of a typical Two-ply cross fiber stent in our study is 12 mm and thus falls into the short length category. However the design of the Two-ply cross fiber stent is sufficiently flexible that increases or decreases in length can be made as required.

4.1.2 Lateral Spreading of Helical Fibers

As noted, the design of the stent should allow gentle implantation in the vicinity of the vulnerable plaque in order to lessen the chance of fibrotic cap rupture. In principle, spreading of the helical fibers in the axial (lateral) direction during stent expansion helps to minimize the compressive forces transmitted from balloon onto the plaque surface, and may also provide stabilizing lateral forces on the vessel wall (at microscale), analogous to the lateral forces (at nanoscale) that enable the gecko foot pad to support a substantial load on a vertical wall, figure 4.1. When the Two-ply cross fiber stent was expanded to completion inside a silicone rubber tube mimicking the arterial wall, lateral spreading of helical fibers along the tube wall was observed for all the specimens tested.

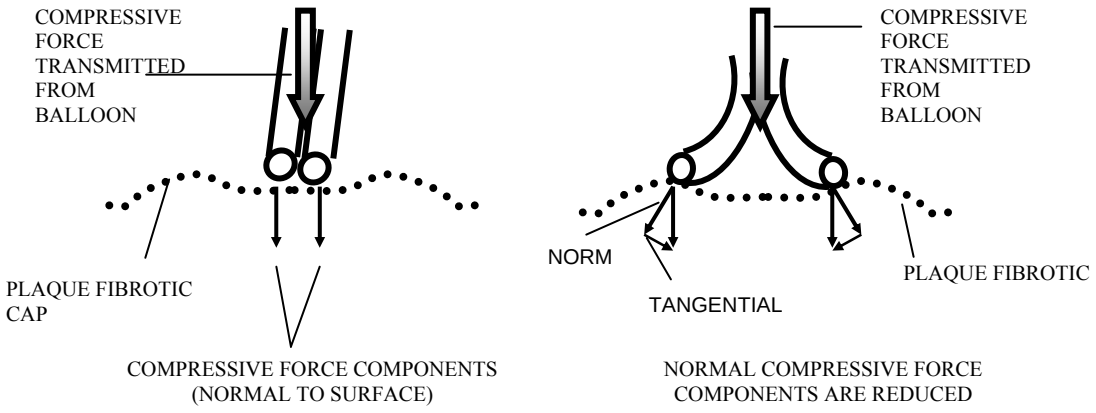

Figure 4.1 Spreading of helical fibers. (A) Stiff metal stent fibers resist spreading, (B) More flexible polymer stent fibers spread laterally.

The spacing among the coils suggests that the design allows very good side branch access after deployment. Many metal stents suffer structural deformation when exposed to side branch balloon dilation. But in the case of the Two-ply design, the PLLA fibers, being more flexible and not malleable, may retain the desired shape, or may recover from balloon-induced distortion of the stent structure. Side branch access and protection are critical when the side branch is large and the runoff subtends a large amount of myocardium [50].

4.1.3 Longitudinal Fibers and Design Integrity

The longitudinal fibers attached to the periphery of the stent at 120º intervals play a critical role in maintaining the integrity of the design. If this structure were to be dismantled from the stent jig without bonding of these axial fibers to both orthogonal plies, the whole structure would fall apart. Furthermore, these longitudinal fibers define and stabilize the criss-crossing pattern in the design. In addition, the longitudinal fibers add to the hoop strength of the expanded structure, which might otherwise collapse under increased pressure. The longitudinal fibers also increase the scaffolding strength of the stent by distributing the load more evenly throughout the coil structure. Another advantage of the longitudinal fibers is that they prevent stent foreshortening upon expansion by anchoring the helical fibers at the glue bonds. Most of the coil-type metal stents were fashioned more like open coil springs, with large gaps between adjacent elements. This type of design was reported to cause tissue prolapse into the gaps [51]. With the Two-ply cross fiber design the presence of longitudinal fibers at 120^{o} intervals adds significantly to the resistance to tissue prolapse. The lateral spreading of helical

fibers also helps to reduce the gaps between adjacent elements, thereby providing more uniform surface area coverage, which in turn helps to reduce tissue prolapse.

4.1.4 Substrate for Multiple Drug Loading

One major advantage of using PLLA fibers to fabricate the stent is that the polymer fibers can serve as drug reservoirs. This permits loading of higher doses of drugs than is available via polymer coating on metal stents. In the 12 mm Two-ply cross fiber stent, two ~ 15 cm PLLA fiber plies are used to fabricate the main coil, and three small fibers (~ 12 mm) are used as longitudinal reinforcing fibers. At ~ 10 % w/v loading (the case for Curcumin), a significant drug supply can be provided that permits ~zero-order kinetics for well over one month, with residual delivery expected for much of the stent lifetime [44]. Furthermore, more than one type of pharmaceutical agent can be loaded into various stent fibers. For example one fiber could be loaded with a lipid-lowering drug; another with an anti-inflammatory agent, and the concentrations of these drugs adjusted as required. Furthermore, the polymer might comprise a blend of differing PLLA molecular weights; the drug release kinetics could be adjusted by altering the molecular weight of the PLLA that is used to extrude the fibers. For example, a low molecular weight PLLA allowing fast release and a high molecular weight PLLA providing prolonged release. Such a combination of low and high molecular weight PLLA fibers might allow required drug release kinetics while providing sufficient mechanical strength.

4.2 Pressure Required for the Expansion of the Stent

Most of the vessels with angiographically significant stenosis are dilated using angioplasty balloons at pressures >10 atm to compress the obstructive plaque. In case the residual diameter stenosis is >30 % stent implantation is carried out using balloon inflation pressures > 12 atm [3, 52]. High inflation pressures are used with metal stents to obtain adequate stent expansion and thereby prevent subacute stent thrombosis [53, 54]. Research over the years has yielded contradicting results regarding the long-term results of high inflation pressures for stent placement. Retrospective angiographic studies in humans indicated that the use of high implantation pressure might result in more than 30-58 % lumen loss when compared to low implantation pressure application [52]. On the other hand in a prospective study, Dirschinger et al found no difference in clinical event rate, minimal lumen diameter or restenosis rate between the high and low pressure implantation techniques [55]. Though there is a controversy revolving around the use of high implantation pressures the main point of using high inflation pressures is to obtain large minimal stent cross sectional area. The Two-ply cross fiber stent achieves adequate expansion at very low inflation pressures. About 96% of the expansion, including lateral spreading, occurs with just 3 atm inflation pressure; complete expansion is achieved at about 4-5 atm. Also the use of low inflation pressures will have little or no traumatic effect on the vessel wall. This feature is especially important when the stent is being considered for implantation in vessels with vulnerable plaque. Since these lesions are not, in many cases, angiographically significant, it may be difficult to detect the vulnerable plaque with current imaging equipment. The recent

introduction of IVUS, with virtual histology capability to image the wall mechanical properties, promises to change this situation. Thus it may become possible to know when greater compressive forces from the inflating balloon are not required. On the other hand the thin fibrotic cap also forbids the use of excessive compressive and shear stresses during stent implantation. The implanted stent is required either to stabilize the plaque by providing a protective seal over the fibrotic cap or to passivate the plaque by delivering therapeutic agents. The advantages of the low pressure Two-ply cross fiber design suggest that it can be placed with less danger of rupture of vulnerable plaque lesions, with loading of higher amounts of multiple drugs as discussed earlier.

4.3 Elastic Recoil and Expansion Ratio

A large minimal stent cross sectional area post-intervention is observed as an important predictor of low restenosis and target vessel revascularization rates [52, 4]. This means that a stent designed to optimize expansion ratio and lower percentage elastic recoil can lead to favorable clinical results [4]. When a stent is placed inside a stenotic artery it is expanded to achieve a diameter close to the desired final lumen diameter of the vessel. During the expansion process of the Two-ply cross fiber stent, the fiber woven into three small peripheral lobes gradually unfolds and converges into the central lobe converting the stent cross section into a single large circular coil. As observed with most of the balloon expandable coronary stents, the diameter of the stent decreased about 2.5% from 3.14 $\pm$ 0.09 mm to 3.06 $\pm$ 0.09 mm within seconds following the deflation of the balloon under the influence of intrinsic elastic recoil. The internal elastic recoil depends both on the material and its mass as well as the three

dimensional structure of the stent design [56, 57]. This may be the reason for the difference in the percentage elastic recoils of the Two-ply cross fiber stent and Single ply inner coil stent (2.5% vs 3.1%). Though they are made with the same high molecular weight PLLA fibers of 0.1 mm diameter, they differ a lot in their three dimensional structural designs. Another reason for the variation in elastic recoil, as well as stent expansion pressure, may have to do with the details of the permanent set induced at the site of inner coil conversion to outer coil loop. As shown in the recent MS thesis of Tré Welch [58], there is a local torsional stress induced in the stent fiber, immediately prior to full conversion of the inner coil, that exceeds the torsional yield point, leading to plastic deformation. The plastic deformation sets the stent diameter without need for further treatment (heating or locking). There may be variance in the "set" conditions, however, that might allow torsional remodeling, and thus introduction of elastic recoil. When comparing the stents made with the low (L) and high (H) molecular weight PLLA blends it is observed that as the percentage of the H-PLLA content decreases, or conversely as the percentage of the L-PLLA content increases, the percentage elastic recoil increases from 3.10 (H/ L - 100/0) to 5.41 (H/ L - 50/50). Though all of these stents were fabricated using the Single-ply inner coil design the properties of the material constituting the stent were different from one and another including molecular weight, material mass and fiber diameter. The diameters of the fibers were 0.1 mm, 0.15mm and 0.2 mm for H/L-100-0, H/L-60-40 and H/L-50-50. Though all the fibers were extruded using the same spinneret their diameters could not

controlled because of limiting drawing ratios. It can be observed that as the diameter increased the percentage elastic recoil also increased accordingly.

In a comparative study using several stent types, Barragan et al showed that the rate of restenosis could be correlated to the elastic recoil of the coronary stents [56, 59]. When the percentage elastic recoil of the stent is high it may dictate the use of compensatory elastic recoil pressure in addition to the normal inflation pressures or large balloon sizes to get adequate expansion during its deployment [4, 56, 57]. The use of high inflation pressures in turn causes undesirable effects like severe wall injury, incisions or ruptures on the arterial wall as noted in the previous section. High elastic recoil may also disturb the flow pattern and cause thrombus formation [60, 61].

The percentage elastic recoil greatly influences the final expansion diameter or expansion ratio of the stent. The expansion ratio of the Two-ply cross fiber stent is slightly higher than that of the single-ply inner coil stent (1.99 ± 0.06 vs 1.90 ± 0.05). The two designs use coil within coil configuration to provide the extra length of fiber required for expansion from the furled state and the length of this extra fiber is same in both designs due to the use of same size mandrels for winding peripheral lobes. So the slightly higher percentage elastic recoil of the single-ply inner coil stent design may have contributed to the lower expanded diameter compared to the Two-ply cross fiber stent. Similar effect of elastic recoil on expansion ratio was observed in the Single-ply inner coil stents made with PLLA blends. The stent made with H/L-50-50 had the highest percentage elastic recoil (5.41%) and the lowest expansion ratio (1.85). The expansion ratio can be increased by increasing the size of the mandrels used for winding

peripheral lobes. The final deployment diameter of the stents is determined partly by the intrinsic elastic recoil and partly by the compressional forces from the stenosed artery wall [57].

4.4 Hoop strength measurements

The hoop strength measures the ability of a stent to withstand the various radial compressive forces from the arterial vessel wall and provide sufficient scaffolding support and luminal patency. The various compressive forces that a stent might experience in vivo include elastic recoil of the atherosclerotic plaque, residual stress of the non-diseased arterial wall, active contraction of smooth muscle within the media, and transmural pressure differentials [62]. A high hoop strength minimizes the recoil of the stent due to these compressive forces and thereby helps to maintain larger minimum lumen diameter (MLD). A large MLD might prevent the need for post-implantation high pressure dilations which may result in clinical complications as discussed above [63, 64]. High radial strength plays a critical role when the stent is implanted in complex lesions, such as strongly calcified stenoses and occlusions.

The Two-ply cross fiber stent had the highest hoop strength (18.8 $\pm$ 2.7 psi) of all the stents studied. Its hoop strength exceeded that of the Single-ply inner coil stent design by a significant 250% though they are made of the same material. This difference in the hoop strengths of the two stent designs could be due to several reasons. During the compression process it was observed that the two fibers anchored between two longitudinal fibers tended to spread apart wider in the lateral direction as the magnitude of radial compressive pressure increased. With the Single-ply inner coil

design there was very little observable change in the gap between the helical coils. However, in the latter design it was observed that all the coils were compacted in the same direction with increasing compressive pressure. Su has reported that fiber-ply and coil density have a direct effect on stent resistance to collapse under compressive pressure [43]. Though the fiber ply is greater for the Two-ply stent its coil density was lower than that of the single-ply stent. This lower coil density helps to optimize the stiffness vs hoop strength relationship. Another reason for the increased strength may relate to the previously described torsional set of the fibers: this may be greater in the two ply configuration, thereby increasing strength. This subject is being explored further in the doctoral studies of Mr. Welch. Others have also observed material influences on hoop strength. Venkatraman et al observed that stents produced from same molecular weight PLLA had higher hoop strength when the load bearing surface area was increased [65]. It is possible that increase in coil density and fiber-ply result in higher hoop strengths due to increased surface area of the stent. In this regard the Two-ply cross fiber stent has the highest surface area of all stents tested due to the use of two fibers instead of one and its longer length. The total mass of the stent determined by its design, length, strut thickness and material was also found to have a direct contribution to its hoop strength [66, 64, 2]. In the case of stents made with fibers of different compositions of H-PLLA/L-PLLA the mass per unit length of stent increases from 0.0016 g/cm (H/ L - 100/0) to 0.0051 g/cm (H/ L - 50/50) due to increase in fiber diameter from 0.1 mm to 0.2 mm respectively. Increase in fiber diameter will also result in increase in the load bearing surface area of the stent. The stents with the

greatest material mass and surface area had the highest hoop strength among the Single-ply inner coil stents studied.

The magnitude of the compressive forces that a stent would experience after its deployment is not established. Agarwal et al have determined the maximal arterial strain that could be created by a severe coronary spasm. Combining their results with those obtained from animal trials and by incorporating a safety margin 5.8 psi was established as a minimum acceptable limit for collapse pressure in coronary stents [67]. This minimum acceptable limit was lowered to 4.35 psi when Rieu et al, comparing the radial forces of 17 metal coronary stents without any history of partial or total collapse in clinical setting, found that none of the stents showed significant deformation upto this compressive pressure [68]. In a recent thesis of biomechanics, Teppaz has evaluated the mean value of radial constraints imposed on the stent by four 3.5-mm arteries, as 3.626 psi [56, 69]. Since the hoop strengths of all the stents tested exceed these pressures it might be supposed that when implanted all these stents will provide sufficient luminal patency and scaffolding.

4.5 Longitudinal Flexibility

Longitudinal flexibility is an important property of the stent in both furled and expanded configurations. Higher flexibility allows stent to bend easily at vessel turns and thereby reduce/avoid vessel irritation during its delivery. Upon expansion a flexible stent can conform to the vessel contour and thereby have beneficial effects on flow dynamics due to reduced turbulence. Longitudinal straightening of vessels after deployment of rigid stents has been associated with late ischemic events [70]. Not many

studies have investigated the effect of longitudinal flexibility on restenosis. Fontaine et al reported that rigid stents developed greater neointima formation than flexible stents in a 5 week swine model [71]. The stiffness (reciprocal of flexibility) of all the stents tested in furled state ranged from 1.06 to 2.23 gforce/mm. Ormiston el al compared the stiffness of 13 currently available stents using a similar experimental technique. They have reported that the stiffness of these stent designs ranged from 0.5 to 91.5 gforce/mm in their unexpanded states [39]. It can be observed that the stiffness of the evaluated stents falls well within the lower end of the reported values leading to the conclusion that the evaluated stents have very good longitudinal flexibilities.

In the furled state the Two-ply cross fiber stent is stiffer than the Single ply inner coil stent design. The use of two fibers considerably reduces the open space between individual coils and the increased total stent mass also may have contributed to the increased stiffness. Upon expansion with equal balloon inflation pressures the stiffness of both the Single and Two-ply stents increases over their furled state but this increase is small in Two-ply stent compared to that of the Single-ply inner coil stent. This could be because of a difference in the magnitude of stresses and strains experienced by the fibers during the expansion process. Due to their resistance to expansion the fibers of the Two-ply stent experience lower stresses and strains whereas a large portion of the fiber mass of the Single-ply stent may be plastically yielded because of greater overall strains, which increase its rigidity and hence bending stiffness. Though the two stent designs have similar stiffness in their expanded states the hoop strength of the Two-ply inner coil stent is significantly higher than that of the

Single-ply inner coil stent making it more attractive. The change in coil pitch from 1 turn/1.0mm to 1 turn/1.4mm has significantly increased the flexibility of the Single ply inner coil stent. There was a strong correlation between coil pitch and flexibility. The increased spacing between the coils creates a more open strcuture which makes it act more like a spring. When the coil pitch of the Single ply inner coil stent was matched with that of the Two-ply cross fiber stent it was observed that the stiffness had dropped almost 25% leading to an increased difference in the longitudinal flexibilities of the two stent designs in the furled state. A small increase in the fiber diameter to 0.13 mm from 0.1 mm has resulted in a significant 50% increase in stiffness of the stent. This might partially explain the increase in hoop strengths of the Single ply inner coil stents made with higher diameter fibers from H-PLLA/L-PLLA blends. Another important design aspect, spiraling of the longitudinal fibers due to torsional preloading could have positively contributed to the longitudinal flexibilities of both Single and Two-ply stents. The effect of spiraling on longitudinal flexibility needs to be tested in future.

4.6 Thermal and Mechanical Analysis of Blends

The DSC thermograms of both H-PLLA/I-PLLA and H-PLLA/L-PLLA blends exhibited a single glass transition temperature indicating that the amorphous portions of the two components are miscible with each other [72]. Since the two polymers used for making the blend are both PLLAs there are no repulsive/cohesive forces among the polymer chains leading to phase separation. The changes in the glass transition temperature are negligible, about 1 ^{0}C, among the various blends of H-PLLA and I-PLLA. Similar trend was observed in the melting temperatures of these blends. The

molecular weight of H-PLLA is ~380 kD and that of I-PLLA is ~300 KD. Since both have a high molecular weight and the difference among their molecular weights is < 100 kD it is highly probable that the length of their polymer chains is very similar except for a fraction of them in the H-PLLA. Because of the closeness of the length of polymer chains the amorphous and crystallite structure of the H-PLLA/I-PLLA blends is not affected to a great extent leading to similar glass transition and melting temperatures. However in the case of 50/50 blend formulation it could have happened that during the blend formulation some of the polymer chains formed larger crystallites which required higher temperatures to uncoil and mobilize.

The thermal behavior of the binary blends of H-PLLA and L-PLLA was very different from that of H-PLLA/I-PLLA blends. The glass transition temperatures of all three blends 60/40, 50/50 and 40/60 were around 53 ^{0}C, independent of the proportion of the L-PLLA in the polymer composition. This represents a decrease of about 5 ^{0}C in the Tg compared to that of the 100% H-PLLA. The molecular weight of H-PLLA is ~380 kD and that of L-PLLA is ~100 kD. Unlike the previous blend system there is a significant difference in the molecular weights of the two polymers. Addition of L-PLLA must have resulted in a significant increase in the amorphous component of the blend leading to a corresponding decrease in the Tg. All the blends containing L-PLLA exhibited cold crystallization exotherm beyond Tg and an asymmetric melting peak. Beyond Tg the mobility of the polymer chains increases and this might have resulted in the alignment of some of the amorphous segments into a crystalline structure [73]. There is a gradual decrease in the melting temperature of the blend with increased

proportion of L-PLLA. The presence of an increased number of chain ends might result in more chain ends being included in crystallites, altering their surface free energy and thereby affecting their melting temperature [72]. The asymmetry in the melting temperature could be due to the coexistence of crystallites of two different sizes one rich in 100 kD PLLA and the other rich in 380 kD PLLA. Von Recum et al reported the presence of crystallites of two types, small and large, in the blends of 8/83 kg/mol PLLA using optical microscopy [74]. The recrystallization process observed when the H-PLLA/L-PLLA blends were heated beyond their Tg's might have resulted in the formation of smaller crystallites that were not incorporated into the larger crystallites of H-PLLA. These have a lower Tm than the crystallites rich in H-PLLA [72]. Hence the asymmetry in the melting peak might be because of the difference in the melting temperatures of the two different crystal sizes present in the blend. However it should be noted that the impurities of L-PLLA could have affected the thermal and mechanical behavior of the blends and fibers containing L-PLLA. Due to problems in SEC measurement it was not possible to analyze the polymer for impurity content.

The H/L-100/0 fiber drawn to 5:1, H/L-60/50 fiber drawn to 4:1 and H/L-50/50 fiber drawn to 4:1 were compared to each other to see the effect of low molecular weight PLLA on fiber crystallinity. The drawing ratio could not be increased beyond 4:1 for 60/40 and 50/50 fibers without significantly increasing the temperature of the heat plate. From the data on Tg and Tm of the films of H-PLLA/L-PLLA blends it was observed that the added L-PLLA had a direct effect on amount of the amorphous portion of the fiber. It is easier for small polymer chains to untangle and align along the

axis than the long polymer chains when drawn at temperature slightly above Tg. The high percentage crystallinity of 50/50 fiber could be due to the high proportion of small polymer chains compared to the other fibers. The cold crystallization exotherm observed with H-PLLA indicate the uncoiling and crystallization of some of the tangled polymer chains which could not be aligned at the draw ratio of 5:1. Higher drawing ratios might untangle and align all the long polymer chains axially and increase the crystallinity in case of high molecular weight polymers. When comparing fibers of high molecular weight PLLA drawn to increasing draw ratios it was observed that the percentage crystallinty increases with increase in the draw ratio [75]. It should be noted that the H-PLLA fiber sample used in the crystallinity studies was from a new batch and these fibers were not used in any of the other studies involving H-PLLA fibers. This fiber had to be used because the fiber from the previous batch was over. Unlike the fiber from the previous batch this fiber was observed to be more brittle and fragile indicating very little crystallization during the fiber extrusion process.

If being considered for loading curcumin by a melt extrusion process, the polymer should have a melting temperature $\leq$ 175 ^{0}C. The melting point of curcumin ranges from 175-183 ^{0}C depending on its purity, so an extrusion temperature $\leq$ 175 ^{0}C ensures that the curcumin is not subjected to thermal degradation, which might affect its potency. Based on the thermal data of the blend systems considered, H-PLLA/L-PLLA blends from 0 % to 50 % of L-PLLA component would be preferred choices. During the random temperature extrusion of fibers from H-PLLA/L-PLLA blends, about 12-13^{0}C higher temperatures than the actual Tm of H/L-0/100 and H/L-40/50 polymers were

used. These higher temperatures must have resulted in the thermal degradation of the polymer hence yielding only molten polymer droplets instead of nice fibers.

The high molecular weight and higher drawing ratio of the H-PLLA might be responsible for its high tensile strength and low percentage strain compared to the fibers of H/L-60/40 and H/L-50/50 blends. All the fibers exhibited ductile failure under constant strain, which is the preferred mode of failure for fibers used for stent fabrication. A brittle fiber makes winding and expansion of the stent very difficult. Increased amorphous portion due to low molecular weight component seemed to increase the ductility. The H/L-60/40 fiber was tougher than the other two fibers due to a higher elastic modulus but exhibited similar ductility beyond its yield strength.

4.7 Molecular Weight Measurements

The values of the Mn and Mw of the blends calculated using the calibration data from polystyrene standards yielded very low values. The retention times and volumes of the PLLA samples were very high compared to the equivalent molecular weights of the polystyrene standards. These unexpected results could be due to several reasons:

1. The interaction of the two polymers with the packing material of the column is not identical. The large retention volumes of samples suggest that the packing material of the column is not inert to PLLA, i.e, either adsorption or absorption, or both, are occurring within the column. According to Yau et al, increased retention volume of solutes indicates the influence of surface effects on the SEC mechanism.

2. The hydrodynamic volumes may not be identical for polystyrene and PLLA in chloroform. The difference in the retention times could be due to differences in the molecular coil dimensions obtained by the polymers in chloroform. Small retention volumes indicate that the chains are too large to permeate the pores of the column. On the other hand large retention times, in theory, imply a small coil dimension that may permit permeation of the pores of the column.
3. The theta temperature of polystyrene/chloroform may be different from PLLA/chloroform. Near the theta temperature the solvent is less effective in preventing polymer solute molecules from adsorbing to the packing surface. Hence it is possible that polystyrene is favored in the solvent phase and PLLA is favored on the stationary packing material at room temperature.
4. μ-Styragel columns are not compatible for storage in chloroform and tetrahydrofuran. The material of the column was not disclosed by the manufacturer, but it is possible that the column was stored in chloroform after the previous use.
5. Contaminants, the nature of solvent polarity, pH and ionic strength all have significant effects on the inertness of the material of the packing. It could be possible that the appropriate solvent was not used, or that water from the tubing of the HPLC instrument was passed through the column, accidentally, from the previous use [76, 77].

CHAPTER 5

CONCLUSIONS

- The objectives of the thesis were to develop a biodegradable stent with a large drug reservoir capacity, lower expansion pressure and sufficient hoop strength for applications at fragile vulnerable plaque lesion sites, and to develop and characterize suitable binary PLLA blends for this application, both thermally and mechanically. The Two-ply cross fiber stent design has been developed in order to accommodate these features, including anticipated gentle implantation at the fragile vulnerable lesion sites, and the feasibility of its fabrication has been demonstrated. Binary PLLA blends were prepared in various proportions of 380/300 kD and 380/100 kD molecular weight PLLAs.
- The unique design feature of the stent, axial spreading of helical fibers during expansion, in principle, helps to minimize the compressive forces transmitted from balloon onto the plaque surface, and may also provide stabilizing lateral forces on the vessel wall.
- The stent has an average furled diameter of 1.54 $\pm$ 0.02 mm, length 12 mm and expanded diameter of 3.06 $\pm$ 0.09 mm. The profile of the stent in both furled and expanded configurations is similar to many metal stents currently used in clinical practice. Both short and longer length stents can be fabricated.

- The use of two PLLA fibers to fabricate the stent not only increases the drug reservoir capacity of the stent but also allows the incorporation of more than one agent onto the stent (this remains to be tested in future).
- An inflation pressure of 4-5 atm is sufficient to completely expand the stent. The major advantage of this is that the Two-ply cross fiber stent may be placed with less danger of rupture of vulnerable plaque lesions.
- The hoop strength of the stent, 18.8 $\pm$ 2.7 psi, was significantly improved by the use of two-ply fibers. This increased hoop strength did not seem to have a significant effect on stent longitudinal flexibility.
- Though it was developed for delicate deployment in vulnerable plaque lesions the good mechanical properties of the stent indicate it can be used as a scaffolding device in lesions of other complexities.
- Blended fibers of 380/100 kD were produced and the feasibility of fabricating stents using blended fibers was demonstrated for a single ply stent design, due to limited availability of fiber. Results showed that the one-ply design had lower expansion ratio, hoop strength and higher elastic recoil than the two ply stent design; nevertheless, the concept of blended fiber stents was validated.
- Mechanical testing showed a decrease in tensile strength, and increase in percentage strain, with an increasing proportion of the low molecular weight component in the PLLA blend.
- Thermal characterization of the blends indicated that 380/300 kD blends behaved similarly in all proportions, unlike 380/100 kD blends, which

demonstrated reduction in Tg and Tm with increasing proportion of the low molecular weight component. Also, the melting temperatures of 380/100 kD systems with 0% to 50% of 100 kD polymer had better melting temperatures for curcumin loading by melt extrusion.

- The manual process of fabricating the stent is tedious and the quality of stents produced by different people may not be identical. The quality of the welds is suboptimal. Furthermore, the PLLA/Chlororform glue that holds the fibers together can cause fiber erosion and weaken it if excess glue/solvent is delivered. Also, the use of two fibers increases the stent mass, which might influence stent thrombosis.
- The low inflation pressure, high hoop strength, low elastic recoil and high drug loading capability and axial flexibility along with axial fiber spreading, tested in vitro, indicate the stent's potential for deployment near fragile lesions.

CHAPTER 6

RECOMMENDATIONS FOR FUTURE WORK

6.1 Degradation Studies of the Fibers From Binary Blends

Using the thermal data on the binary blends good fibers can be produced under controlled temperature conditions. The effect of blending on the degradation behavior of the fiber must be studied to determine which blend compositions are preferable for future drug loading applications.

6.2 Curcumin Incorporation Studies

Curcumin can be loaded at various concentrations into the fibers. The determination of drug distribution characteristics, drug elution kinetics and the effect on the mechanical characteristics must be studied to optimize the amount of drug that can be incorporated into the fibers without seriously affecting its mechanical characteristics.

6.3 Improvement in Weld Quality

The effect of the following techniques on the improvement of glue quality must be studied:

1. Coat the fiber crossover points with a reactive biodegradable polymer. Subject the stent weld to UV/ Thermal/ gaseous environments to initiate the chemical reaction that can yield improved weld with minimal mass
2. Remove the residual solvent by blowing hot air/ applying vacuum at the glue point.

3. Expose the glue point to a nonsolvent aerosol for rapid removal of solvent.
4. Solvent polishing by the use of a very mild solvent to remove unnecessary trails of filaments at the glue point.
5. Use a microject injector with ultrasonically vibrated tip to direct a microscopically small drop of solvent onto glue that has spread out wider than required.

APPENDIX A

SIZE EXCLUSION CHROMATOGRAPHY DATA

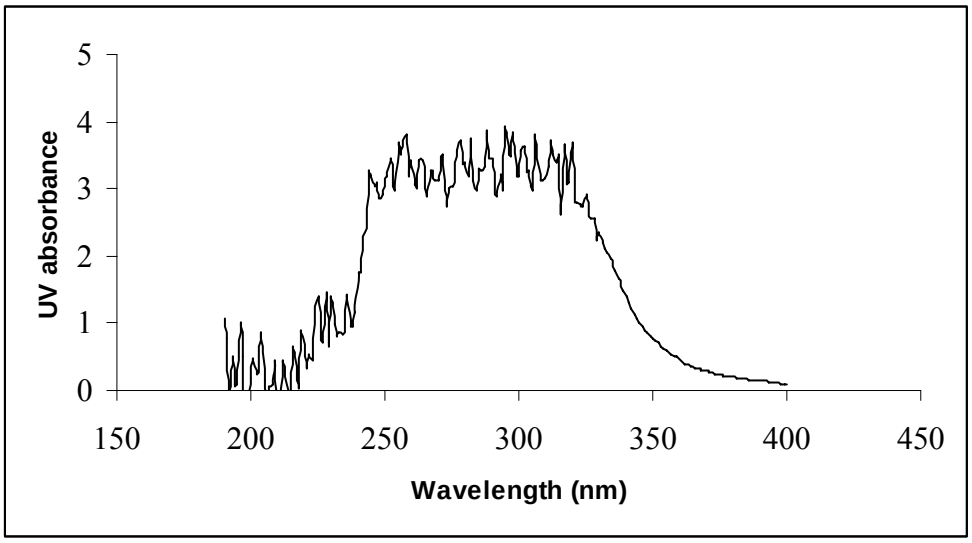

Figure A.1 UV absorbance spectrum of 380 kD polymer.

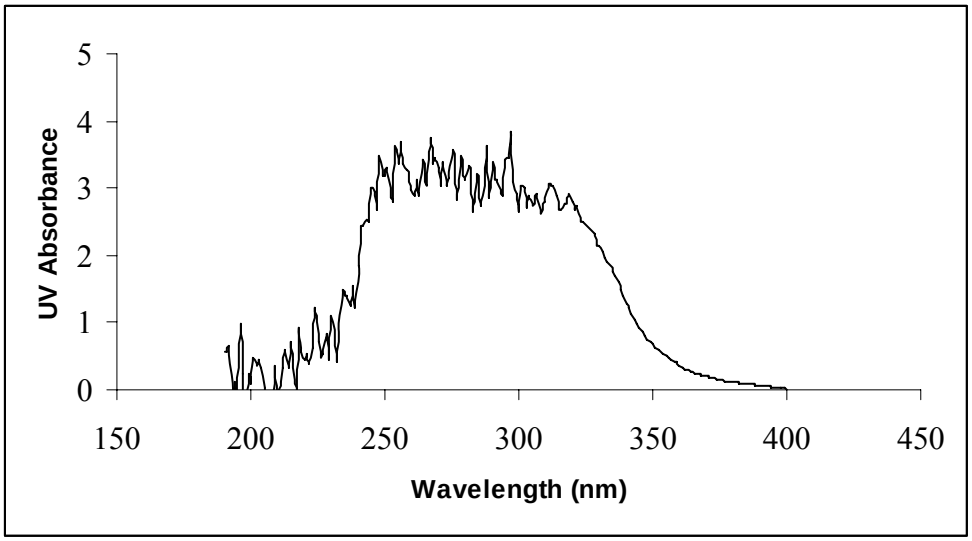

Figure A.2 UV absorbance spectrum of 300 kD polymer.

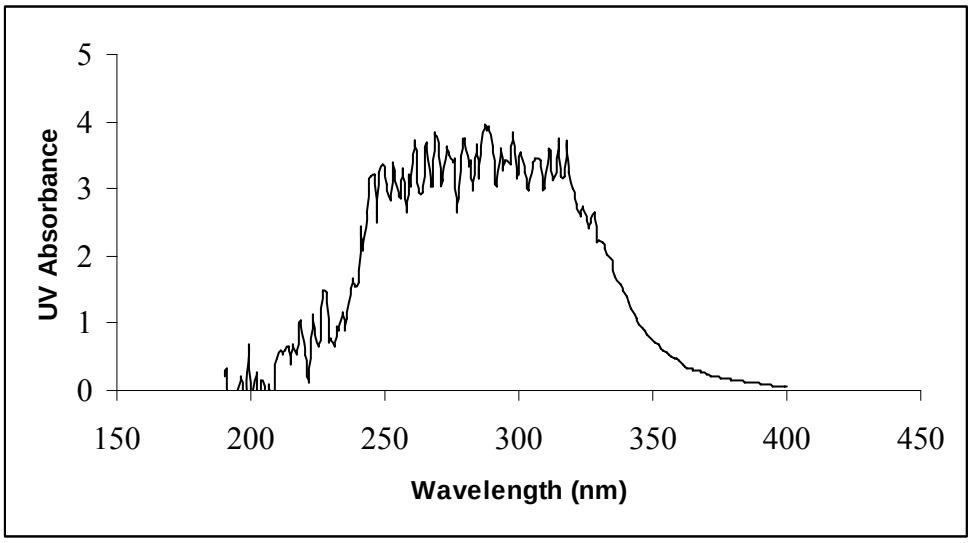

Figure A.3 UV absorbance spectrum of 100 kD polymer.

Table A.1 Molecular Weight and Retention Volume Data of Polystyrene Standards

Molecular weight (Dalton)	Retention volume (ml)
50000	9.49
110000	8.81
220000	8.26
400000	7.80
600000	7.48
900000	7.10

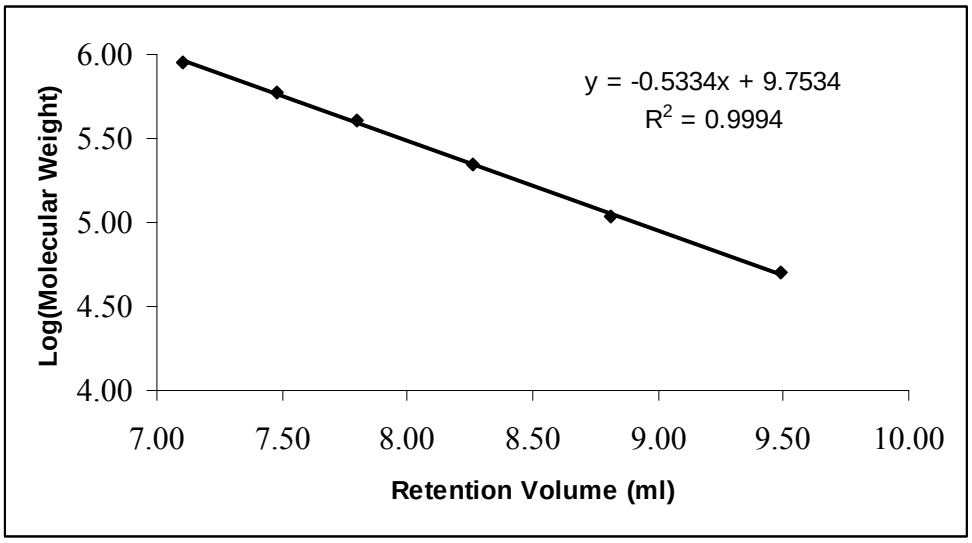

Figure A.4 Molecular Weight Calibration Curve

Table A.2 Number and Weight Average Molecular Weights of H-PLLA/I-PLLA Blends

H-PLLA/I-PLLA	Mn (Dalton)	Mw (Dalton)
0/100	385.9318	696.1497
40/60	314.3976	638.5486
50/50	380.9497	655.9102
60/40	361.9809	698.0633
100/0	361.2646	717.9091

Table A.3 Number and Weight Average Molecular Weight of H-PLLA/L-PLLA Blends

H-PLLA/L-PLLA	Mn (Dalton)	Mw (Dalton)
0/100	324.1501	673.4605
40/60	377.0890	665.7649
50/50	417.2017	725.6810
60/40	217.7870	659.4299
100/0	361.2646	717.9091

APPENDIX B

FIXTURE FOR THREE POINT BEND TEST

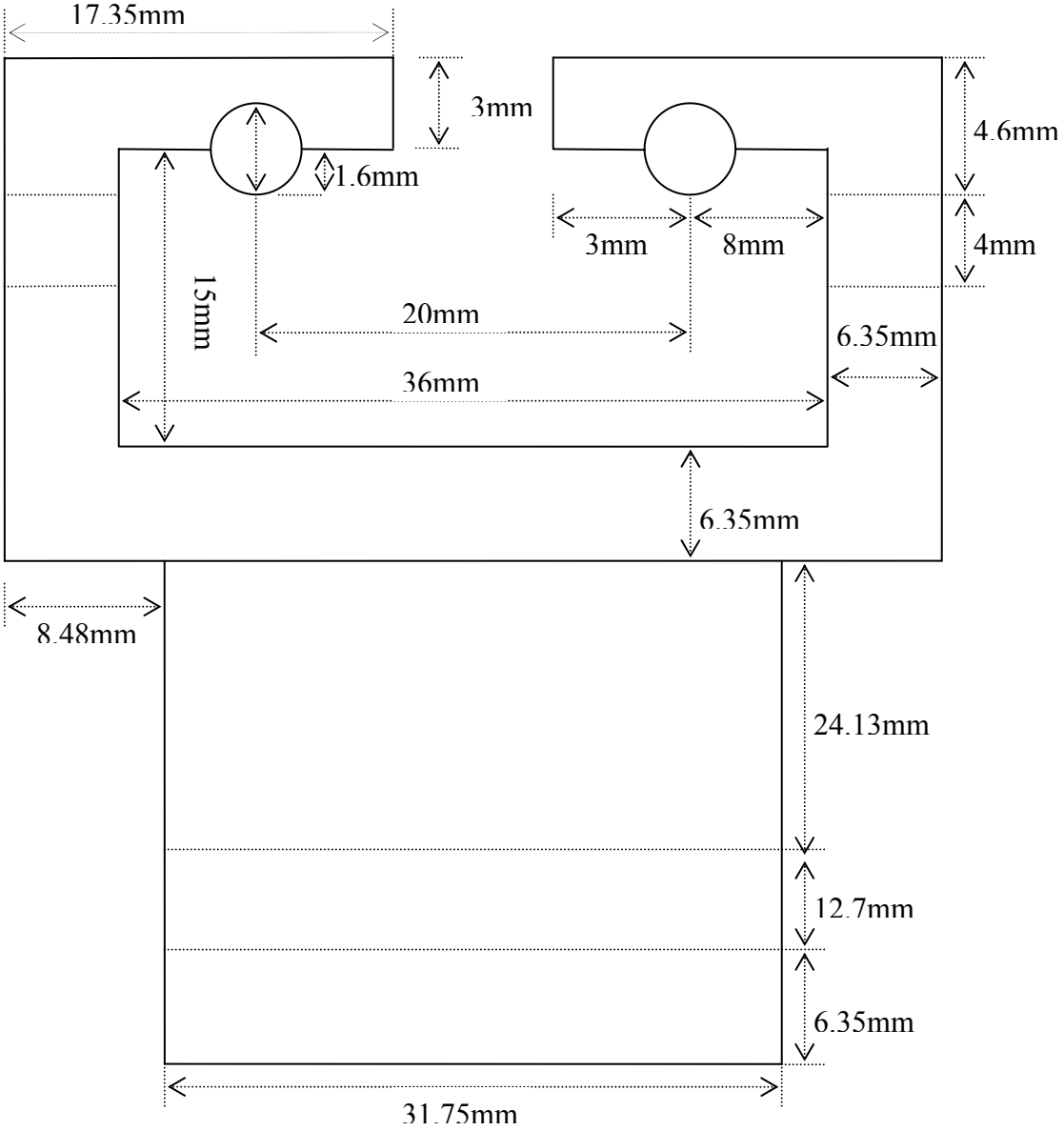

Figure B.1 Front view of the Y-fixture

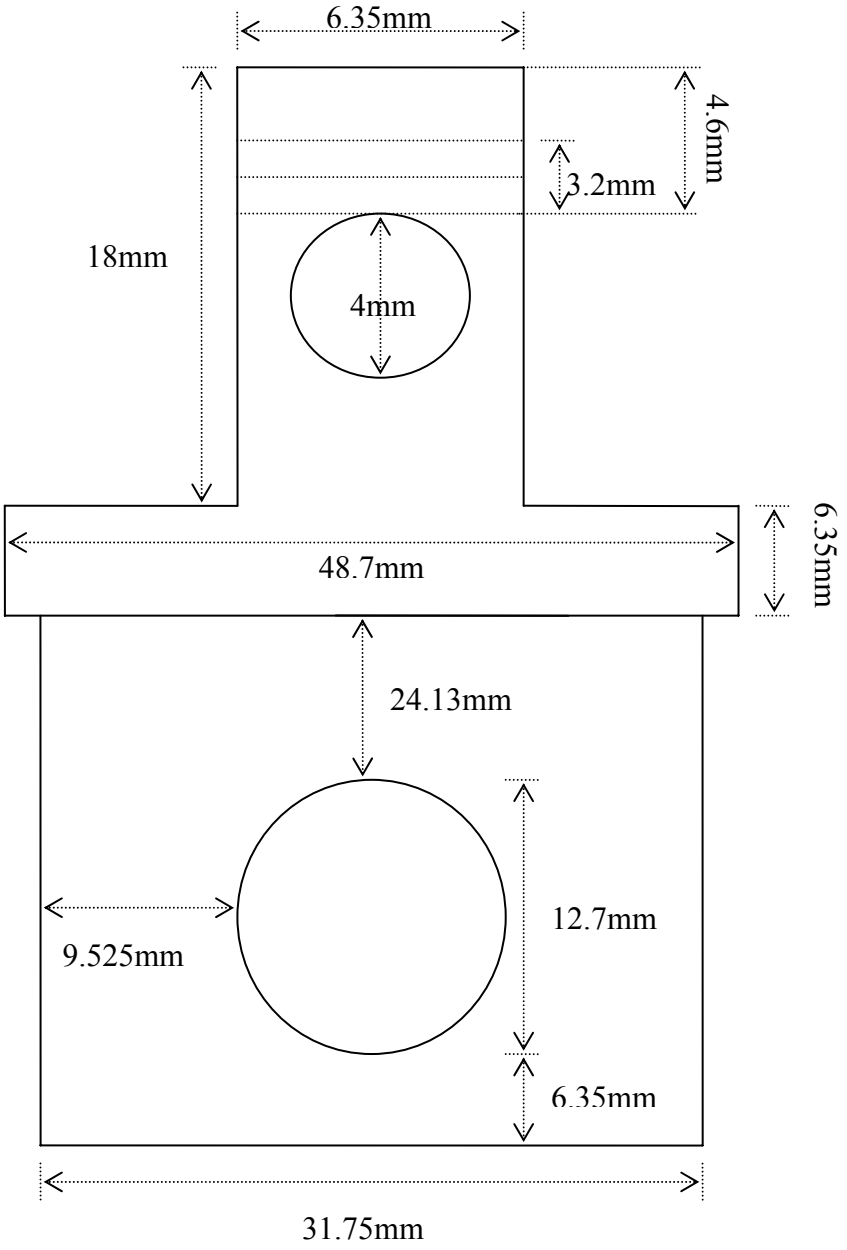

Figure B.2 Side view of the Y-fixture

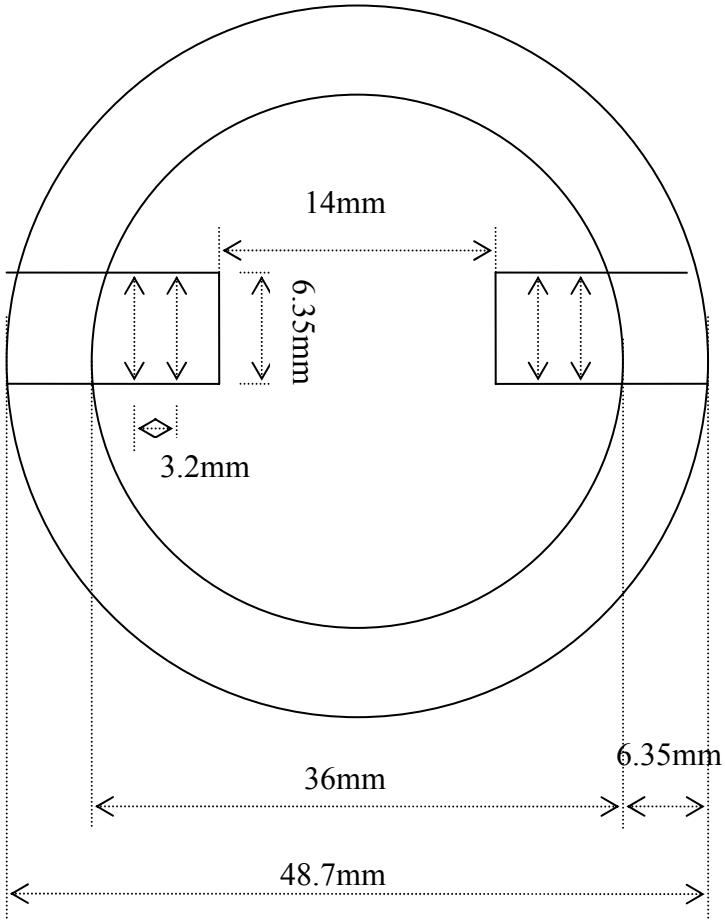

Figure B.3 Top view of the Y-fixture

REFERENCES

1. Heart disease and stroke statistics-2005 update. American Heart Association.

2. Leung DA, Spinosa DJ, Hagspiel KD, et al. Selection of stents for treating iliac arterial occlusive disease. J Vasc Interven Radiol. 2003; 14: 137.

3. Morton AC, Crossman D, Gunn J. The influence of physical stent parameters upon restenosis. Pathologie Biologie 2004; 52: 196.

4. MacClean DR, Eigler NL. Stent design: Implications for restenosis. Reviews in Cardiovascular medicine 2002; 3(Suppl5): S16.

5. Costa MA, Foley DP, Serruys PW. Restenosis: the problem and how to deal with it. In: Grech ED, Ramsdale DR, eds. Practical interventional cardiology. 2002; 2nd ed: 279.

6. Campbell DK Rogers. Optimal stent design for drug delivery. Reviews in Cardiovascular medicine 2004; 5(Suppl2): S9.

7. Sousa JE, Serruys PW and Costa MA. New frontiers in cardiology drug-eluting stents: Part 1. Circulation 2003; 107: 2274.

8. Naghavi M, Libby P, Falk E, et al . From vulnerable plaque to vulnerable patient a call for new definitions and risk assessment strategies: Part I. Circulation 2003; 108: 1664.

9. Myerburg RJ, Interian A Jr, Mitrani RM, et al. Frequency of sudden cardiac death and profiles of risk. Am J Cardiol 1997; 80: 10F.

10. Virmani R, Kolodgie FD, Burke AP, et al. Lesson from sudden cardiac death: a comprehensive morphological classification scheme for atherosclerotic lesions. Arterioscler Thromb Vasc Biol 2000; 20: 1262.

11. Ambrose JA, Tannenbaum MA, Alexopoulos D, et al. Angiographic progression of coronary artery disease and the development of myocardial infarction. J Am Coll Cardiol 1988; 12: 56.

12. Little WC, Constantinescu M, Applegate RJ, et al. Can coronary angiography predict the site of a subsequent myocardial infarction in patients with mild-to-moderate coronary artery disease? Circulation 1988; 78….: 1157.

13. Glagov, S. Intimal hyperplasia, vascular modeling, and the restenosis problem. Circulation. 89:2888-91; 1994.

14. Schoenhagen P, Ziada KM, Kapadia SR, et al. Extent and direction of arterial remodeling in stable versus unstable coronary syndromes. Circulation 2000; 101: 598.

15. Kotani, J., et al. Intravascular ultrasound analysis of infarct-related and non-infarct-related arteries in patients who presented with an acute myocardial infarction. Circulation 107:2889-93; 2003.

16. Gertz SD, Roberts WC. Hemodynamic shear force in rupture of coronary arterial atherosclerotic plaques. Am J Cardiol 1990; 66: 1368.

17. Yamagishi M, Terashima M, Awano K, et al. Morphology of vulnerable coronary plaque: insights from follow-up of patients examined by intravascular ultrasound before an acute coronary syndrome. J Am Coll Cardiol. 2000; 35: 106.

18. Van der Wal AC, Becker AE, van der Loos CM, Das PK. Site of intimal rupture or erosion of thrombosed coronary atherosclerotic plaques is characteized by an inflammatory process irrespective of the dominant plaque morphology. Circulation 1994; 89: 36.

19. Fuster V, Badimon L, Badimon JJ, et al. The pathogenesis of coronary artery disease and the acute coronary syndromes. N Engl J Med 1992; 326: 242.

20. Nakamura M, David Lee and Yeung AC. Identification and treatment of Vulnerable plaque. Reviews in cardiovascular medicine 2004. 5(suppl 2): S22.

21. Kolodgie FD, Burke AP, Farb A, et al. The thin-cap fibroatheroma: a type of vulnerable plaque: the major precursor lesion to acute coronary syndromes. Curr Opin Cardiol 2001; 16: 285.

22. Tenaglia AN, Peters KG, Sketch MH Jr, Annex BH. Neovascularization in atherectomy specimens from patients with unstable angina: implications for pathogenesis of unstable angina. Am Heart J 1998; 135: 10.

23. Moreno PR, Falk E, Palacios IF, et al. Macrophage infiltration in acute coronary syndromes. Implications for plaque rupture. Circulation 1994; 90: 775.

24. Toschi V, Gallo R, Lettino M, et al. Tissue factor modulates the thrombogenicity of human atherosclerotic plaques. Circulation 1997; 95: 594.

25. Dangas G, Mehran R, Harpel PC, et al. Lipoprotein(a) and inflammation in human coronary atheroma : association with the severity of clinical presentation. J Am Coll Cardiol. 1998; 32: 2035.

26. Fernandez-Ortiz A, Badimon JJ, Falk E, et al. Characterization of the relative thrombogenicity of atherosaclerotic plaque components: implications for consequences of plaque rupture. J Am Coll Cardiol. 1994; 23: 1562.

27. Loree HM, Tobias BJ, Gibson LJ, et al. Mechanical properties of model atherosclerotic lesion lipid pools. Arterioscler Thromb 1994; 14: 230.

28. Libby P. Molecular bases of the acute coronary syndromes. Circulation 1995; 91: 2844.

29. Galis ZS, Sukhova GK, Lark MW, Libby P. Increased expression of matrix metalloproteinases and matrix degrading activity in vulnerable regions of human atherosclerotic plaques. J Clin Invest. 1994; 94: 2493.

30. Cheng GC, Loree HM, Kamm RD, et al. Distribution of circumferential stress in ruptured and stable atherosclerotic lesions. A structural analysis with histopathological correlation. Circulation 1993; 87: 1179.

31. Stein PD, Hamid MS, Shivkumar K, et al. Effects of cyclic flexion of coronary ar tries on progression of atherosclerosis. Am J Cardiol. 1994; 73: 431.

32. Spratt JC and Camenzind E. Plaque stabilization by systemic and local drug administration. Heart 2004; 90: 1392.

33. Vaughan CJ, Gotto AM, Basson CT. The evolving role of statins in the management of atherosclerosis. J Am Coll Cardiol 2000; 35: 1.

34. Schartl M, Bocksch W, Koschyk DH, et al. Use of intravascular ultrasound to compare effects of different strategies of lipid-lowering therapy on plaque volume and composition in patients with coronary artery disease. Circulation 2001; 104: 387.

35. Shepherd J, Cobbe SM, Ford I, et al. Prevention of coronary heart disease with pravastatin in men with hypercholesterolemia. West of Scotland Coronary Prevention Study Group. N engl J Med. 1995; 333: 1301.

36. Downs JR, Clearfield M, Weis S, et al. Primary prevention of acute coronary events with lovastatin in men and women with average cholesterol levels: results of AFCAPS/TexCAPS. Air Force/Texas Coronary Atherosscleross Prevention Study. JAMA 1998; 279: 1615.

37. Maron DJ, Fazio S, Linton MF. Current perspectives on statins. Circulation 2000; 101: 207.

38. Libby P, Aikawa M. Mechanism of plaque stabilization with statins. Am J Cardiol. 2003; 91: 4B.

39. Ormiston JA, Dixon SR, Webster MWI, Ruygrok PN, Stewart JT, Minchington I, West T. Stent longitudinal flexibility: a comparison of 13 stent designs before and after balloon expansion. Catheterization and Cardiovascular Interventions 2000; 50: 120.

40. Pankaj Satasiya, MS Thesis, University of Texas at Arlington, 2004.

41. Zilberman M, Schwade ND, Meidell RS, Eberhart RC. Structured drug-loaded bioresorbable films for support structures. J. Biomater. Sci. Polymer Edn 2001; 12 (8): 875.

42. Cecil A, Scandola M. Thermal properties and physical ageing of poly(L-lactic acid). Polymer 1992; 33: 2699.

43. Yau WW, Kirkland JJ and Bly DD. Modern size exclusion liquid chromatography. Wiley-Interscience Publication 1979.

44. Su, S-H., New Expandable Biodegradable Polymeric Endovascular Stent Designs, in Biomedical Engineering, 2000. The University of Texas at Arlington p. 160.

45. Intravascular ultrasound findings of the RIBS II (Restenosis Intra-stent:Balloon angioplasty versus rapamycin-eluting stenting) randomized study. F. Alfonso, C. Macaya, Hospital Clinico San Carlos, Madrid. AHA Annual Meeting, Dallas, TX. Abstract #3580, November 16, 2005.

46. The vascular remodeling at the site of post-procedural incomplete stent apposition after sirolimus-eluting stent implantation. M. Kimura and M.B. Leon, Columbia University Medical Center & Cardiovascular Research Foundation, New York. AHA Annual Meeting, Dallas, TX. Abstract #3576, November 16, 2005.

47. Mauri L, O'Malley AJ, Cutlip DE et al. Effects of stent length and lesion length on coronary restenosis. Am J Cardiol 2004; 93: 1340.

48. Foley DP, Pieper M, Wijns W, et al. The influence of stent length on clinical and angiographic outcome in patients undergoing elective stenting elective stenting for native coronary artery lesions. Eur Heart J 2001; 22: 1585.

49. Dietz U, Holz N, Dauer C et al. Short stent implantation for routine use is feasible in a high proportion of coronary interventions and yields a low restenosis rate. Cardiology 2005; 103: 212.

50. Lau KW, Johan A, Sigwart U, Hung JS. A stent is not just a stent: stent construction and design do matter in its clinical performance. Singapore Med J 2004; 45(7) : 305

51. Leon MB, Popma JJ, O'Shaughnessy C, et al. Quantitative angiographic outcomes after Gianturco-Roubin stent implantation in complex lesions. Circulation 1997; 96: I-593.

52. Hoffmann R, Haager P, Mintz GS, et al. The impact of high pressure vs low pressure stent implantation on intimal hyperplasia and follow-up lumen dimensions. Eur Heart J 2001; 22: 2015.

53. Colombo A, Hall P, Nakamura S, et al. Intracoronary stenting without anticoagulation accomplished with intravascular ultrasound guidance. Circulation 1995; 91: 1676.

54. Goldberg SL, Colombo A, Nakamura S et al. Benefit of intracoronary ultrasound in the deployment of Palmaz-Schatz stents. J Am Coll Cardiol 1994; 24: 996.

55. Dirschinger J, Kastrati A, Neumann FJ, et al. Influence of balloon pressure during stent placement in native coronary arteries on early and late angiographic and clinical outcome. Circulation 1999; 100: 918.

56. Barragan P, Rieu R, Garitey V, et al. Elastic recoil of coronary stents: A comparative analysis. Cathet. Cardiovasc. Intervent. 2000; 50: 112.

57. Tré Welch, MS Thesis, University of Texas at Arlington, June 2005.

58. Etave F, Finet G, Boivin M, et al. Mechanical properties of coronary stents determined by using finite element analysis. J Biomechanics 2001; 34: 1065.

59. Rieu R, Barragan P, Garitey V, et al. Assessment of the trackability, flexibility, and conformability of coronary stents: A comparative analysis. Cathet Cardiovasc Intervent 2003; 59: 496.

60. Schmidt W, Behrens P, Behrend D, et al. Experimental study of peripheral, balloon-expandable stent systems. Progress in Biomedical Research 2001; May: 246.

61. Muller-hulsbeck S, Grimm J, Jahnke T, et al. Flow pattern from metallic vascular enderposthesis: in vitro results. Eur Radiol. 2001; 11: 893.

62. Kalmár G, Hübner F, Voelker W, et al. Radial force and wall apposition of balloon-expandable vascular stents in eccentric stenoses: An in vitro evaluation in a curved vessel model. J Vasc Interv Radiol 2002; 13: 499.

63. Schiele F, Meneveau N, Vuillemenot A, et al. Intermediate outcome after stent implantation with and without intracoronary ultrasound guidance: intermediate results of a randomized study. Eur Heart J 1996; 17 (supp l): 173.

64. Duda SH, Wiskirchen J, Tepe G, et al. Physical properties of endovascular stents: An experimental comparison. JVIR 2000; 11:645.

65. Venkatramana S, Poha TL, Vinaliaa T, et al. Collapse pressures of biodegradable stents Biomaterials 2003; 24: 2105.

66. Wiskirchen J, Pusich B, Kramer U, et al. Stent struts and articulations their impact on balloon-expandable stents' hoop strength, pushability, and radiopacity in an experimental setting. Investigative Radiology 2002; 37(6): 356.

67. Agrawal CM, Haas KF, Leopold DA, et al. Evaluation of poly L-lactic acid as a material for intravascular polymeric stents. Biomaterials 1992; 13: 176.

68. Rieu R, Barragan P, Masson C, et al. Radial force of coronary stents: a comparative analysis. Cathet Cardiovasc Intervent 1999; 46: 380.

69. Teppaz P. Mechanical behaviour of the composite atherosclerotic plaque and numerical simulations of angioplasty in human coronary arteries. PhD Thesis, Le Bourget du Lac: University of Savoie; 1999.

70. Gyongyosi M, Yang P, Khorsand A, et al. Longitudinal straightening effect of stents is an additional predictor for major adverse cardiac events. J Am Coll Cardiol. 2000; 35: 1580.

71. Fontaine AB, Spigos DG, Eaton G, et al. Stent-induced intimal hyperplasia: are there fundamental differences between flexible and rigid stent designs? J Vasc Interv Radiol 1994; 5 :739.

72. Liggins RT and Burt HM. Paclitaxel-loaded Poly(L-lactic acid) microspheres 3: blending low and high molecular weight polymers to control morphology and drug release. Int J Pharm 2004; 282: 61.

73. Weir NA, Buchanan FJ, Orr JF, et al. Degradation of poly-L-lactide. Part I: in vitro and in vivo physiological temperature degradation. Proc. Instn Mech. Engrs 2004; 218: 307.

74. Von Recum H, Cleek RL, Eskin SG, et al. Degradation of polydispersed poly(L-lactic acid) to modulate lactic acid release. Biomaterials 1995; 16: 441.

75. Zilberman M, Schwade ND and Eberhart RC. Protein-loaded bioresorbable fibers and expandable stens: Mechanical proerties and protein release. J Biomed Mater Res PartB: Appl Biomater 2004; 69B: 1.

76. Yau WW, Kirkland JJ and Bly DD. Modern size-exclusion liquid chromatography. Wiley publications, 1979.

77. Hunt BJ and Holding SR. Size exclusion chromatography. Chapman and Hall publications, 1989.

BIOGRAPHICAL INFORMATION

Sushma Gampa recieved her Bachelor of Technology degree in Chemical Engineering from Kakatiya University, India, in 2001. She worked as a Junior Chemical Consultant at Sri Sai Enterprises, India, for one year. In Spring 2003, she joined the graduate program at the University of Texas at Arlington to pursue her Master of Science degree in Biomedical Engineering. Her research interests in Biomaterials and Tissue Engineering drew her attention to the biodegradable stent project in Dr. Eberhart's lab. In Spring 2004 she started working on the stent project as a graduate research assistant and has successfully designed and fabricated a new stent design. She also had an opportunity to work on numerous school projects in Biomaterials and Tissue Engineering areas and her future plans are to pursue career opportunities in these areas. Under Dr. Robert Eberhart's mentoring, she received her M.S. Degree in fall 2005.